Draft version 0.4

ATLAS NOTE

June 12, 2017

Search for Higgs pair production in the final state of $\gamma\gamma WW^{*}(\rightarrow l\nu jj)$ using 36.1 fb^{-1} pp collision data at $\sqrt{s}$ = 13 TeV with the ATLAS detector

Yaquan Fang[1], Douglas Gingrich[3], Qi Li[1], Xinchou Lou[1,2], Bruce Mellado Garcia[4], Abdualazem Fadol Mohammed[4], Tshidiso Sydwell Molupe[4], Xifeng Ruan[4], Xiaohu Sun[3], Jin Wang[5], Maosen Zhou[1], Yu Zhang[1]

[1.] *Institute of High Energy Physics, Chinses Academy of Siences, Beijing, China*
[2.] *University of Texas at Dallas, USA*
[3.] *University of Alberta, Canada*
[4.] *University of the Witwatersrand, ZA*
[5.] *University of Sydney, AU*

Abstract

A search is performed for resonant and non-resonant Higgs pair production with one Higgs boson decaying to semi-leptonic WW and the other to $\gamma\gamma$ using proton-proton collision data corresponding to an integrated luminosity of 36.1 fb^{-1} at a 13 TeV centre-of-mass energy recorded with the ATLAS detector. The observed (expected) upper limit at 95% confidence level on the cross section for $gg \rightarrow hh$ is XXX pb (5.02 pb) for the non-resonant Higgs pair production. For resonant Higgs pair production, the observed (expected) upper limits at 95% confidence level on cross section times the branching ratio of $X \rightarrow hh$ range from XXX pb (12.2 pb) to XXX pb (4.15 pb) as a function of the resonant mass from 260 GeV to 500 GeV assuming a narrow-width resonance.

Contents

1 Statements **3**
1.1 List of contributions . . . 3
1.2 Version 0.X . . . 4
1.3 Version 0.4 . . . 4
1.4 Version 0.3 . . . 4
1.5 Version 0.2 . . . 4
1.6 Version 0.1 . . . 4
1.7 Version 0.0 . . . 4

2 Introduction **5**

3 Data and Monte Carlo samples **6**
3.1 Data samples . . . 6
3.2 Monte Carlo samples . . . 6
3.2.1 MC samples for signals . . . 6
3.2.2 MC samples for SM single Higgs backgrounds . . . 9
3.2.3 MC samples for continuum backgrounds . . . 9

4 Object definition **11**
4.1 Photons . . . 11
4.2 Jets . . . 11
4.3 Electrons . . . 11
4.4 Muons . . . 12
4.5 Missing transverse momentum . . . 12
4.6 Overlap removal . . . 12

5 Event selection **13**
5.1 Selection and efficiency . . . 13

6 Selection optimizations **15**
6.1 Optimal b-tagging working point . . . 15
6.2 Cuts optimization . . . 15

7 Signal and background estimations **17**
7.1 Model of signals, SM single Higgs and SM di-Higgs backgrounds . . . 17
7.2 Signal estimation . . . 17
7.3 Single Higgs background estimation . . . 21
7.4 Continuum background estimation . . . 21
7.4.1 Function form . . . 23
7.4.2 Lepton dependence . . . 26
7.4.3 Spurious signal . . . 28
7.4.4 $Z\gamma$ background . . . 33

8 Systematic uncertainties **35**
8.1 Luminosity uncertainties . . . 35
8.2 Theoretical uncertainties . . . 35
8.3 Experimental Uncertainties . . . 35
8.4 Uncertainty on continuum background estimation . . . 38

9 Statistical interpretation **39**
9.1 Statistical model 39
9.2 Model inspection 39
9.3 Upper limit setting 61

10 Summary **63**

Appendices **67**

A MadGraphs5 cards used for signals **67**

B Systematic uncertainties in details for one lepton region **71**

C Selections optimization **120**

D Fake lepton estimation **123**

E Discusssion on continuum background modeling **125**

F Parameters extraction for signals and SM backgrounds **125**

G Systematics on photon resolution and scale **130**

1 Statements

1.1 List of contributions

Yaquan Fang	Paper editor, supervision of IHEP students
Qi Li	Supporting note editor, main analyzer (signal, background estimations, systematics and statistics), plot production
Douglas Gingrich	Supervisor of Xiaohu
Xinchou Lou	Supervision of Yu Zhang
Bruce Mellado Garcia	Supervision of Witwatersrand students
Abdualazem Fadol Mohammed	Cross check of the cutflow
Tshidiso Sydwell Molupe	Continuum background decomposition
Xifeng Ruan	Background decomposition, spurious signal, supervision of Witwatersrand students
Xiaohu Sun	Supporting note/paper editor, analyzer, statistics, supervision of IHEP students
Jin Wang	Statistics, background modeling
Maosen Zhou	Signal and background sample validation, Wh uncertainty from jet multiplicity
Yu Zhang	Photon purity checks, derivations of MC samples, cross check of the data

1.2 Version 0.X

Finalized analysis strategy and answered CDS comments

- Determine the fit strategy with only 1-lep region 9.1
- ...

1.3 Version 0.4

Fully updated version answering all CDS comments so far and aiming at unblinding approval.

1.4 Version 0.3

Please focus on the fully updated Section 7, while sections of statistics and systematics are under developing not ready for reading. Thanks.

- Fully update to h15 HGam framework and final CP recommendation for Moriond
- Fully update the structure and content of Section 7 ”Signal and background estimations”
- Drop fully hadronic channel given no gain in sensitivity
- Apply $p_T(\gamma\gamma)$ cut
- Study photon purity
- Study spurious signal
- Study electron faking photons
- Study jet faking leptons

1.5 Version 0.2

- Upgrade to the shape fit
- Include combination and introduce orthogonal cuts between the fully hadronic and this analysis.
- Explore additional kinematic cuts besides what have been applied; no one shows promising results.

1.6 Version 0.1

Almost all the results and plots are updated to 36.47 fb^{-1}.

1.7 Version 0.0

This version is based on ICHEP INT note

2 Introduction

A Higgs boson was discovered by the ATLAS and CMS collaborations [1, 2] in 2012 and has been subsequently studied by spin and coupling measurements [3, 4, 5], which have established that its properties are very similar to the ones of the Standard Model (SM) Higgs boson. These measurements are mainly based on Higgs production via gluon-fusion, vector-boson-fusion and in association with a W or Z boson. Higgs pair production has not been measured and, if its cross section is similar to the SM predicted value 33.41 fb [6], it is impossible to measure with the current data. However, the non-resonant Higgs pair production can be significantly enhanced either by altering the Higgs boson self-coupling λ_{HHH} [7] or in extended Higgs sectors such as 2-Higgs-Doublet Models (2HDM) [8] where a heavy resonance decaying into a pair of SM-like Higgs bosons could exist. In RUN I, various channels were explored with the ATLAS detector, such as $bb\gamma\gamma$ [9], $bbbb$ [10], $bb\tau\tau$ and $WW\gamma\gamma$ [11]. In RUN II, $bb\gamma\gamma$ [12], $bbbb$ [13] and $WW\gamma\gamma$ [14] continue searching for the Higgs boson pair production.

This note provides supporting material for the search of Higgs pair either from the non-resonant production or from the resonant one, with the subsequent decay chain of $hh \to WW\gamma\gamma \to l\nu jj\gamma\gamma$, namely one of the W bosons decays hadronically while the other decays leptonically, leading to a final state with two jets, one charged lepton (either electron or muon), missing transverse momentum and two photons. In terms of the mass scan on the resonant search, we start from 260 GeV and stop at 500 GeV based on our RUN I sensitivity [11]. The object and event selections inherits the ICHEP analysis as much as possible. With a set of similar selections, around two times more data are accumulated and examined for the Higgs pair search. The featured update is that a shape fit on $m_{\gamma\gamma}$ is adopted rather than the simple event counting method given more sufficient statistics.

Section 3 introduces the data and MC samples used in this analysis. Section 4 defines the objects used in the event selection. Section 5 gives the event selection definitions and relevant cut efficiencies. Section 6 describes the optimization on selection criteria. Section 7 discusses the signal and background estimations in the non-resonant and resonant Higgs pair searches. Section 8 describes the systematic uncertainties. In Section 9, statistical interpretation and relevant checks are done.

Section 10 summarizes the results and compares them to RUN I and RUN II (13.3 fb^{-1}). Appendix A gives the details of MG5 cards used for signal event generation. Appendix B records the details of systematic uncertainties related to detectors in one lepton region. Appendix C provides the discussions on the cuts optimizations.

3 Data and Monte Carlo samples

3.1 Data samples

The data samples used in this analysis correspond to the data recorded by ATLAS in the whole 2015 and 2016, which sums up to an integrated luminosity of 36.1 fb^{-1}. The whole dataset is recorded with all subsystems of ATLAS operational [1].

3.2 Monte Carlo samples

SM single Higgs backgrounds and signals are estimated with MC samples that are documented in this section, while the continuum photon background of the SM processes with multiphotons and multijets is determined with the data in sideband [2] with the data-driven method. Nevertheless, two relevant MC samples are used to check and consolidate the modeling of the continuum photon background and they are described in this section.

The simulation under MC15c configuration is used in the analysis. The samples are generated with the consideration of multiple interactions per bunch crossing by introducing pileup noise at the stage of digitalization. MC15c configuration incorporates the pileup condition that is an average of the actual pileup condition in 2015 data and an estimation for 2016 data. Any residual difference in pileup conditions is corrected for through a re-weighting. The vertex z distribution is also re-weighted to better match data.

3.2.1 MC samples for signals

Signal samples are generated with MadGraph5_aMC@NLO [15]. For both non-resonant and resonant productions, the event generation is performed using a next-to-leading-order SM Higgs pair model developed by the Cosmology, Particle Physics and Phenomenology (CP3) theory group [16]. Events are generated with a Higgs Effective Field Theory (HEFT) using aMC@NLO method [17] and are reweighted to take into account top quark mass dependence [13]. The top mass can become an important effect [18], particularly for the non-resonant case. The shower is implemented by Herwig++ [19] with UEEE5 underlying-event tune [20], and the PDF set CTEQ6L1 [21] is used. The heavy scalar, H, is assumed to have a narrow width. Technically its decay width is set to 10 MeV in the event generation for the following masses: 260 GeV, 300 GeV, 400 GeV and 500 GeV. The card used in MadGraph5 for signal event generations is attached in Appendix A. Subsequently, the H boson is required to decay into a pair of SM Higgs bosons, one of which decays into a pair of photons and the other into two W bosons. W inclusively decays. The generator level filter *ParentChildFilter* implements the selection of these decay products. Details on the signal samples are listed in Table 1. All signal samples are produced with the Atlas fast simulation framework (AF2).

The kinematic distributions after hadronization and parton shower before interacting with the materials in the detector are shown for non-resonant and resonant Higgs pair productions. In Figure 1 and Figure 2, the transverse momentum p_T and pseudorapidity η distributions are shown for each object in the final state at truth level [22]. The p_T spectrum of the decay products get harder as the resonant mass rises and the non-resonant one is the hardest under the centre-of-mass energy of 13 TeV.

[1] Good Run Lists are data15_13TeV.periodAllYear_DetStatus-v79-repro20-02_DQDefects-00-02-02_PHYS_StandardGRL_All_Good_25ns.xml for 2015 data and data16_13TeV.periodAllYear_DetStatus-v88-pro20-21_DQDefects-00-02-04_PHYS_StandardGRL_All_Good_25ns.xml for 2016 data

[2] The sideband is defined as $m_{\gamma\gamma} \in [105, 125.09 - 2\sigma_{\gamma\gamma}] \cup [125.09 + 2\sigma_{\gamma\gamma}, 160]$ GeV orthogonal to the signal region defined in Section 5. The $\sigma_{\gamma\gamma}$ is the resolution of invariant mass of di-photon and is 1.7 GeV

DSID	Processes	Generators, tunes and PDFs	Tags
342621	non-resonance	MadGraph + Herwigpp UEEE5 CTEQ6L1	*e4419_a766_a821_r7676_p2691*
343756	$X \to hh$, 260 GeV	MadGraph + Herwigpp UEEE5 CTEQ6L1	*e5153_a766_a821_r7676_p2691*
343758	$X \to hh$, 300 GeV	MadGraph + Herwigpp UEEE5 CTEQ6L1	*e5153_a766_a821_r7676_p2691*
343761	$X \to hh$, 400 GeV	MadGraph + Herwigpp UEEE5 CTEQ6L1	*e5153_a766_a821_r7676_p2691*
343763	$X \to hh$, 500 GeV	MadGraph + Herwigpp UEEE5 CTEQ6L1	*e5153_a766_a821_r7676_p2691*

Table 1: Simulated signal samples

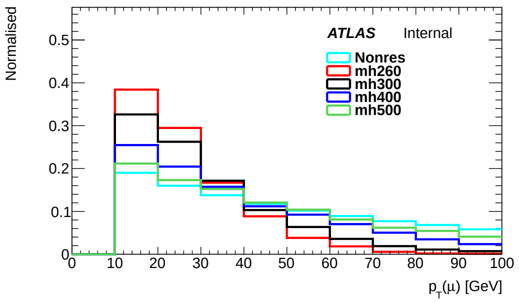

(a)

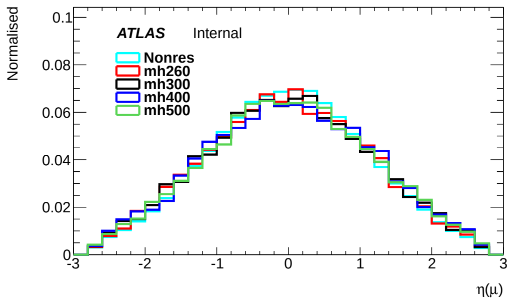

(b)

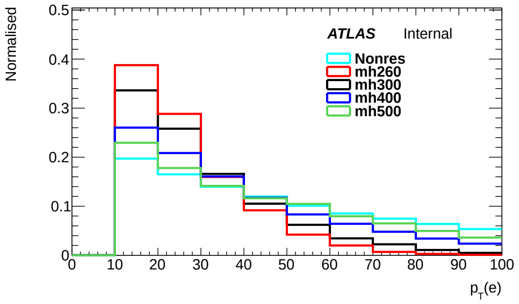

(c)

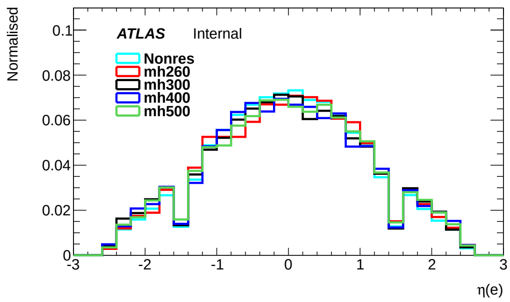

(d)

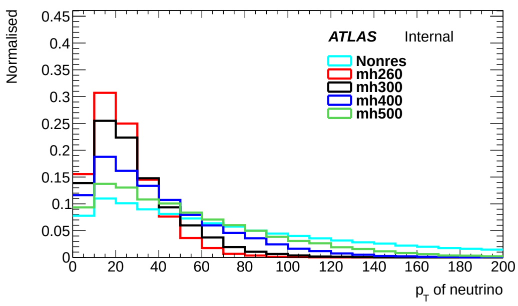

(e)

Figure 1: Kinematic distributions at truth level for the production of $hh \to WW\gamma\gamma$: (a) p_T of muons, (b) η of muons, (c) p_T of electrons, (d) η of electrons, (e) p_T of neutrino. Distributions are normalized to unity. Some kinematic cuts are applied for particles. For photon : $p_T > 25GeV$, $|\eta| < 2.37$, remove crack region, truth isolation; for electron : $p_T > 10GeV$, $|\eta| < 2.47$; for muon : $p_T > 10GeV$, $|\eta| < 2.7$; for jet : $p_T > 25GeV$, $|\eta| < 4.4$

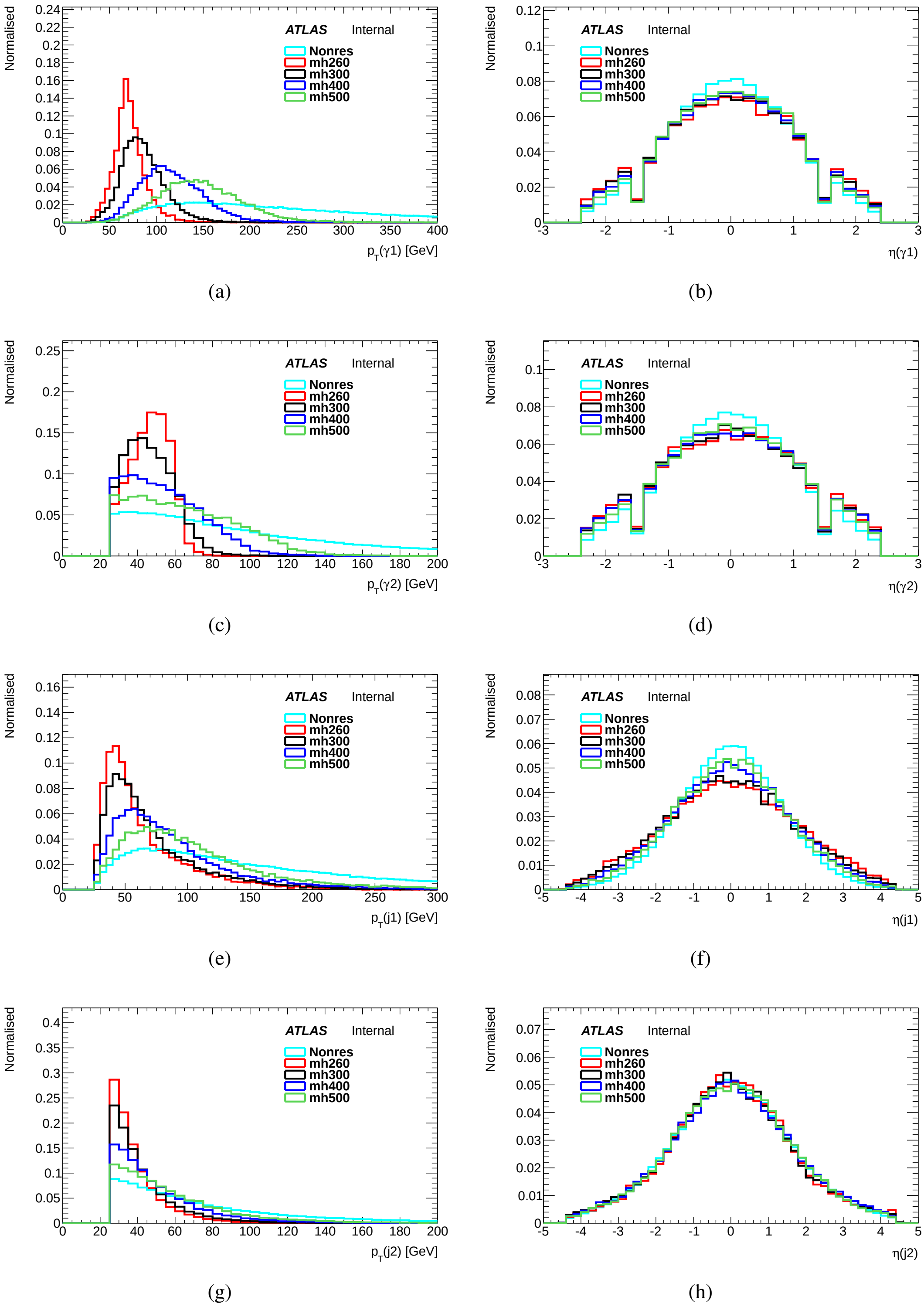

Figure 2: Kinematic distributions at truth level for the production of $hh \to WW\gamma\gamma$: (a) p_T of leading photon, (b) η of leading photon, (c) p_T of subleading photon, (b) η of subleading photon, (e) p_T of leading jet, (f) η of leading jet, (g) p_T of subleading jet, (h) η of subleading jet. For jet, the truth jet is plotted in the plots. Distributions are normalized to unity.

3.2.2 MC samples for SM single Higgs backgrounds

Simulated samples for SM single Higgs background are produced to investigate the components of this background in $m_{\gamma\gamma}$ and to estimate their contributions. The SM single Higgs background considered here is assumed to be produced via five production modes: ggh, VBF, Wh, Zh and tth, where h is the light (SM-like) 125 GeV Higgs boson. These samples are simulated using the full ATLAS simulation and reconstruction chain. The mass of the SM Higgs boson is set to 125 GeV. More details on generator, parton shower and simulation tags are listed in Table 2.

The cross sections at $\sqrt{s}$ = 13 TeV corresponding to each production mode are listed in Table 3. In the analysis, these cross sections will be multiplied by the $h \to \gamma\gamma$ branching ratio of 0.00227 due to all simulated samples are produced with SM Higgs decaying into photon pairs.

DSID	Processes	Generators, tunes and PDFs	Tags
341000	ggh	Powheg+Pythia8 AZNLO CTEQ6L1	$e3806\_s2608\_r7772\_r7676\_p2669$
341001	VBF	Powheg+Pythia8 AZNLO CTEQ6L1	$e3806\_s2608\_r7772\_r7676\_p2669$
341067	Wh	Pythia8 A14 NNPDF2.3LO	$e3796\_s2608\_s2183\_r7772\_r7676\_p2669$
341068	Zh	Pythia8 A14 NNPDF2.3LO	$e3796\_s2608\_s2183\_r7772\_r7676\_p2669$
341069	tth	Pythia8 A14 NNPDF2.3LO	$e3796\_s2608\_s2183\_r7772\_r7676\_p2669$

Table 2: Simulated SM single Higgs background samples.

production	cross sections
ggh	48.52 pb
VBF	3.779 pb
Wh	1.369 pb
Zh	0.8824 pb
tth	0.5065 pb
$gg \to hh$	33.41 fb

Table 3: Cross sections for SM single Higgs processes at $\sqrt{s}$ = 13 TeV with m_h = 125.09 GeV and the SM Higgs pair productions, $gg \to hh$ [23].

3.2.3 MC samples for continuum backgrounds

The simulated sample of the $pp \to l\nu jj\gamma\gamma$ background is used to study the components with the SM background with the same final states of signal. The background sample $pp \to jjj\gamma\gamma$ is generated by HGam group. The $pp \to jjj\gamma\gamma$ as well as $pp \to l\nu jj\gamma\gamma$ is used to validate the $m_{\gamma\gamma}$ modeling. These processes are listed in Table 4.

DSID	Processes	Generators, tunes and PDFs	Tags	Cross section
343363	$pp \to l\nu jj\gamma\gamma$	MadGraph + Pythia8 AU2 NN23LO1ME	$e4852\_a766\_a821\_r7676\_p2691$	31.739 fb
341065	$pp \to jjj\gamma\gamma$	Sherpa + CT10 + 2DP20	$e4407\_s2726\_s2183\_r7725\_r7676\_p2666$	40.127 pb

Table 4: The simulated samples for continuum background.

4 Object definition

The photon selections follow the recommendations in HGam analysis and are exactly the same as what the team of $bb\gamma\gamma$ uses. This analysis additionally requires leptons and jets. The analysis framework of $hh \to WW\gamma\gamma$ is based on the HGamAnalysisFramework that is centrally developed by HGam group. The tag of the framework is HGamAnalysisFramework-00-02-77-01 which is used to produce official MxAOD samples of version h015.

4.1 Photons

- The E_T of leading (sub-leading) photon is required to be large than 35% (25%) of the invariant mass of the leading two photons.
- The $|\eta|$ of photon is considered up to 2.37, vetoing the crack region $1.37 < |\eta| < 1.52$.
- Photons are required to pass the loose identification criteria on the shape of the electromagnetic shower in the LAr accordion calorimeter and on the fraction of energy leaking in the hadronic calorimeter. Photons are further required to pass the Tight ID cut to suppress the fake photon.
- The isolation working point FixedCutLoose is used. It is one of the recommended points from the isolation forum. The photons are required to satisfy both a calorimeter-based and a track-based isolation requirements. The calorimeter isolation requires $topoetcone20 < 0.065 \times E_T$ in which the 20 means a cone of $\Delta R = 0.20$. The track isolation requires $ptcone20 < 0.05 \times p_T$.
- The neural network photon pointing information that is default in HGam is used to select the primary vertex (PV) and recalculate the photons' four momenta and other quantities including JVT and track isolation. The NN training takes into account the inputs from the weighted average of the z position obtained from photon pointing, the beam spot position, the conversion vertex for converted photons, $log(\Sigma p_T$ of tracks), $log(\Sigma p_T^2$ of tracks) and $\Delta\phi(\gamma\gamma,\mathrm{PV})$.
- The invariant mass of two leading photons is required to be within [105,160] GeV.

4.2 Jets

- The Anti-k_t algorithm [24] with the distance parameter of $R = 0.4$ is used.
- Jets are required to have $p_T > 25$ GeV and $|y| < 2.5$.
- Jets from pileup are rejected by applying a JVT (Jet Vertex Tagger) cut. The jet is rejected if JVT< 0.59 for $p_T < 60$ GeV and $|y| < 2.4$.
- Events with a jet passing the LooseBad cut are rejected. The LooseBad jet quality requirement is designed to reject fake jets caused by detector readout problems and non-collision backgrounds.

4.3 Electrons

Electrons are reconstructed from energy clusters in the EM calorimeter matched with tracks reconstructed in the inner detector.

- E_T is required to be larger than 10 GeV.
- $|\eta|$ is required to be less than 2.47 vetoing the transition region with $1.37 < |\eta| < 1.52$.

- The $|d_0|$ significance ($d_0/\sigma(d_0)$) with respect to the hardest vertex in the event is required to be less than 5.
- The $|z_0 sin\theta|$ with respect to the hardest vertex in the event is required to be less than 0.5mm.
- Identification: MediumLH quality electrons are used.
- Isolation: Loose electrons are used. It requires that the calorimeter isolation in a cone size $\Delta R < 0.2$ satisfies $topoetcone20 < 0.020 \times E_T$ as well as track isolation in a cone size $\Delta R < 0.2$ satisfing $ptcone20 < 0.15 \times P_T$.

4.4 Muons

Muons are reconstructed from tracks in the inner detector and the muon spectrometer.

- p_T is required to be larger than 10 GeV.
- $|\eta|$ is required to be less than 2.7.
- The significance $|d_0/\sigma(d_0)|$ with respect to the hardet vertex in the event is required to be less than 3.
- The $|z_0 sin\theta|$ with respect to the hardest vertex in the event is required to be less than 0.5mm.
- Identification: Medium quality muons are used.
- Isolation: GradientLoose is used.

4.5 Missing transverse momentum

The missing transverse momentum E_T^{miss} is calculated as the negative vector sum of the transverse momentum of the reconstructed objects including jets, electrons, muons and photons, with relevant calibrations and soft terms which are not associated to any reconstructed objects [25, 26]. Various algorithms have been explored to improve the soft term measurement. The default one used in this analysis is Track-base Soft Term (TST) [27] thanks to its outstanding resolution performance and pileup robustness. In this algorithm, the momentum of the soft terms are calculated based on inner detector measurements.

4.6 Overlap removal

Since objects are reconstructed with different algorithms in parallel, i.e. no check to see if a same set of clusters or tracks are used for reconstructing two different object, one needs to implement a set of rules to remove objects close to each other to avoid double counting. The rule is defined as below:

- The two leading photons are always kept.
- Electrons with $\Delta R(e, \gamma) < 0.4$ are removed.
- Jets with $\Delta R(jet, \gamma) < 0.4$ are removed.
- Jets with $\Delta R(jet, e) < 0.2$ are removed.
- Muons with $\Delta R(\mu, \gamma) < 0.4$ or $\Delta R(\mu, jet) < 0.4$ are removed
- Electrons with $\Delta R(e, jet) < 0.4$ are removed.

5 Event selection

5.1 Selection and efficiency

The event selection procedure identifies two photons and then applies requirements on the multiplicities of jets and leptons in order to increase the signal purity and background rejection for events with at least 2 jets, at least 1 lepton and 2 photons. The event selection for the analysis starts with the full di-photon selection from the $h \rightarrow \gamma\gamma$ analysis in RUN II to select two high p_T isolated photons.

- **Trigger**: di-photon trigger HLT_g35_loose_g25_loose is used.
- **Good Run List and Detector Quality**: Events must belong to the luminosity blocks specified in the Good Run Lists:
  - data15_13TeV.periodAllYear_DetStatus-v79-repro20-02_DQDefects-00-02-02_PHYS_StandardGRL_All_Good_25ns.xml for 2015 data
  - data16_13TeV.periodAllYear_DetStatus-v88-pro20-21_DQDefects-00-02-04_PHYS_StandardGRL_All_Good_25ns.xml for 2016 data

  Events with data integrity errors in the calorimeters and incomplete events where some detector information is missing are rejected, as well as events which are corrupted due to power supply trips in the tile calorimeter.
- **Primary Vertex**: The primary vertex is selected using the neural network (NN) algorithm form HGam group. The photons' four momenta, JVT and track isolation are corrected with respect to this origin, and the mass of the diphoton system is accordingly recalculated. Figure 5.1 shows the difference of NN vertex and primary vertex in z axis. The difference is very small after full selection which requires at least one lepton and two jets in the final state.
- **2 loose photons**: At least two loose photons with $E_T > 25$ GeV and within the detector acceptance are selected.
- The other cuts on photons involving **Identification (tight ID), Isolation, Rel.Pt cuts** and $m_{\gamma\gamma} \in [105, 160]$ **GeV** have been discussed in Section 4.1
- **Number of jets**: At least two jets.
- **b-veto**: In order to suppress backgrounds with top quarks and keep orthogonality to other hh channels $bb\gamma\gamma$, $bbbb$, $bb\tau\tau$ etc, the event is rejected if there is any b-jet. The b-tagger is MV2c10 with a b-tagging efficiency of 70%. The optimization is discussed in Section 6.1.
- **Number of leptons**: At least one muon or electron.[3]
- **Tight mass window**: The tight mass window is used to define the final signal region which is blinded till the background estimation is consolidated. In the final fit on the shape of $m_{\gamma\gamma}$ in Section 7, the events both in the window and out are used.

The efficiencies of event selection are listed in Table 5. These efficiencies are derived for signals from simulated samples. After the selection of the two photons, the signal efficiencies range from 35.6% to 42.2%, while after the additional selection on the jets and the leptons , the signal efficiencies range from 6.56% to 12.0%, for a resonant mass from 260 to 500 GeV.

[3] There is one comparison about exact one lepton and at least one lepton. See link

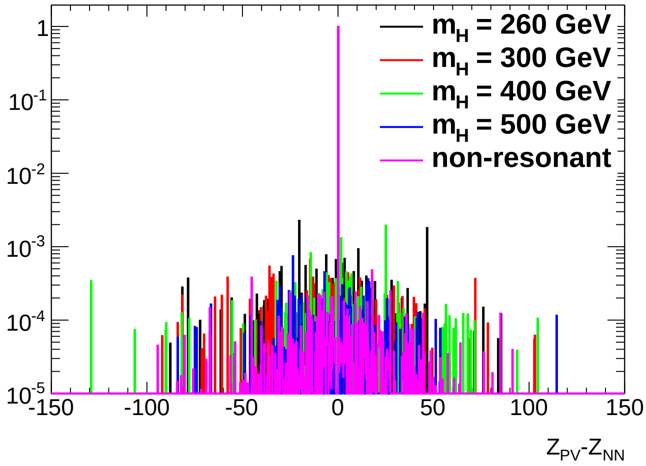

Figure 3: The lines show the difference of two algorithms in signal sample. If require $|Z_{PV} - Z_{NN}| <$ 0.3 mm , the efficiency is 97.7%, 98.4%, 98.3%, 98.8%, 99.0% for m_H = 260 GeV, m_H = 300 GeV, m_H = 400 GeV, m_H = 500 GeV and non-resonant.

	SM Higgs pair	Resonant 260 GeV	300 GeV	400 GeV	500 GeV
All Events	100.0%	100.0%	100.0%	100.0%	100.0%
Duplicate	100.0%	100.0%	100.0%	100.0%	100.0%
GRL	100.0%	100.0%	100.0%	100.0%	100.0%
Pass Trigger	73.8%	68.4%	69.4%	71.8%	74.5%
Detector Quality	73.8%	68.4%	69.4%	71.8%	74.5%
has PV	73.8%	68.4%	69.4%	71.8%	74.5%
2 loose photons	59.3%	56.6%	56.1%	57.5%	59.7%
Trig Match	59.0%	56.3%	55.8%	57.2%	59.4%
Tight ID	49.3%	46.2%	45.5%	47.5%	50.2%
Isolation	44.6%	39.3%	39.3%	42.6%	45.7%
Rel.Pt cuts	41.0%	36.6%	35.6%	38.8%	42.4%
$105 < m_{\gamma\gamma} < 160$ GeV	40.9%	36.6%	35.6%	38.6%	42.2%
At least 2 central jets	29.7%	17.7%	20.1%	26.5%	32.1%
B-veto	27.8%	16.7%	19.0%	25.0%	30.2%
At least 1 lepton	11.1%	6.56%	7.60%	10.4%	12.0%
$pT_{\gamma\gamma} > 100$ GeV					

Table 5: Efficiencies for event selection

ϵ(btag)	ggh	VBF	Wh	Zh	tth	Cont.	Non-res	ϵ(non-res)	Sig.
60%	0	0.001	0.042	0.016	0.093	1.60	0.128	8.7%	0.09556σ
70%	0	0.001	0.042	0.012	0.067	1.60	0.127	8.6%	0.09568σ
77%	0	0.001	0.042	0.012	0.050	1.60	0.126	8.5%	0.09548σ
85%	0	0.001	0.039	0.012	0.035	1.60	0.100	7.1%	0.07625σ

Table 6: The event yields (SM single Higgs, continuum background and non-resonant signal), signal efficiencies and the expected significance for difference b-tagging working points. Non-resonant signal is used as a benchmark. Events pass all selections defined for signal region. The backgrounds in this table were estimated with the luminosity (3.2 fb^{-1}) from 2015 data.

$p_T(\gamma\gamma)$ selection	$p_T(\gamma\gamma)$ >50 GeV	$p_T(\gamma\gamma)$ >80 GeV	$p_T(\gamma\gamma)$ >100 GeV
Limits (pb)	5.42	4.64	4.22

Table 7: The limits scan with different $p_T(\gamma\gamma)$ cuts including all systematic uncertainties for mh = 500 GeV.

6 Selection optimizations

Optimizations on object or event selection are discussed in this section. In general, the expected significance formula for low-statistical analyses is used as a figure-of-merit.

$$Z = \sqrt{2 \times [(S + B) \times (\ln \frac{S+B}{B}) - S]} \tag{1}$$

where S is the signal yield and B is the background yield after a set of selections. The higher the significance is, the better the expected sensitivity would be. Normally, we choose the selections that give the highest expected significance. When doing the optimization, the cross section $\sigma(gg \to hh)$ for non-resonance and $\sigma(gg \to H) \times BR(X \to hh)$ for resonances are assumed to be 1 pb.

6.1 Optimal b-tagging working point

As recommended by the performance groups, the btagger MV2c10 is used for b-veto to suppress tth background. Several working points corresponding to difference b-tagging efficiencies are tested as shown in Table 6. As expected, the b-tagging working point only affects the SM tth process significantly. Eventually, we choose working point with 70% b-tagging efficiency based on the expected significance.

6.2 Cuts optimization

Details of optimizations are documented in the Appdendix C. Given that the improvement is small and the loss on statistics is large, there is no more cut applied except $p_T(\gamma\gamma)$, which shows significant improvement on sensitivity for high mass points and non-resonance. Figure 4 shows the distribution of $p_T(\gamma\gamma)$, the expected significance against the cut threshold and the signal efficiencies against the cut threshold. Table 7 then shows a limit scan with several different $p_T(\gamma\gamma)$ cuts using the full statistical machinary including all systematic uncertainties. A threshold of 100 GeV is chosen considering the sensitivity improvement and the loss of statistics as Figure 4(c) shown. This selection is applied to resonant mass points 400 GeV and 500 GeV as well as non-resonant analysis considering the improvements as shown in the Figure 4(b) for these signals.

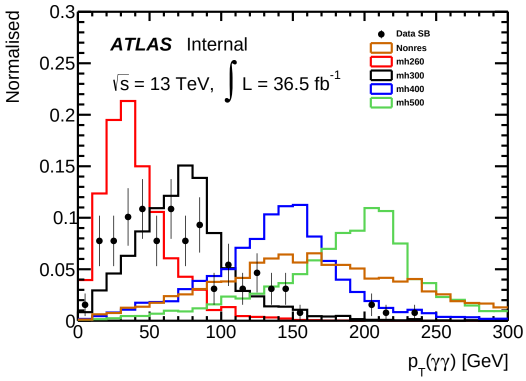

(a)

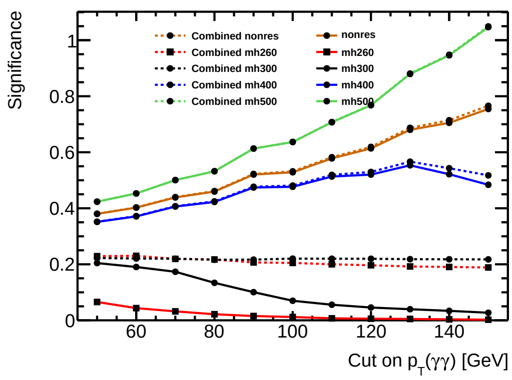

(b)

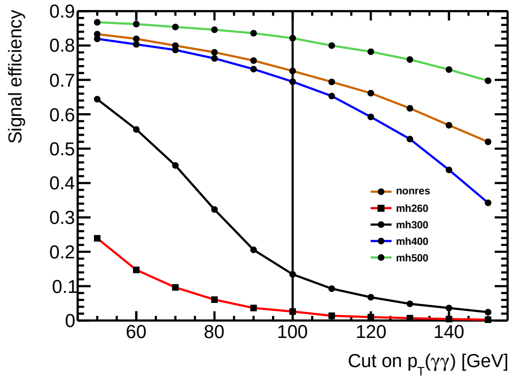

(c)

Figure 4: (a) The distribution of $p_T(\gamma\gamma)$, (b) the expected significance as a function of $p_T(\gamma\gamma)$ cut, (c) the signal efficiencies as a function of $p_T(\gamma\gamma)$ cut.

7 Signal and background estimations

Previously a number counting method was used given a limit statistics, while now a shape fit on $m_{\gamma\gamma}$ is performed to capture the features of signal events. The signal region is defined with all the cuts described in Section 5 for both non-resonant and resonant searches, while the background region (sideband region) is defined with the same selections but reversing the Tight mass window cut. A control region is defined by asking exactly no lepton and 2 jets inclusively to constrain the shape and the normalization of the continuum background. In the end, events in any of the above regions are used in the final fit of $m_{\gamma\gamma}$. The background estimation are exactly same for non-resonance and resonances with masses larger than 400 GeV (inclusive), and the same for all lower masses less than 400 GeV (exclusive), respectively, which differ only by a $p_T(\gamma\gamma)$ cut.

The detailed shape fit strategy is to perform the fit in the signal regions. The fit is performed to whole $m_{\gamma\gamma}$ spectrum ranging from 105 GeV to 160 GeV. The contributions from signal, SM single Higgs, SM di-Higgs and continuum background consist of the $m_{\gamma\gamma}$ shape in the whole range from 105 GeV to 160 GeV. The shape parameters for signals, SM single Higgs and SM di-Higgs are extracted from the MC and fixed in the final model. The shape parameters of continuum background and normalization are floating in the final model.

7.1 Model of signals, SM single Higgs and SM di-Higgs backgrounds

The $m_{\gamma\gamma}$ distribution is modelled by the fitting a double-sided Crystal Ball (DSCB) to the MC simulation with m_h = 125 GeV. The analytic form of this function is presented in Eq 2.

$$CB(m_{\gamma\gamma}) = N \times \begin{cases} e^{-t^2/2}, & \text{if } -\alpha_{\text{low}} \le t \le \alpha_{\text{high}} \\ e^{-\frac{1}{2}\alpha_{\text{low}}^2}\left[\frac{1}{R_{\text{low}}}(R_{\text{low}} - \alpha_{\text{low}} - t)\right]^{-n_{\text{low}}}, & \text{if } t < -\alpha_{\text{low}} \\ e^{-\frac{1}{2}\alpha_{\text{high}}^2}\left[\frac{1}{R_{\text{high}}}(R_{\text{high}} - \alpha_{\text{high}} - t)\right]^{-n_{\text{high}}}, & \text{if } t > \alpha_{\text{high}} \end{cases} \tag{2}$$

Where $t = (m_{\gamma\gamma - \mu_{CB}})/\sigma_{CB}$, $R_{low} = \alpha_{low}/n_{low}$, and $R_{high} = \alpha_{high}/n_{high}$. Here N is a normalization parameter, μ_{CB} is mean of the Gaussian distribution, σ_{CB} is the width of the Gaussian distribution, α_{low} and α_{high} are the positions of the transitions from Gaussian core to the exponential tails on the low and high mass sides, and the n_{low} and n_{high} are the exponents of the low and high mass tails. An example of this shape is shown in Figure 5.

Each of the shape parameters is determined by performing a fit to the simulated $H \to \gamma\gamma$ decays at $m_{\gamma\gamma}$ =125 GeV. The resulting μ_{CB} variables are shifted up by 0.09 GeV to simulate a Higgs boson of mass 125.09 GeV. The fits are shown in the App F.

7.2 Signal estimation

The contributions are estimated with MC for both non-resonant and resonant signals. The expected signal yields of non-resonance with the recommended cross section $\sigma(gg \to hh)$ [6] and the ones of resonance at each mass point with the assumption of $\sigma(gg \to H) \times BR(X \to hh) = 1pb$ are listed in Table 8.

Signal yields	non-resonance	260 GeV	300 GeV	400 GeV	500 GeV
At least one leptons	1.732	0.964	1.12	1.623	1.873
$p_T(\gamma\gamma) > 100$ GeV	1.357	-	-	1.233	1.631

Table 8: Event yields in one lepton region assuming the cross section $\sigma(gg \to hh)$ or $\sigma(gg \to H) \times BR(X \to hh)$ of 1 pb, with the integrated luminosity of 36.1 fb^{-1}.

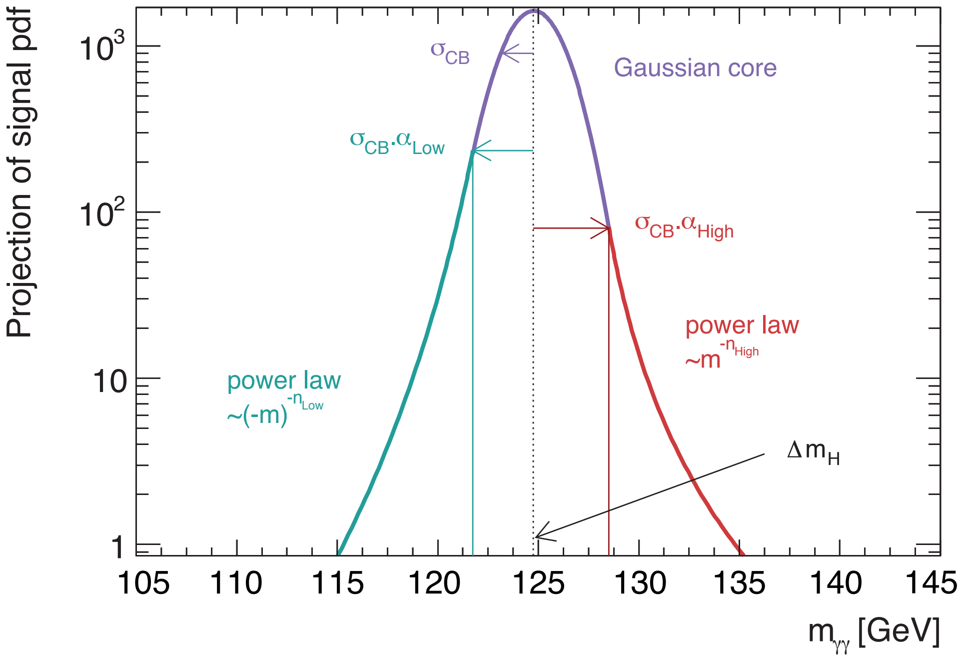

Figure 5: Example of a double-sided crystal ball function.

Important kinematic distributions are shown in Figures 6, 7 and 8 for comparisons among non-resonant, 260 GeV, 300 GeV, 400GeV, 500 GeV resonant signals and data sideband.

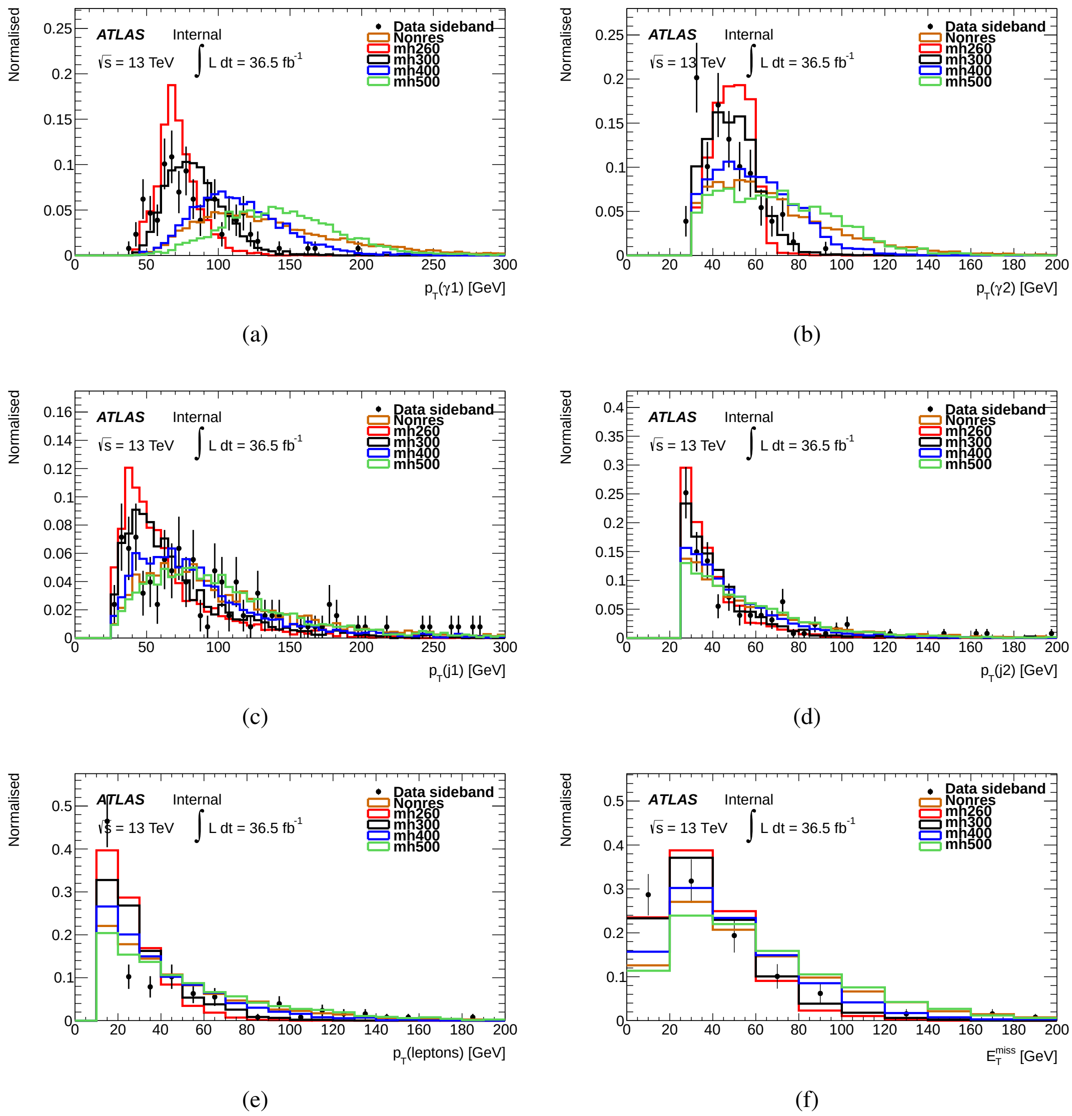

Figure 6: (a) p_T of leading photon, (b) p_T of sub-leading photon, (c) p_T of leading jet, (d) p_T of sub-leading jet, (e) p_T of leading lepton. (f) missing transverse energy. Events pass all selections defined in signal region.

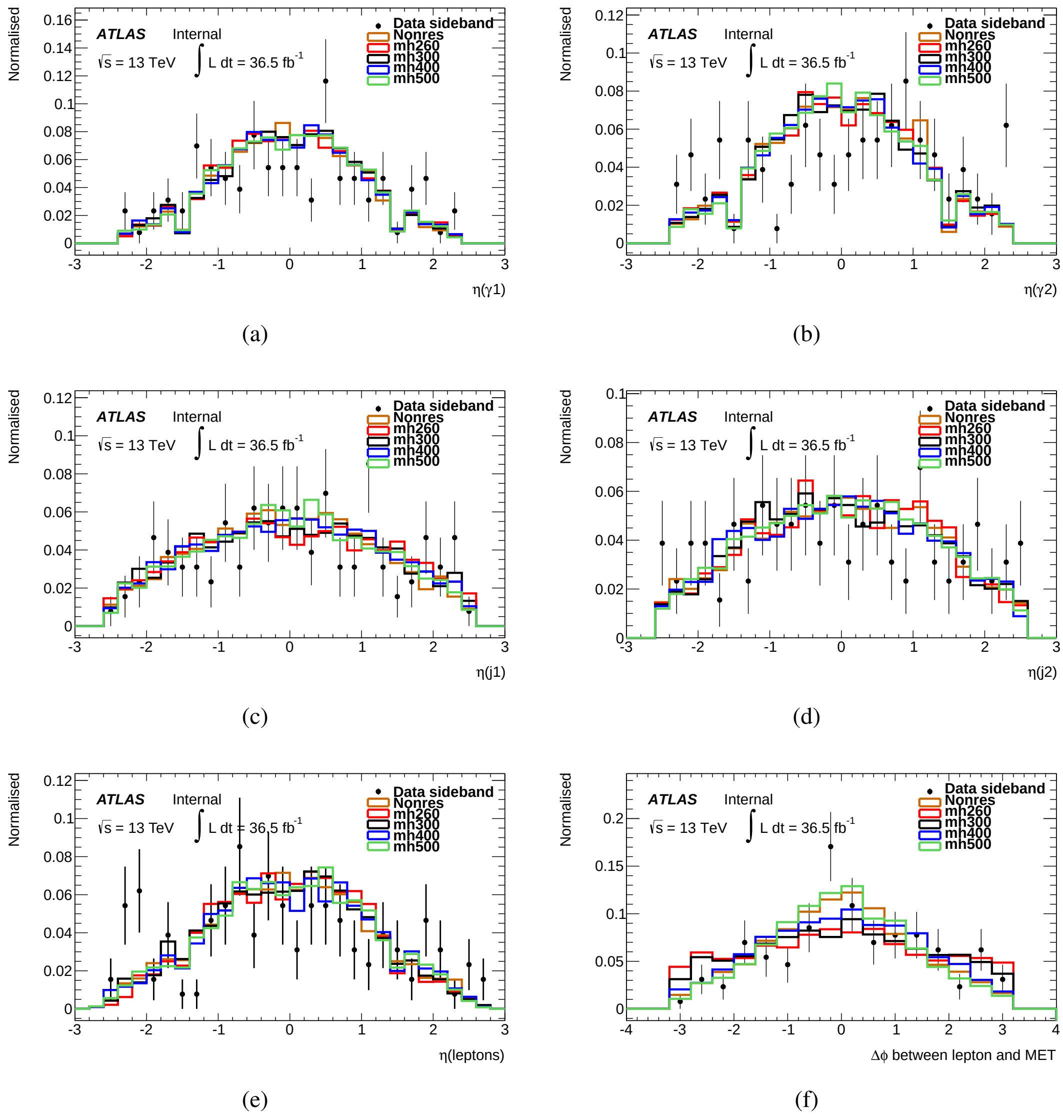

Figure 7: (a) η of leading photon, (b) η of sub-leading photon, (c) η of leading jet, (d) η of sub-leading jet, (e) η of leading lepton, (f) $\Delta\phi$ between leading lepton and MET. Events pass all selections defined in signal region.

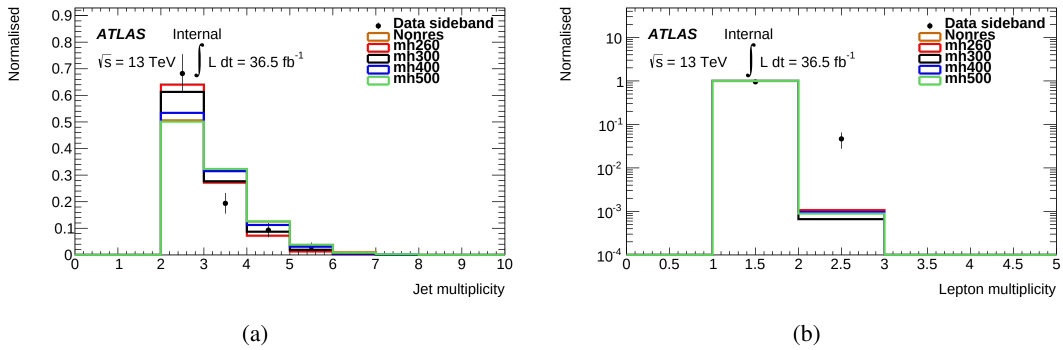

Figure 8: (a) jet multiplicity, (b) lepton multiplicity. Events pass all selections defined in signal region.

7.3 Single Higgs background estimation

Backgrounds with final states similar to signal are considered including SM single Higgs boson production and continuum photon background. SM single Higgs production is estimated using MC samples. The cut efficiencies and events yields are summarized in Table 9 and 10 The tth production contributes the most among all SM single Higgs productions due to its higher jet multiplicity in the central region and real leptons from top decays.

	ggh	VBF	Wh	Zh	tth
All Events	100.0%	100.0%	100.0%	100.0%	100.0%
Duplicate	100.0%	100.0%	100.0%	100.0%	100.0%
GRL	100.0%	100.0%	100.0%	100.0%	100.0%
Pass Trigger	59.6%	61.3%	56.5 %	56.0%	72.8%
Detector Quality	59.6%	61.3%	56.5 %	56.0%	72.8%
has PV	59.6%	61.3%	56.5 %	56.0%	72.8%
2 loose photons	49.8%	51.2%	44.5 %	45.2%	58.3%
Trig Match	49.7%	51.1%	44.4 %	45.1%	57.9%
Tight ID	43.4%	43.4%	38.2 %	38.9%	48.3%
Isolation	39.0%	40.2%	33.9 %	34.4%	40.0%
Rel.Pt cuts	36.1%	36.5%	31.0 %	31.4%	36.5%
$105 < m_{\gamma\gamma} < 160$ GeV	36.1%	36.4%	30.8 %	31.2%	36.0%
At least 2 central jets	5.51%	10.2%	14.9 %	15.8%	35.4%
B-veto	5.23%	9.65%	14.2 %	12.9%	6.18%
At least 1 lepton	0.00365%	0.0109%	0.533%	0.354%	1.89%
$pT_{\gamma\gamma} > 100$ GeV					

Table 9: Cut efficiencies for SM single Higgs processes.

Background yields	ggh	VBF	Wh	Zh	tth	SM Higgs Pair
At least one lepton	0.153	0.032	0.58	0.25	0.74	0.055
$p_T(\gamma\gamma) > 100$ GeV	0.079	0.018	0.31	0.12	0.44	0.045

Table 10: The yields for SM single Higgs and SM Higgs pair processes.

7.4 Continuum background estimation

The continuum background shape and normalization are determined simultaneously in the final fit to the invariant mass $m_{\gamma\gamma}$. The constrain power mainly comes from the sideband by reveising tight mass window as described above. Figure 9(a) shows the sideband in 1-lep region requiring at least one leptons. Figure 9(b) shows the sideband in 0-lep region requeing exactly zero lepton. Similarly, Figure 10 shows $m_{\gamma\gamma}$ after $p_T(\gamma\gamma)$ cut. 0-lep region was used to perform the continuum background estimation in the past. Now with more data, 1-lep region turns to have sufficient statistics and it is the only region used in the final fit in the current analysis. Nevertheless, 0-lep region is still studied and presented for determining and examining the background modeling function given a larger statistics.

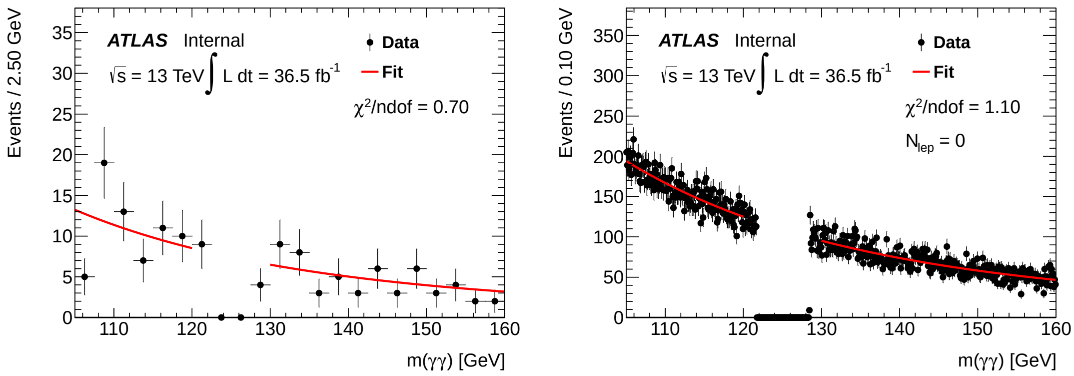

(a) (b)

Figure 9: Sideband $m_{\gamma\gamma}$ distribution with data (a) in signal-like sideband (number of leptons is larger than zero) and (b) in control region sideband (number of leptons is equal to zero) where a background fit is performed.

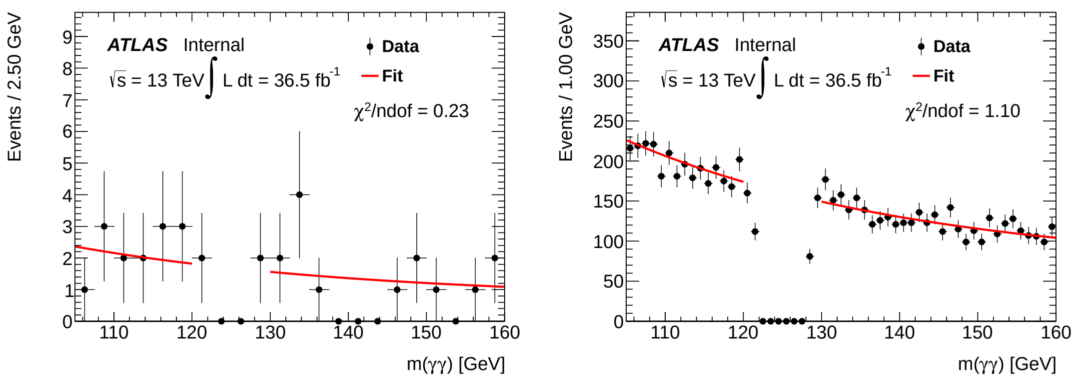

(a) (b)

Figure 10: Sideband $m_{\gamma\gamma}$ distribution with data (a) in signal-like sideband and (b) in control region sideband where a background fit is performed, after $p_T(\gamma\gamma)$ cut.

7.4.1 Function form

Different function forms are tested to choose the modeling of continuum background. Table 11 records the quality of fit. Figure 11 shows the fits in 0-lep region, Figure 12 in the same region with RevID on photons, Figure 13 with RevIso on photons. Here, RevID means at least one of the two leading photons fail the tight ID selection, and similarly, RevIso means at least one of the two leading photons fail the isolation criteria, as described in Section 4.1. The exponential function with a second-order polynomial is chosen given that it well accommodates all data in different background control regions.

Control regions	Nominal	RevID	RevIso
1^{st}-order polynomial	2.79	4.44	4.72
2^{nd}-order polynomial	1.10	1.15	1.02
Exp	1.19	1.29	0.99
ExpPoly2	1.10	1.09	0.95

Table 11: $\chi^2/ndof$ in different background control regions for various functions.

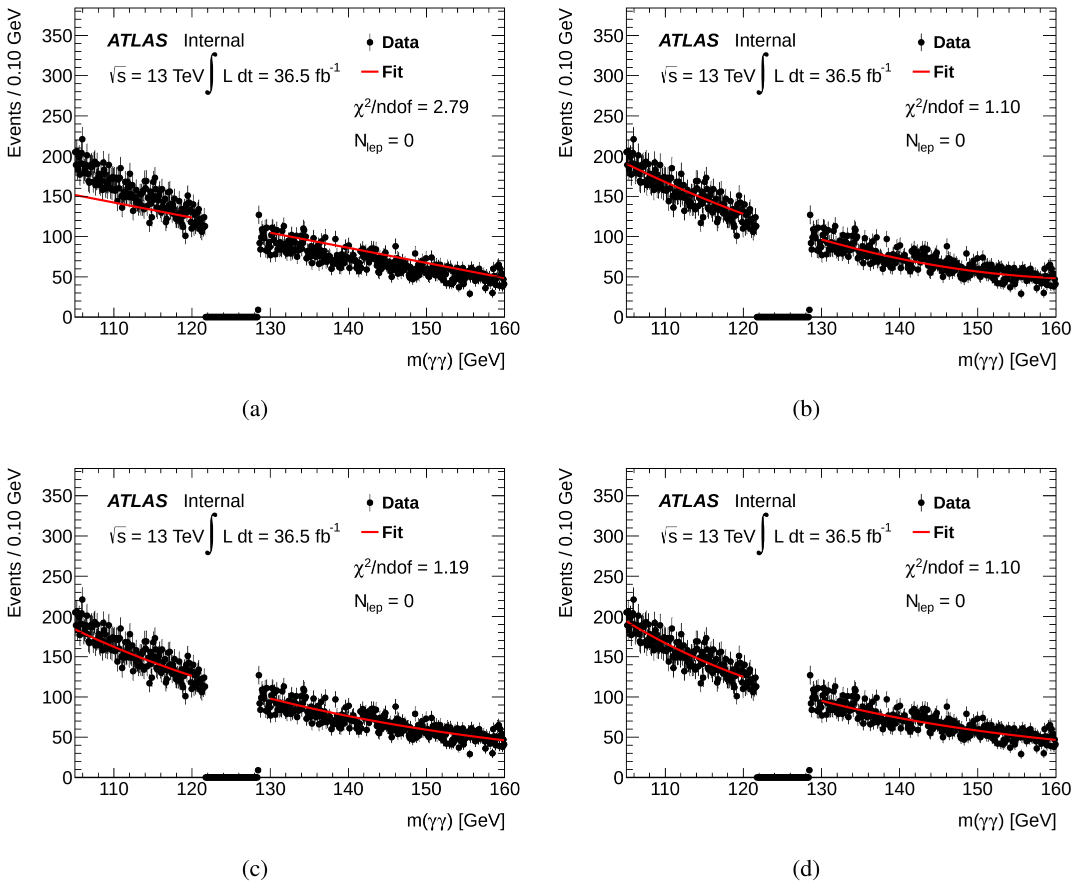

Figure 11: $m_{\gamma\gamma}$ Fits using different background modeling functions: (a) with a 1^{st}-order polynomial function; (b) with a 2^{nd}-order polynomial function; (c) with an exponential function; (d) with an exponential function carrying a 2^{nd}-order polynomial.

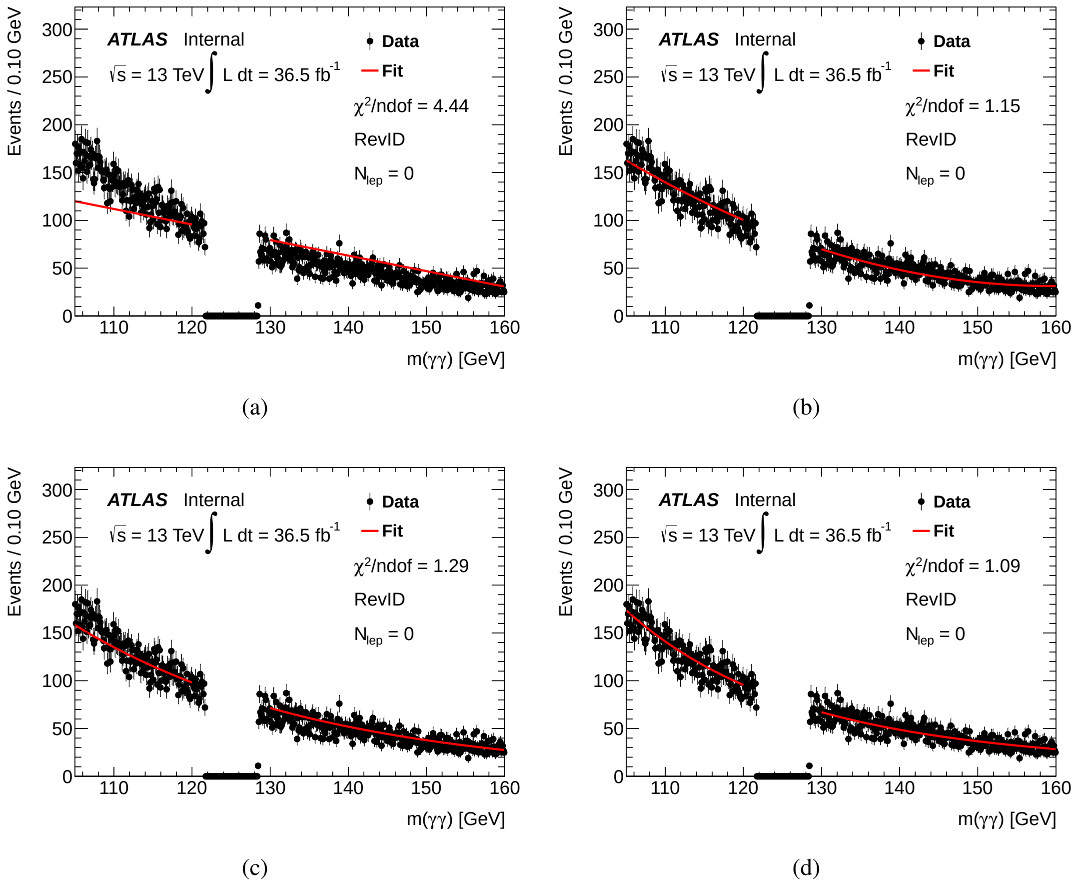

Figure 12: $m_{\gamma\gamma}$ Fits using different background modeling functions with RevID on photons: (a) with a 1^{st}-order polynomial function; (b) with a 2^{nd}-order polynomial function; (c) with an exponential function; (d) with an exponential function carrying a 2^{nd}-order polynomial.

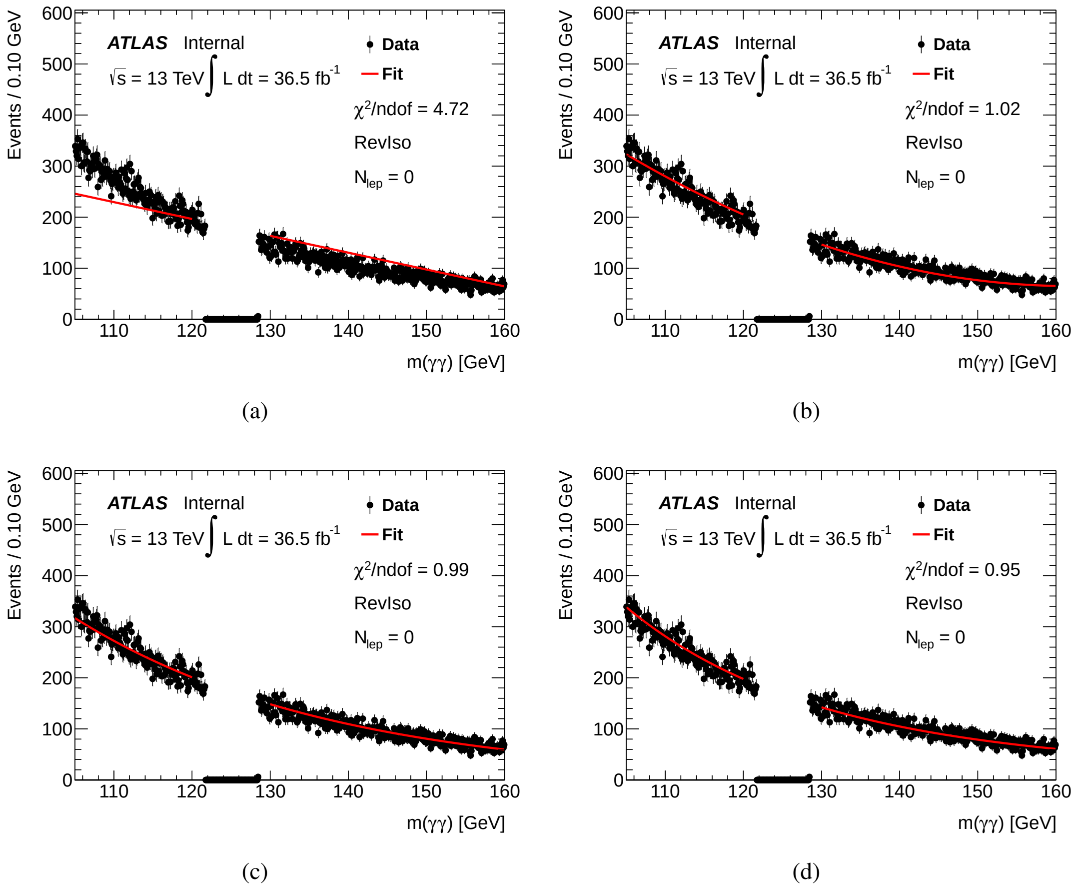

Figure 13: $m_{\gamma\gamma}$ Fits using different background modeling functions with RevIso on photons: (a) with a 1^{st}-order polynomial function; (b) with a 2^{nd}-order polynomial function; (c) with an exponential function; (d) with an exponential function carrying a 2^{nd}-order polynomial.

7.4.2 Lepton dependence

Benefiting from a larger statistics, 0-lep region is used to determine and examine the continuum background modeling for 1-lep region. A validation is performed to check the consistency of the shape in both regions. Basically, the exponential with 2^{nd}-order polynomial function is freely fit to the data sideband in 0-lep region. Applying the fitted parameters which are obtained from the fit in 0-lep region to 1-lep region, the quality of fit $\chi^2/ndof$ is calculated. Effectively, the shape obtained from 0-lep is tested by $\chi^2/ndof$ in 1-lep region.

Firstly, two MC samples are used to check the consistency as shown in Figure 14. They are SM processes of $l\nu jj\gamma\gamma$ and $jjj\gamma\gamma$. The two MC samples above only mimic real photon processes whose photon purity is extremely high. This is not necessarily true in real data and the lepton dependence might vary with photon purity. Thus additional tests with RevIso photons and RevID-RevIso photons are performed as these control regions have very low photon purity. The fits are shown in Figure 15. In general, a consistent shape between 0-lep and 1-lep is seen in various scenarios. The bais observed in the two plots will be covered by the spurious signal discussed in Sec 7.4.3. The detailed shape difference in 1-lep and 0-lep region is discussed in E.

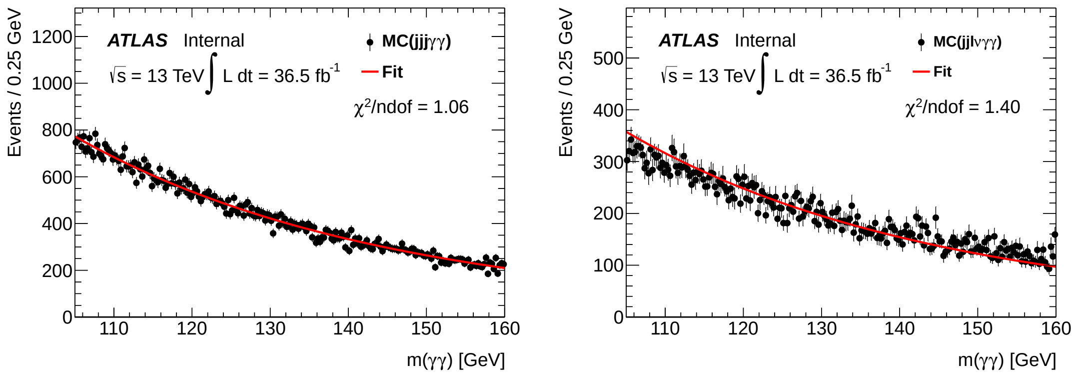

(a) (b)

Figure 14: Fits with sideband events to test lepton dependence (a) with $jjj\gamma\gamma$ MC sample and (b) with $l\nu jj\gamma\gamma$ MC sample.

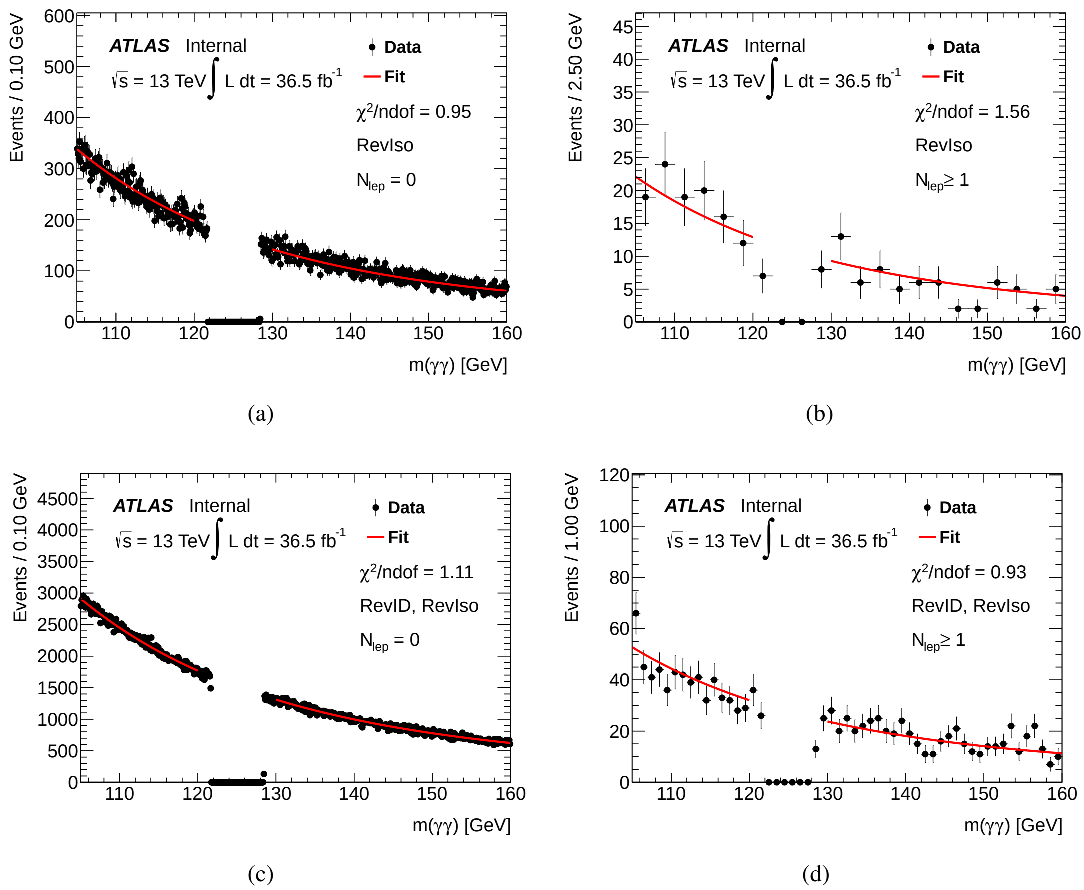

Figure 15: Fits with sideband events to test lepton dependence in reversed photon ID or isolation (a) with RevIso and zero lepton, (b) with RevIso and non-zero lepton. (c) with RevID-RevIso and zero lepton, (d) with RevID-RevIso and non-zero lepton;

Component	SR no $pT_{\gamma\gamma}$ cut	CR no $pT_{\gamma\gamma}$ cut	SR $pT_{\gamma\gamma} > 100GeV$	CR $pT_{\gamma\gamma} > 100GeV$
data	165	54762	39	8415
$\gamma\gamma$	146±15	46855±876	35.4±6.4	7829±120
$\gamma - jet$	6.25±5.08	4139±218	2.78±1.85	501±54
$jet - \gamma$	7.37±5.30	2971±129	1.00±1.00	449±42
jet-jet	5.65±2.72	780±43	0.22±0.25	46.6±9.5
purity	0.884±0.063	0.856±0.006	0.898±0.074	0.881±0.010

Table 12: The purity of diphoton in one lepton SR and zero lepton CR after different $pT_{\gamma\gamma}$ cut is shown.

7.4.3 Spurious signal

The bias for a given background parametrization is estimated by fitting background MC samples with a function combining this parametrization and signal model, and measuring the fitted number of signal events N_{ss} [28]. The fits are performed in the mass range of $m_h \in [110, 160]$ GeV, in which the mean of signal shape is shifted with a step of 0.5 GeV. The fitted bias is evaluated as the maximum value of $|N_{ss}|$ over the fit range from 120 GeV to 130 GeV. The simultaneous fit is performed to one lepton signal region and zero lepton control region and the function of ExpPoly2 is used. The irreducible background is modeled by large statistic $l\nu\gamma\gamma jj$ MC sample and the reducible background is modeled by reverse ID or reverse ISO sample from data. They are merged according to diphoton purity.

The diphoton purity is measured by 2x2D sideband method described in Ref [29]. The so-called "Matrix method" is utilized to measure the photon purity. According to whether the loose leading or subleading photon passes the tight ID requirement or isolation requirement, the events can be splitted into 16 regions. The predicted yield of each region can be calculated by the absolute yield of different component like $\gamma\gamma, \gamma - jet, jet - \gamma, jet - jet$,ID and Isolation efficiency, ID and Isolation fake rate. These parameter can be estimated by minimizing the χ^2. The result of purity measurement with 36.1 fb^{-1} 2015+2016 data is shown in Table 12.

The parametrization is kept if N_{ss} satisfies at least one of the following two criteria:

- $Max(N_{ss}/S_{ref}) < 10\%$
- $Max(N_{ss}/\Delta S) < 20\%$

Where S_{ref} is the expected number of the signal events passing the "At least one lepton", and ΔS is the statistical uncertainty on the spurious signal. "Max" means the largest ratio in $m_{\gamma\gamma}$ [120, 130] GeV. The S+B fit results of maximum fitted spurious signal are shown in Figure 18and 23. The yields are summarized in Table 18.

In conclusion, current 2nd-exponential can pass the spurious signal criteria mentioned above, even though a bias can be seen in low mass and high mass region in S+B fit plots. The spurious signal will be taken as the background modeling uncertainty and added in to the statistic model. More tests on other functions are discussed in

Since the uncertainty of purity is around 7% in one lepton signal region, the comparison of purity with one sigma up and down is shown in Figure 17. The difference is about 1% and only the nominal distribution is used for spurious signal in the following part. The spurious signal test for other function is discussed in Appendix E.

Function	Max(S)	Max(S/DeltaS)	Max(S/RefS)	Result
Exponential	0.81309	0.160835	1.57252	pass
ExpPoly2	-0.438693	-0.105086	-0.848438	pass
Poly1	-1.69689	-0.448545	-3.28181	fail
Poly2	-1.11274	-0.291617	-2.15205	fail

Table 13: The spurious signal test for $m_H = 260 GeV$. ExpPoly2 and Exponential function pass the criteria.

Function	Max(S)	Max(S/DeltaS)	Max(S/RefS)	Result
Exponential	0.826848	0.162524	1.45369	pass
ExpPoly2	-0.45901	-0.109038	-0.806992	pass
Poly1	-1.73049	-0.454291	-3.0424	fail
Poly2	-1.13824	-0.296309	-2.00116	fail

Table 14: The spurious signal test for $m_H = 300 GeV$. ExpPoly2 and Exponential function pass the criteria.

Function	Max(S)	Max(S/DeltaS)	Max(S/RefS)	Result
Exponential	0.24593	0.105271	0.318951	pass
ExpPoly2	-0.264615	-0.106127	-0.343184	pass
Poly1	-0.272567	-0.118275	-0.353496	pass
Poly2	-0.277345	-0.11856	-0.359693	pass

Table 15: The spurious signal test for $m_H = 400 GeV$. All the function pass the criteria.

Function	Max(S)	Max(S/DeltaS)	Max(S/RefS)	Result
Exponential	0.240416	0.10547	0.280103	pass
ExpPoly2	-0.259126	-0.107353	-0.301901	pass
Poly1	-0.269504	-0.120466	-0.313992	pass
Poly2	-0.253425	-0.11074	-0.295259	pass

Table 16: The spurious signal test for $m_H = 500 GeV$. All the functions pass the criteria.

Function	Max(S)	Max(S/DeltaS)	Max(S/RefS)	Result
Exponential	0.243031	0.105582	0.300664	pass
ExpPoly2	-0.260077	-0.106422	-0.321752	pass
Poly1	-0.274957	-0.121043	-0.340161	pass
Poly2	-0.261354	-0.113135	-0.323331	pass

Table 17: The spurious signal test for non-resonant. All the functions pass the criteria.

Mass	Max(N_{ss})	Max($N_{ss}/\Delta S$)	Max($_{ss}/S_{ref}$)
$m_H = 260 GeV$	0.845848	0.194842	1.6359
$m_H = 300 GeV$	0.826406	0.189248	1.45292
$m_H = 400 GeV$	-0.398046	-0.169399	-0.516232
$m_H = 500 GeV$	-0.395486	-0.172747	-0.460771
non-resonant	-0.402366	-0.174128	-0.497784

Table 18: The difference between low mass and high mass is due to $pT_{\gamma\gamma}$ cut.

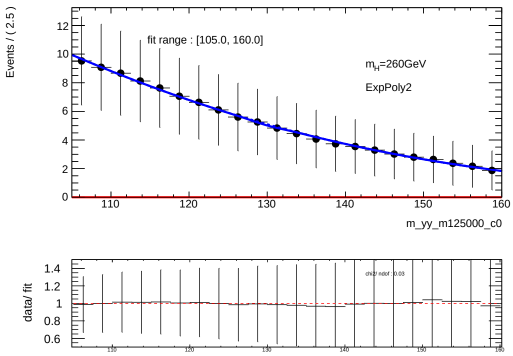

(a) S+B fit to 1-lep SR for $m_H = 260 GeV$

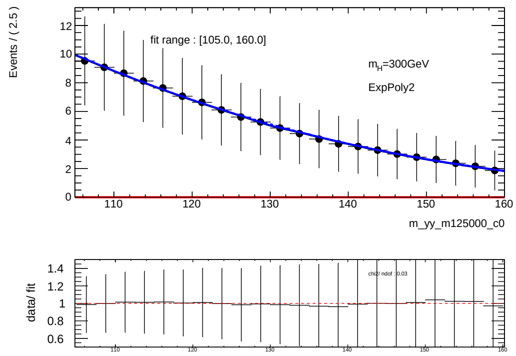

(b) S+B fit to 1-lep SR for $m_H = 300 GeV$

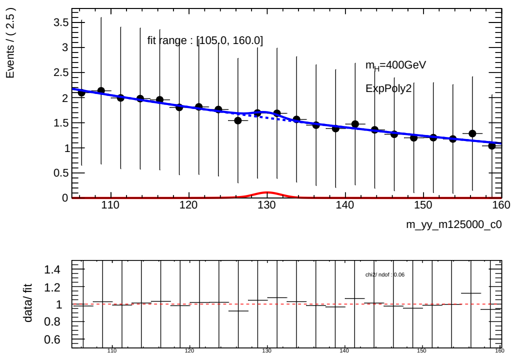

(c) S+B fit to 1-lep SR for $m_H = 400 GeV$

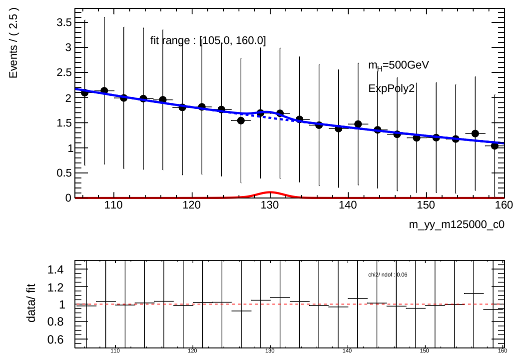

(d) S+B fit to 1-lep SR for $m_H = 500 GeV$

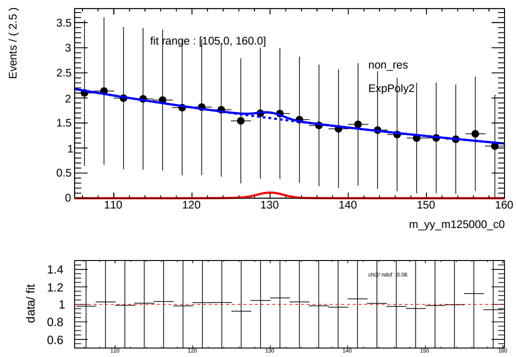

(e) S+B fit to 1-lep SR for non-resonant

Figure 16: S+B fit 1-lep SR for difference mass point.

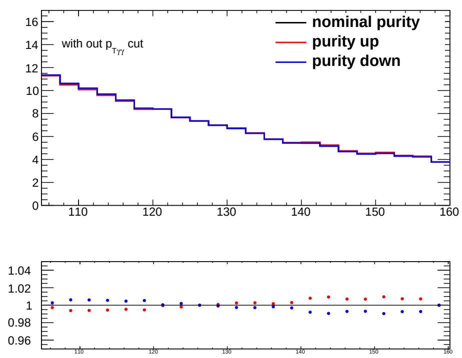

(a) without $p_T(\gamma\gamma)$ cut

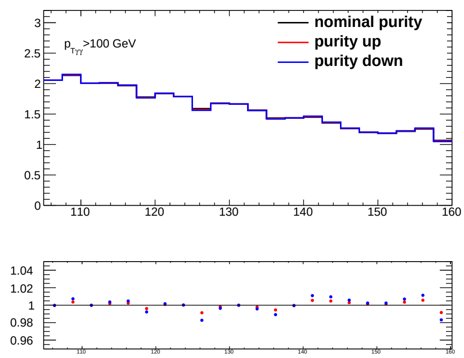

(b) $p_T(\gamma\gamma) > 100$ GeV

Figure 17: Left plot is for low mass search and right plot is for high mass search. In the ratio plot, the difference is 1%.

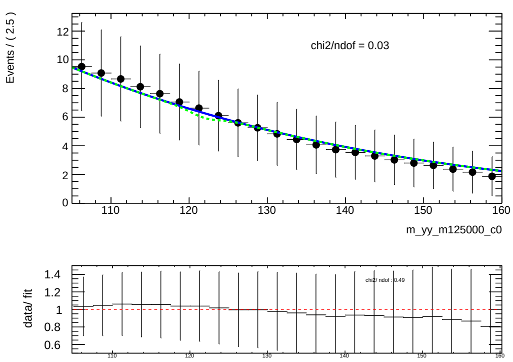

(a)

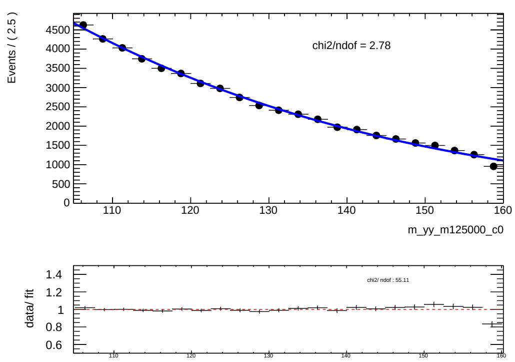

(b)

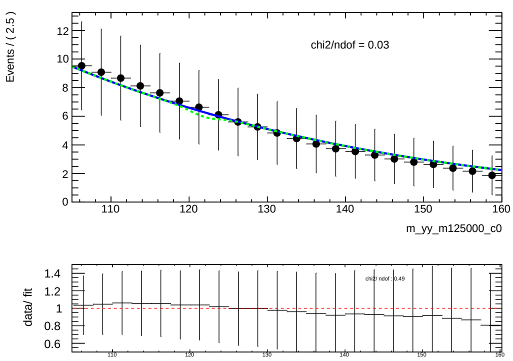

(c)

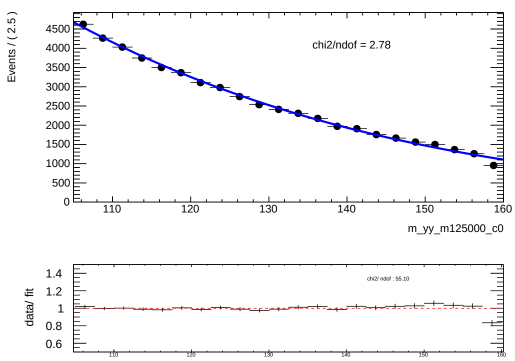

(d)

Figure 18: The S+B fit to background only dataset. Left is one lepton signal region, right is zero lepton control region. The shape is constrained by control region, which has higher statistic. The blue line is background-only function and the green is the fitted signal. (a)(b) for $m(H)$=260 GeV, (c)(d) for $m(H)$=300 GeV,

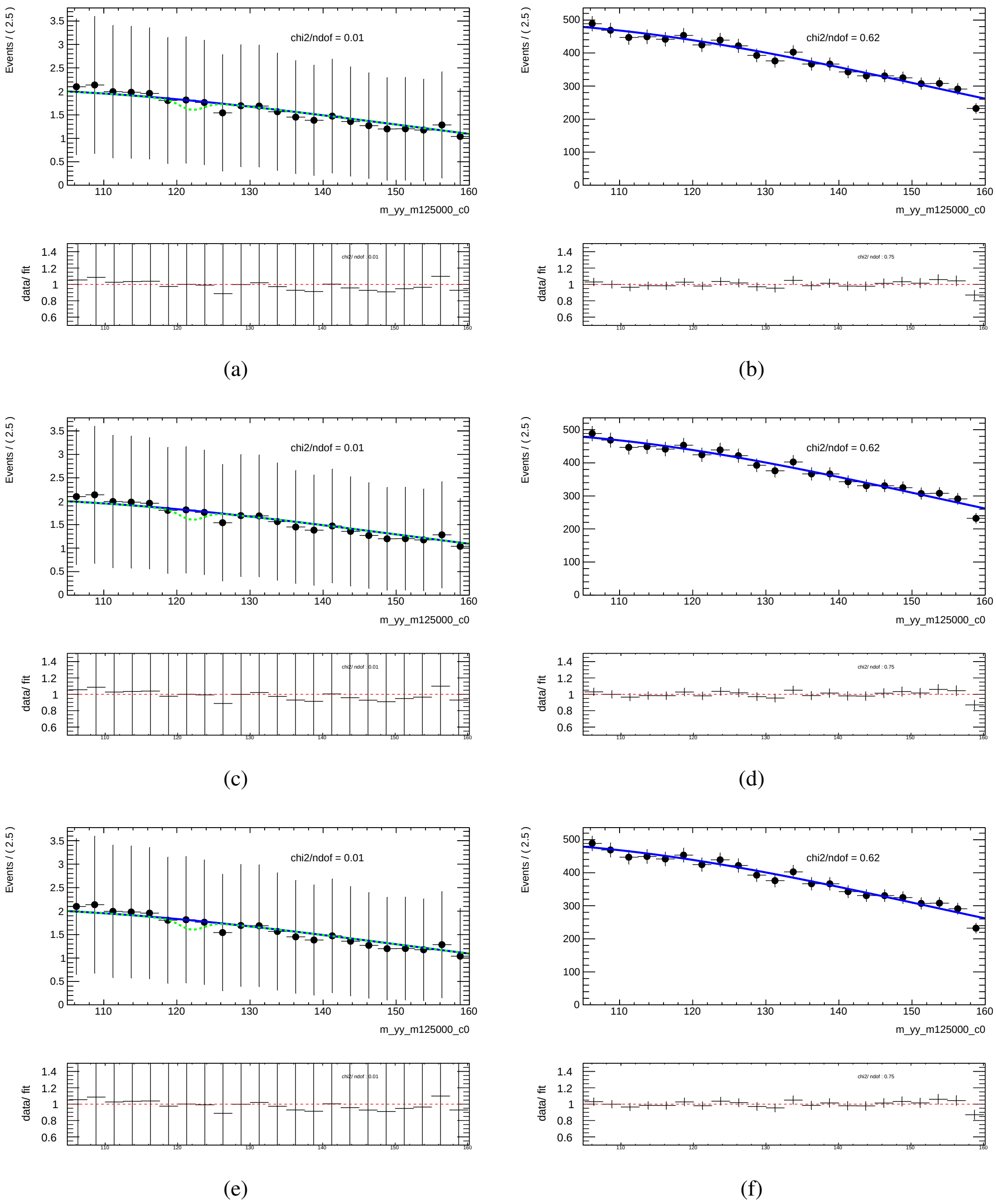

Figure 19: The S+B fit to background only dataset. Left is one lepton signal region, right is zero lepton control region. The shape is constrained by control region, which has higher statistic. The blue line is background-only function and the green is the fitted signal. (a)(b) for $m(H)$=400 GeV, (c)(d) for $m(H)$=500 GeV, (e)(f) for non-resonant

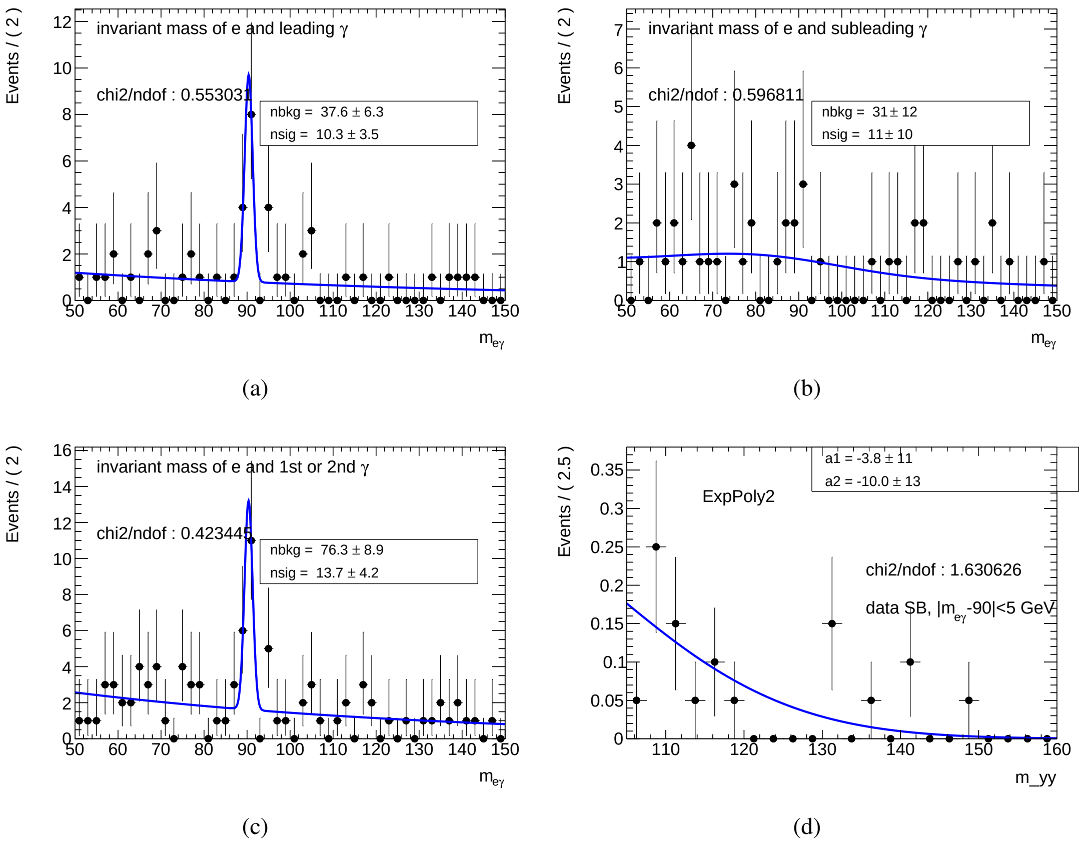

Figure 20: 20(a) : Invariant mass of electron and leading photon in data sideband. 20(b) : Invariant mass of electron and subleading photon. 20(c) The sum of previous two plots. 20(d) : A second order exponential fit to Z peak events in data sideband.

7.4.4 $Z\gamma$ background

The Z($\rightarrow ee$)γ events are also considered as background since one of the electron could be misidentified as a photon. The yield of $Z\gamma$ events could be estimated from $M_{e\gamma}$ spectrum in data sideband and the $m_{\gamma\gamma}$ shape could be obtained with events in Z peak. Figure 20 shows the $m_{e\gamma}$ distribution and the estimated yield is 13.7. Since the statistic is very low, the selection of at least 2 central jets is dropped to enlarge the statistic. Figure 22 shows the fit of $m_{\gamma\gamma}$ shape in Z peak. Since there is no Z peak in $M_{e\gamma}$ spectrum after $pT_{\gamma\gamma} > 100GeV$ in Figure 21, $Z\gamma$ component is only added to the search of $m_H = 260\ GeV$ and $m_H = 300\ GeV$. The $\gamma\gamma$, γ-jet and jet-jet are normalized to yields in data sideband after $Z\gamma$ subtraction. In this case, the sum of all the background components is corresponding to data sideband. This normalization is same as VH leptonic analysis in HGam group.

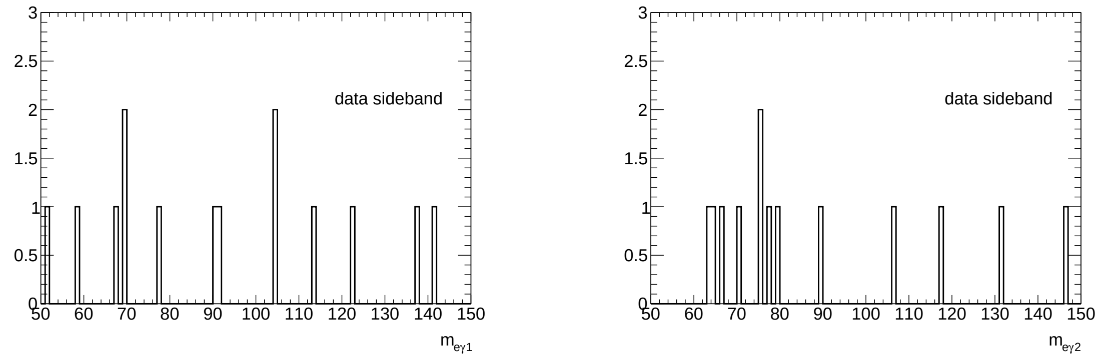

(a) (b)

Figure 21: These two plots show the invariant mass of electron and leading or subleading photon with $p_{T\gamma\gamma} > 100GeV$. No Z peak is observed.

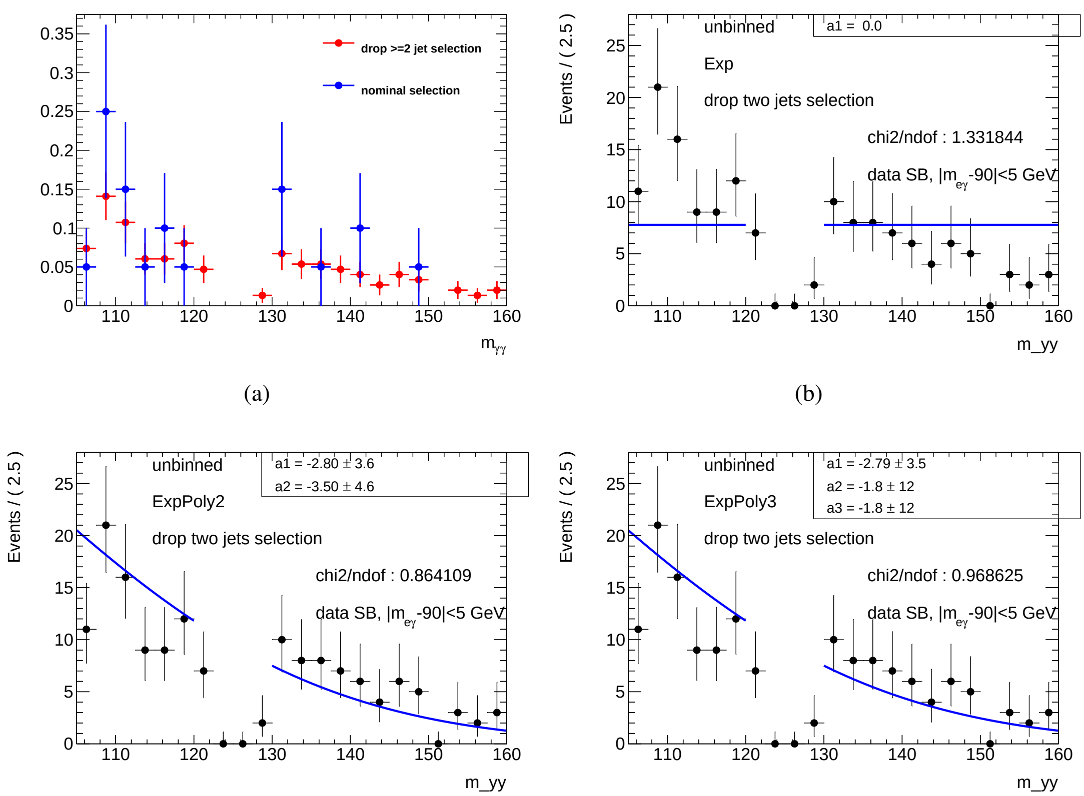

(a) (b)

(c) (d)

Figure 22: 22(a) shows the comparison before and after dropping 2 jets requirements to demonstrate this loose selection does not change the $m_{\gamma\gamma}$ shape. 22(b) 22(c) 22(d) show the exponential, 2nd exponential, 3rd exponential fit to $m_{\gamma\gamma}$ shape in Z peak.

8 Systematic uncertainties

8.1 Luminosity uncertainties

The uncertainty in the combined 2015+2016 integrated luminosity is 3.2%. It is derived, following a methodology similar to that detailed in Ref. [30], from a preliminary calibration of the luminosity scale using x-y beam-separation scans performed in August 2015 and May 2016.

8.2 Theoretical uncertainties

The LHCHXSWG recommended scale and PDF uncertainties on SM single Higgs processes are documented in Ref [31], and they are used in the analysis as presented in Table 19.

Processes	+QCD Scale %	-QCD Scale %	$\pm PDF$ %	$\pm\alpha_s$ %
ggh	+3.9	-3.9	± 1.9	± 2.6
VBF	+0.4	-0.3	± 2.1	± 0.5
Wh	+0.5	-0.7	± 1.7	± 0.9
Zh	+3.8	-3.0	± 1.3	± 0.9
tth	+5.8	-9.2	± 3.0	± 2.0

Table 19: SM single Higgs scale and PDF uncertainties.

The LHCHXSWG recommended scale and PDF uncertainties on SM Higgs pair production are used in the analysis as presented in Table 20.

$\sqrt{s}$	$\sigma^{NNLO}_{gg\to hh}$	Scale	$\pm PDF$ %	$\pm\alpha_s$ %	EFT
13 TeV	33.41 fb	+4.3% -6.0%	±2.1%	±2.3%	±5%

Table 20: SM Higgs pair process (ggF) scale and PDF uncertainties, taken from Ref [32], only applied to the non-resonant analysis

Additional uncertainty of +2.1%/-2.0% applies to the $h \to \gamma\gamma$ branching ratio, and +1.5%/-1.5% to the $h \to WW$ branching ratio according to recommendations from Ref [23], since the final upper limits is set on $\sigma(gg \to hh)$ and $\sigma(gg \to H) \times BR(X \to hh)$.

The Wh process is generated with Pythia8, which uses parton shower to model the additional jets. To take into account the uncertainties that is caused by parton-shower originated jets, we generate the $Wh+jj$ (jets from matrix element) process with MadGraph5 and compare the difference in 2-jet-inclusive bin. This result is in a 37.5% uncertainty for Wh process. Also, the Zh sample generated by MadGraph5 is produced to compare the difference in 2-jet-inclusive bin. 6.02% uncertainty is introduced for Zh process.

8.3 Experimental Uncertainties

The uncertainties from trigger efficiency, photon energy scale, lepton efficiency, jet energy scale/resolution and b-tagging efficiency are estimated following CP group recommendations (Moriond2017) and the rate variations are summarized in Table 21for signals and Tables 22, 23 for SM single Higgs backgrounds and SM Higgs pair process. In the tables, the numbers in each line are the quadratic sum of their respective individual components. In these tables, the uncertainty due to the photon identification efficiency is computed by varying the indendification efficiency scale factors, obtained from control samples of photons from radiative Z boson decays and from γ+jet evnets and of electrons from $Z \rightarrow ee$ by $\pm\sigma$. The photons isolation uncertainty is obtained as the sum of two contributions. For the track isolation, the corresponding effciency scale factors are varied by $\pm\sigma$. For the calorimeter isolation, the data-MC shifts are used to correct the simulation are truned off ($PH\_Iso\_DDonoff$). The extrapolation uncertainties in b-tagging include two components: one is from the extrapolation to high-p_T (p_T >300 GeV) jets and the other one is from extrapolating c-jets to τ-jets. The further breakdowns are documented in Appendix B.

Source of uncertainties		Non-resonance	260 GeV	300 GeV	400 GeV	500 GeV
Photon	identification	1.664	1.447	1.439	1.462	1.670
	isolation	0.765	0.748	0.745	0.751	0.728
Jet	energy resolution	0.146	1.494	0.229	1.009	0.198
	energy scale	4.017	9.849	7.242	4.589	3.370
b-tagging	b-jets	0.058	0.089	0.057	0.082	0.056
	c-jets	1.541	1.047	1.194	1.366	1.523
	light jets	0.293	0.310	0.300	0.293	0.291
	extrapolation	0.018	0.001	0.001	0.004	0.010
Lepton	electron	0.530	0.708	0.626	0.545	0.482
	muon	0.459	0.707	0.623	0.578	0.406
Pileup re-weighting		0.494	0.714	0.670	0.058	1.392

Table 21: Summary of systematic uncertainties propagated to the yields, in percent, for signals in one lepton region.

Source of uncertainties		ggh	VBF	Wh	Zh	tth	SM Higgs pair
Photon	identification	1.563	1.434	1.690	1.707	1.707	1.664
	isolation	0.786	3.439	0.837	0.821	0.800	0.765
Jet	energy resolution	6.199	1.563	5.958	1.976	0.149	0.146
	energy scale	3.527	2.690	7.425	6.131	2.115	4.017
b-tagging	b-jets	0.553	0.110	0.096	0.273	8.622	0.058
	c-jets	0.487	1.663	0.595	0.630	1.605	1.541
	light jets	0.287	0.265	0.288	0.260	0.270	0.293
	extrapolation	0	0.076	0.021	0.095	0.436	0.018
Lepton	electron	0.638	0.668	0.511	0.470	0.510	0.530
	muon	4.067	0.424	0.809	0.465	0.408	0.459
Pileup re-weighting		10.834	2.832	0.849	0.476	1.177	0.494

Table 22: Summary of systematic uncertainties propagated to the yields, in percent, for SM single Higgs and SM Higgs pair processes in one lepton region with $p_T(\gamma\gamma)$ cut applied. The ggH sample has large pileup reweighting uncertainty here. It quite depends on the selection and https://cds.cern.ch/record/2137502/files/ATL-COM-PHYS-2016-222.pdf has similar results in certain categories.

The uncertainty from egamma calibration including energy scale and resolution can have impact on signal $m_{\gamma\gamma}$ shape, particularly on the parameters of μ (mean) and σ (width) of the Gaussian core. The

Source of uncertainties		ggh	VBF	Wh	Zh	tth	SM Higgs pair
Photon	identification	1.564	1.451	1.621	1.589	1.612	1.625
	isolation	0.745	2.005	0.830	0.812	0.796	0.768
Jet	energy resolution	7.446	3.299	5.205	3.861	1.941	0.232
	energy scale	13.020	3.691	9.704	8.541	1.621	4.275
b-tagging	b-jets	0.953	0.434	0.092	0.445	8.700	0.056
	c-jets	0.375	1.204	0.572	0.639	1.568	1.503
	light jets	0.306	0.278	0.288	0.269	0.264	0.294
	extrapolation	0	0.042	0.012	0.080	0.284	0.015
Lepton	electron	0.428	0.477	0.462	0.448	0.488	0.538
	muon	5.411	1.692	0.617	0.425	0.414	0.526
Pileup re-weighting		2.845	2.760	0.523	1.641	1.386	0.554

Table 23: Summary of systematic uncertainties propagated to the yields, in percent, for SM single Higgs and SM Higgs pair processes in one lepton region without $p_T(\gamma\gamma)$ cut applied.

457 variation are calculated and shown in Tables 24, 25, 26 and 27.

	Non-resonane	260 GeV	300 GeV	400 GeV	500 GeV
Variation on μ in 1 lepton region	+0.503%	+0.415%	+0.434%	+0.474%	+0.510%
	-0.500%	-0.414%	-0.444%	-0.477%	-0.502%

Table 24: The variation on μ due to the uncertainty of energy scale in egamma calibration for signals.

	Non-resonane	260 GeV	300 GeV	400 GeV	500 GeV
Variation on σ in 1 lepton region	+8.24%	+4.58%	+5.76%	+7.92%	+8.95%
	-7.22%	-5.78%	-6.07%	-8.02%	-7.32%

Table 25: The variation on σ due to the uncertainty of energy resolution in egamma calibration for signals.

	SM single Higgs	SM di-Higgs
Variation on μ in 1 lepton region with $p_T(\gamma\gamma)$ cut applied	+0.541%	+0.503%
	-0.557%	-0.500%
Variation on μ in 1 lepton region without $p_T(\gamma\gamma)$ cut applied	+0.509%	+0.491%
	-0.512%	-0.496%

Table 26: The variation on μ due to the uncertainty of energy scale in egamma calibration for SM backgrounds.

	SM single Higgs	SM di-Higgs
Variation on σ in 1 lepton region with $p_T(\gamma\gamma)$ cut applied	+11.6% -11.1%	+8.24% -7.22%
Variation on σ in 1 lepton region without $p_T(\gamma\gamma)$ cut applied	+11.7% -6.9 %	+8.12% -6.23%

Table 27: The variation on σ due to the uncertainty of energy resolution in egamma calibration for SM backgrounds.

8.4 Uncertainty on continuum background estimation

The uncertainty on the continuum background modeling depends how much the background function can fake signal from background only fits, i.e. the so-called spurious signal. The spurious signals are calculated by performing a signal plus background fit on the background only sample as descriibed in Section 7.4.3. The results are shown in the Table 18. The relevent spurious signal numbers are taken into account as the uncertainty by adding in the statistical model a spurious signal component that shares a same shape as our signal.

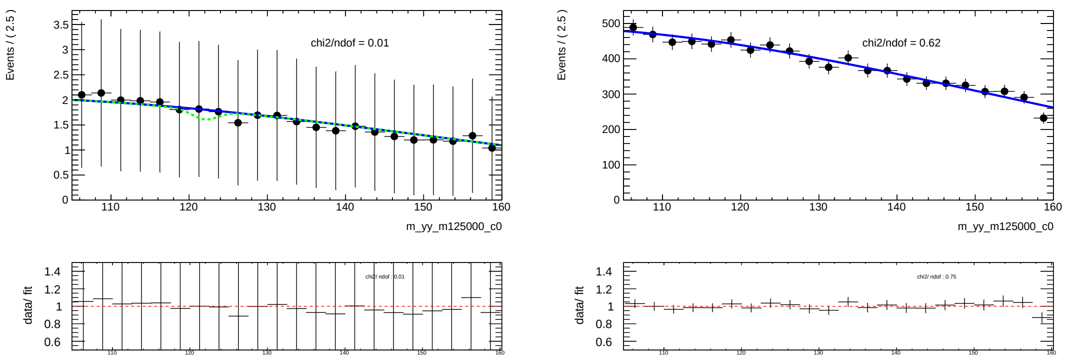

(a) (b)

Figure 23: The fitted number of spurious signal. Left is one lepton signal region, right is zero lepton control region. The shape is constrained by control region, which has higher statistic. The blue line is background-only function and the green is the fitted signal. (a)(b) for $m(H)$=400 GeV, (c)(d) for $m(H)$=500 GeV, (e)(f) for non-resonant

Expected	Non-res	mh260	mh300	mh400	mh500
Case1	7.78	13.5	11.6	8.42	7.09
Case2	6.74	12.2	10.4	7.35	6.42
Case3	6.77	12.2	10.4	7.39	6.44
Case4	6.38	11.6	9.88	6.94	6.09
Case5	6.69	12.2	10.4	7.3	6.42

Table 28: Expected upper limit with different fit strategies. Full systematic is applied in all cases. Case 1: counting; Case 2: fit to the 1Lep region with parameters c1 and c2 fixed in ExpPoly2. The fixed value is from 1-lep signal region; Case 3: fit to the 1Lep region with floating parameters c1 and c2; Case 4: fit to the 1Lep and 0Lep regions with nConBkg (continuum BKG in 1Lep) constrained with nConBkgCR (continuum BKG in 0Lep), nConBkg = Transfer factor * nCongBkgCR; Case 5: fit to the 1Lep and 0Lep regions with floating nConBkg and nConBkgCR.

9 Statistical interpretation

9.1 Statistical model

The statistical model is built up with an unbinned likelihood function. The model is constructed in the following form.

$$\mathcal{L}(\mu,\theta) = \begin{array}{l} \prod_i (n_{BSM}(\mu,\theta) \times f_{DSCB}(m^i_{\gamma\gamma},\theta) + n_{SM}(\theta) \times f_{DSCB}(m^i_{\gamma\gamma},\theta) \\ + n_{Cont} \times f_{Cont}(m^i_{\gamma\gamma},\theta) + n_{ss} \times f_{DSCB}(m^i_{\gamma\gamma},\theta)) \prod Norm(\theta|0,1) \end{array} \tag{3}$$

where i stands for the event index, n_{BSM} the number of expected signal events, n_{SM} the number of expected single Higgs events, n_{Cont} the number of expected continuum background events, f_{DSCB} the pdf of a double-sided crystal ball function shared by both BSM signal and SM Higgs, f_{Cont} the pdf of the continuum background i.e. the second order exponential, n_{ss} the expected spurious signal yield, μ the cross section (time the branching ratio of $X \to hh$) of non-resonant (resonant) production, and $Norm$ the probability density function of a Gaussian distribution used for constraining the nuisance parameters. The systematic uncertainties are introduced by a set of nuisance parameters θ which can vary the acceptance of signal and single Higgs processes as well as the function parameters of either f_{DSCB} or f_{Cont}.

Possible fit strategies are studied and compared. The expected upper limit is used to choose the best strategy as presented in Table 28. From case3 to case5, compared with direct fit to 1-lep signal region, the shape difference in simultaneous fit does not affect the limit very much. From case5 to case4, the constrain on normalization factor improves the limit by about 5%, which is very limited. In conclusion, case3 is chosen given its simplicity and no obvious improvement from adding 0-lep region.

9.2 Model inspection

To test the S+B fit performance, a signal injection is performed. Table 29 shows the fiitted signal strength and upper limit of signal injection.

To inspect the statistical model and the behaviour of nuisance parameters, checks on the pull of nuisance parameters $(\theta_{fit} - \theta_0)/\Delta\theta$ are performed with an unconditional fit to the amount of expected backgrounds, as shown in Figures 24, 25, 26, 27 and 28. The values of the pull of nuisance parameteres are always close to 0, which suggests a correct implementation of the staistical model. Similar checkes are done with the observed data in order to check the data constraints on nuisance parameters, as shown in Figures 29, 30,31, 32 and 33.

Then, checks on the correlation between all parameters in the statistical model are performed, as shown in Figure 34, 35, 36, 37 and 38, with an unconditional fit to the amount of expected backgrounds,

	Bands	Non-res	mh260	mh300	mh400	mh500
$\mu = 0$	Median	5.3401	13.352	11.3597	5.97878	4.38764
	Observed	5.34409	13.3682	11.3681	5.98912	4.39495
	$\hat{\mu}$	-0.00396	0.077449	0.0447662	0.0269317	0.0179568
$\mu = 2$	Median	5.42712	13.4182	11.426	6.06536	4.47178
	Observed	7.40385	15.113	13.1348	8.01421	6.47877
	$\hat{\mu}$	2.00019	2.08285	2.05854	2.00257	1.9984

Table 29: The number is the 95% CL upper limit on $\sigma(pp \to H \to hh)$ for resonance or on the $\sigma(pp \to hh)$ for non-resonance. The number after signal injction. $\hat{\mu}$ is the best fited value for certain signal injection.

and in Figure 42, 43, 44, 45 and 46, with an unconditional fit to observed data. Additionally, the reduced correlation matrix for all the signal mass points are shown in the Figures 39, 40 and 41. Also, the Figures 47, 49, 51, 53 and 55 show the ranking of the nuisance parameters.

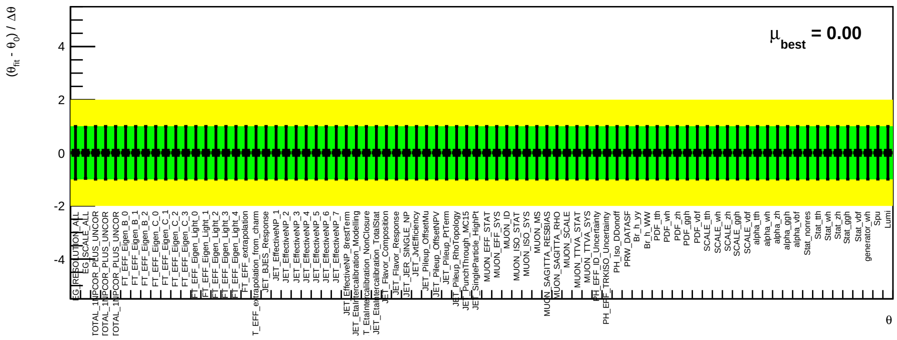

Figure 24: Nuisance parameter pull checks for non-resonance with a fit to expected backgrounds only.

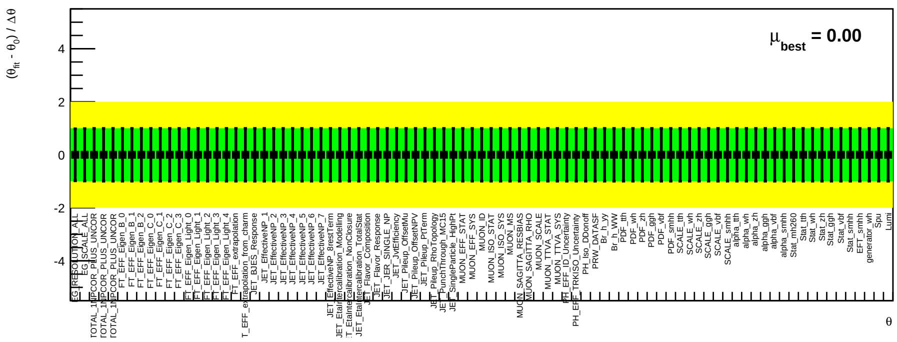

Figure 25: Nuisance parameter pull checks for resonance m_H = 260 GeV with a fit to expected backgrounds only.

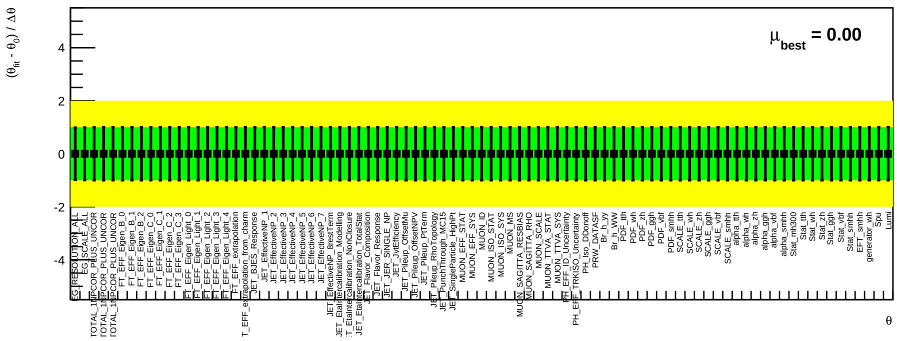

Figure 26: Nuisance parameter pull checks for resonance m_H = 300 GeV with a fit to expected backgrounds only.

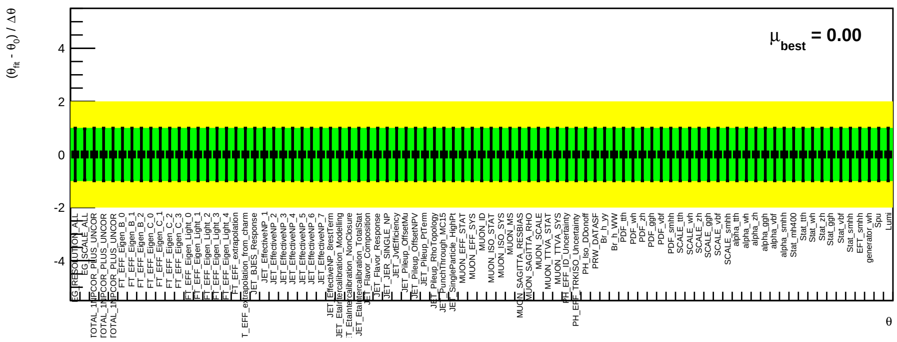

Figure 27: Nuisance parameter pull checks for resonance m_H = 400 GeV with a fit to expected backgrounds only.

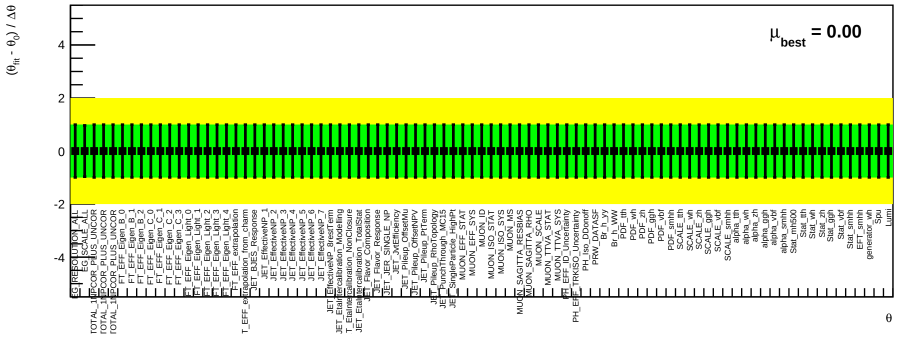

Figure 28: Nuisance parameter pull checks for resonance $m_H = 500$ GeV with a fit to expected backgrounds only.

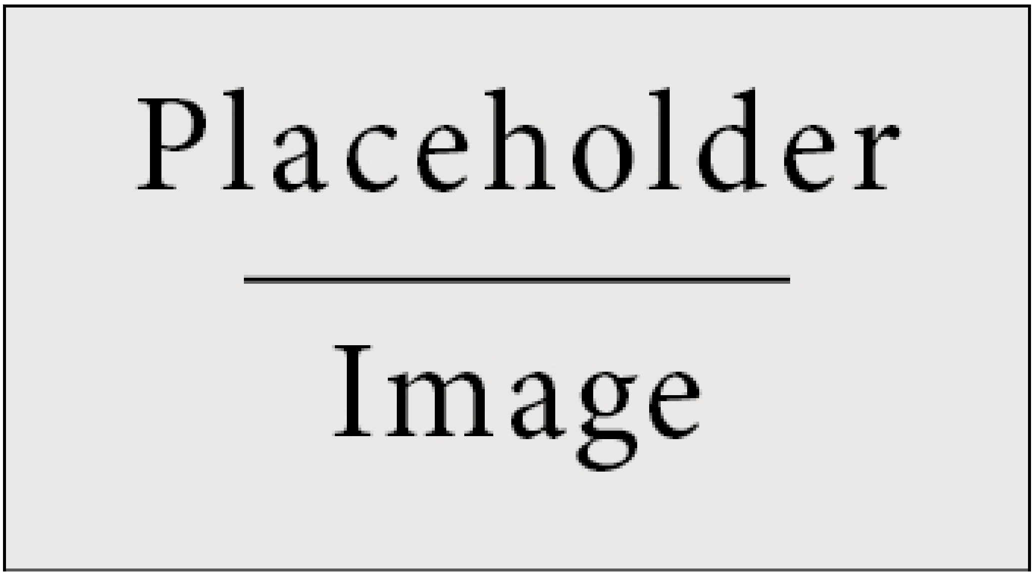

Figure 29: Nuisance parameter pull checks for non-resonance with a fit to observed data.

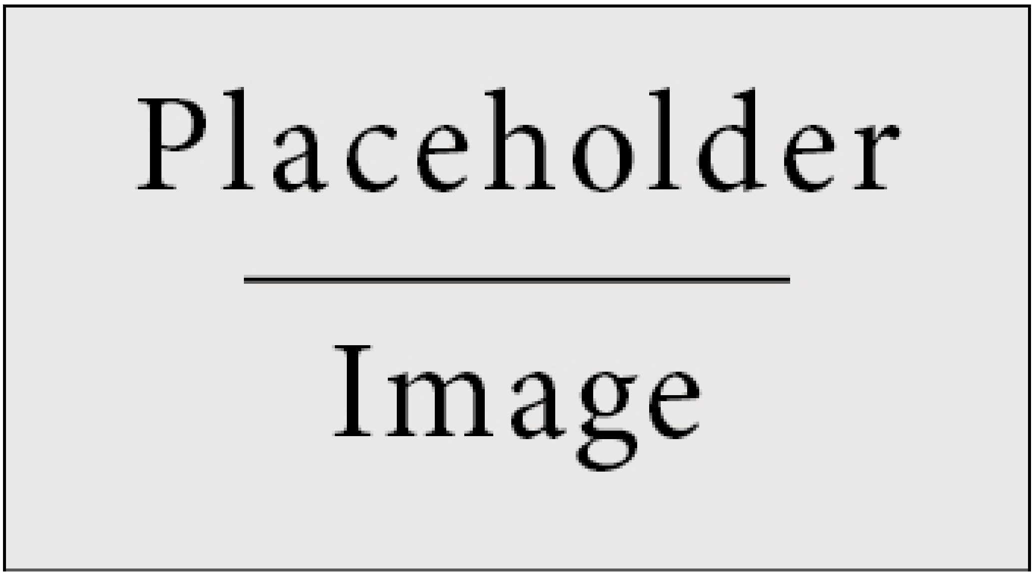

Figure 30: Nuisance parameter pull checks for resonance $m_H = 260$ GeV with a fit to observed data.

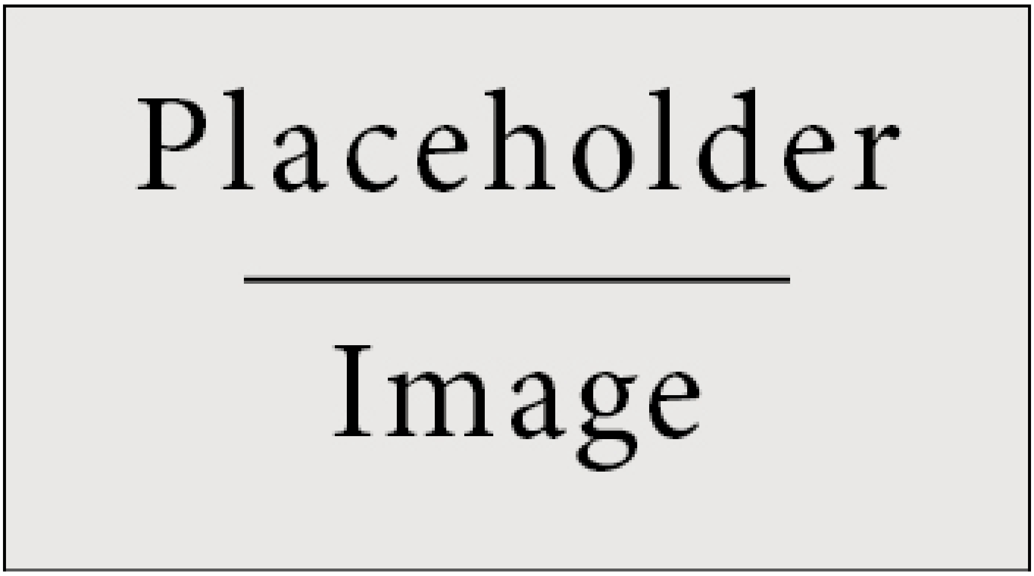

Figure 31: Nuisance parameter pull checks for resonance $m_H = 300$ GeV with a fit to observed data.

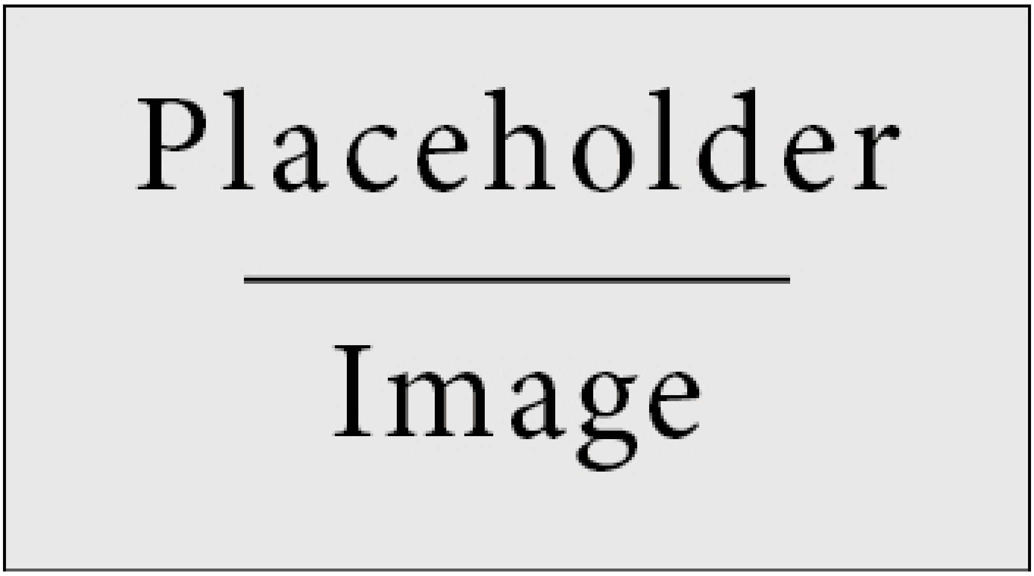

Figure 32: Nuisance parameter pull checks for resonance m_H = 400 GeV with a fit to observed data.

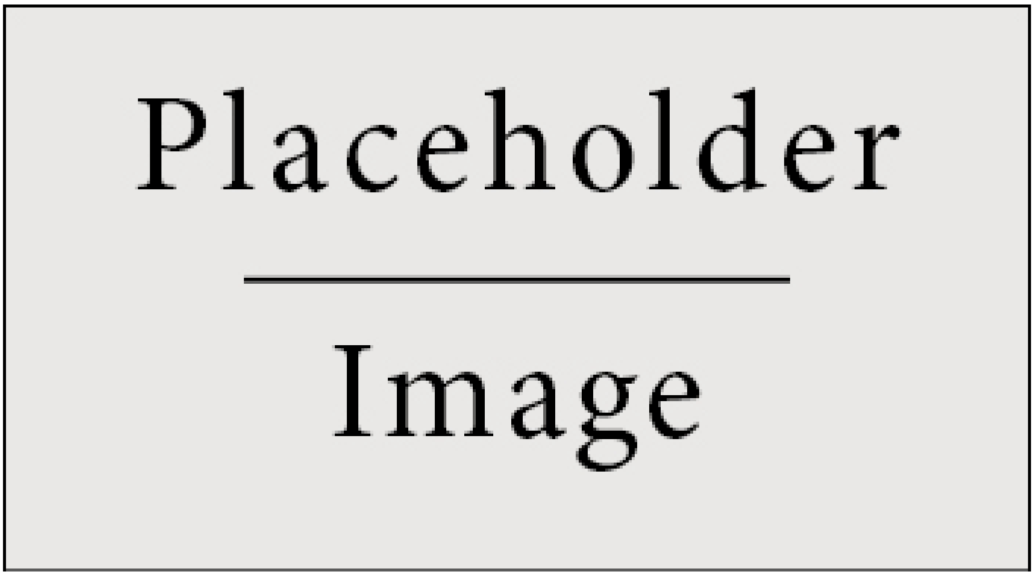

Figure 33: Nuisance parameter pull checks for resonance m_H = 500 GeV with a fit to observed data.

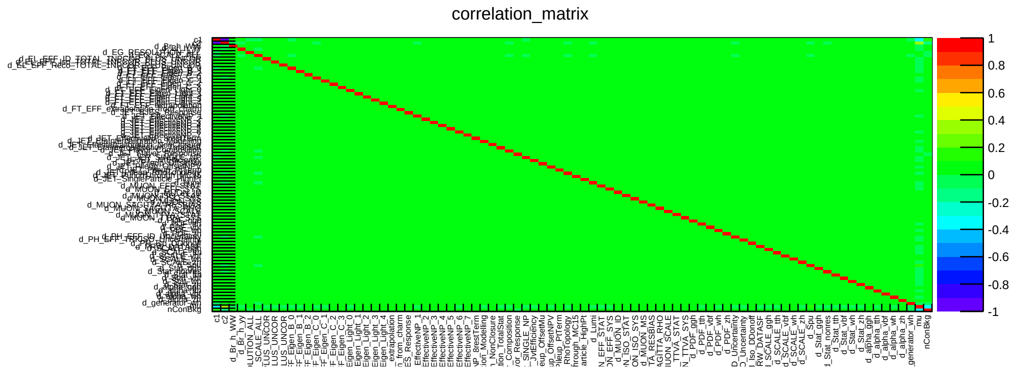

Figure 34: Correlation matrix for nuisance parameters for non-resonance with a fit to expected backgrounds only.

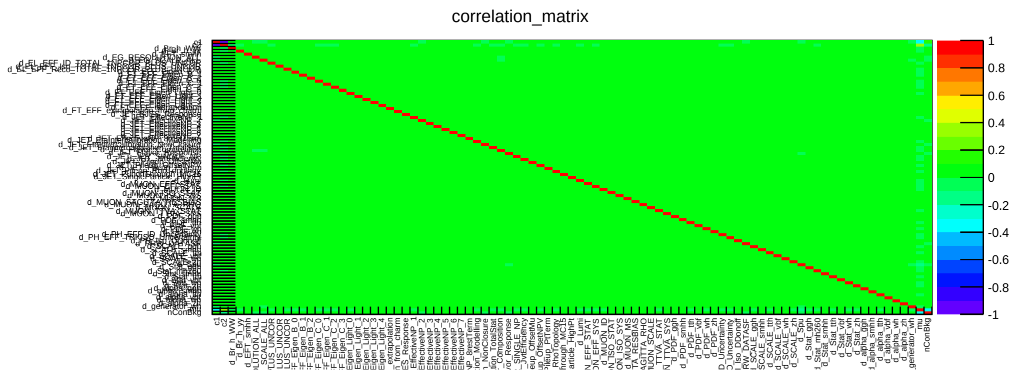

Figure 35: Correlation matrix for nuisance parameters for resonance $m_H = 260$ GeV with a fit to expected backgrounds only.

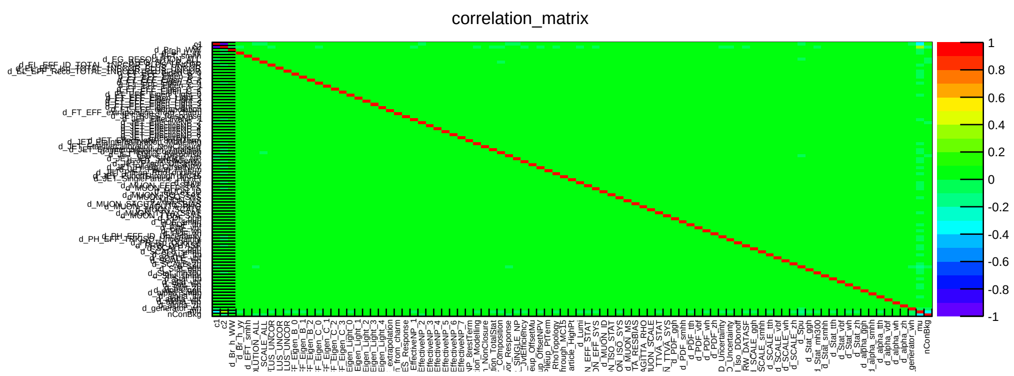

Figure 36: Correlation matrix for nuisance parameters for resonance $m_H = 300$ GeV with a fit to expected backgrounds only.

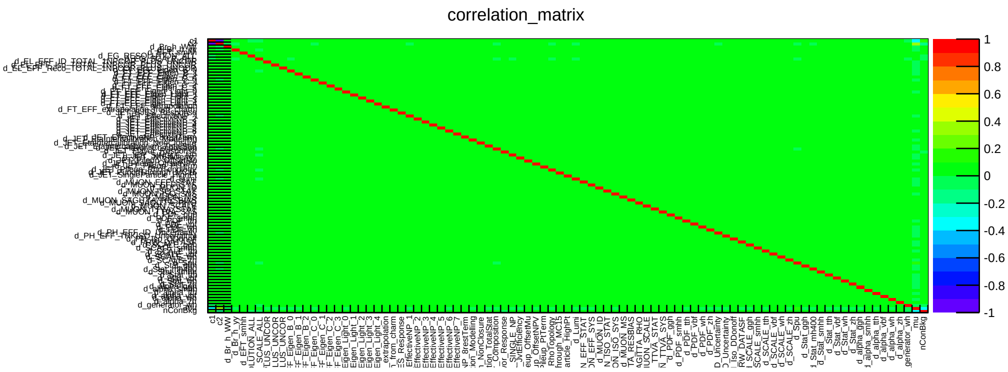

Figure 37: Correlation matrix for nuisance parameters for resonance $m_H = 400$ GeV with a fit to expected backgrounds only.

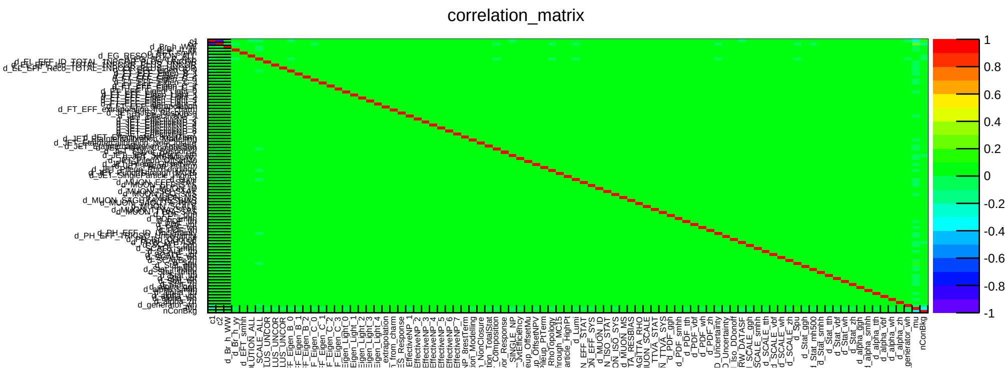

Figure 38: Correlation matrix for nuisance parameters for resonance $m_H = 500$ GeV with a fit to expected backgrounds only.

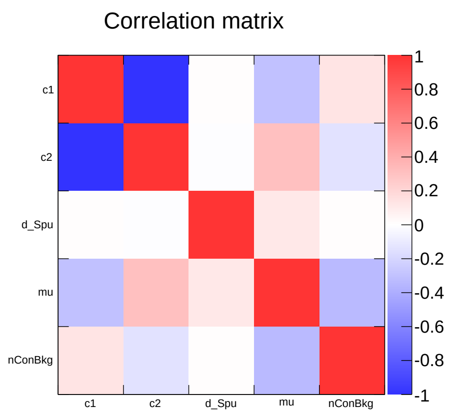

Figure 39: Reduced correlation matrix for nuisance parameters for non-resonance.

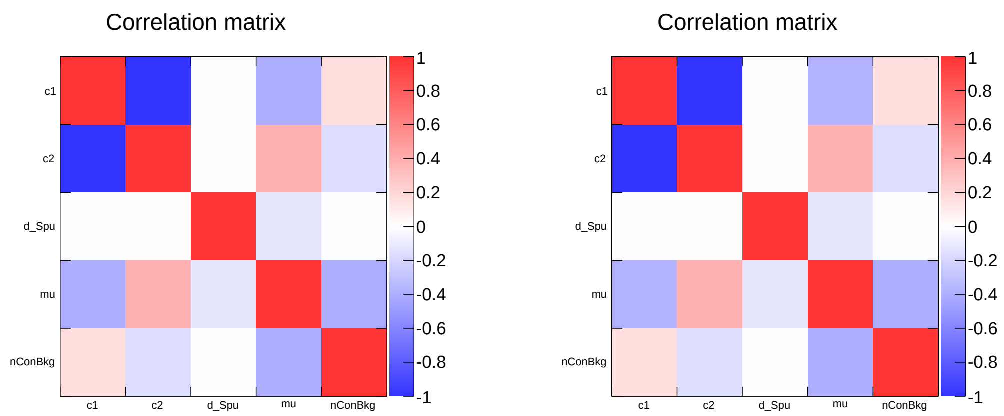

(a) (b)

Figure 40: Reduced correlation matrix for nuisance parameters for (a)m_H = 260 GeV, (b)m_H = 300 GeV.

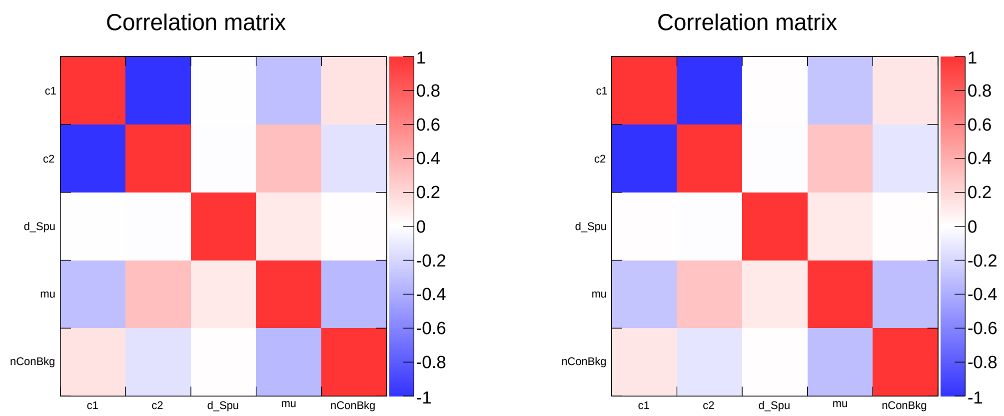

(a) (b)

Figure 41: Reduced correlation matrix for nuisance parameters for (a)m_H = 400 GeV, (b)m_H = 500 GeV.

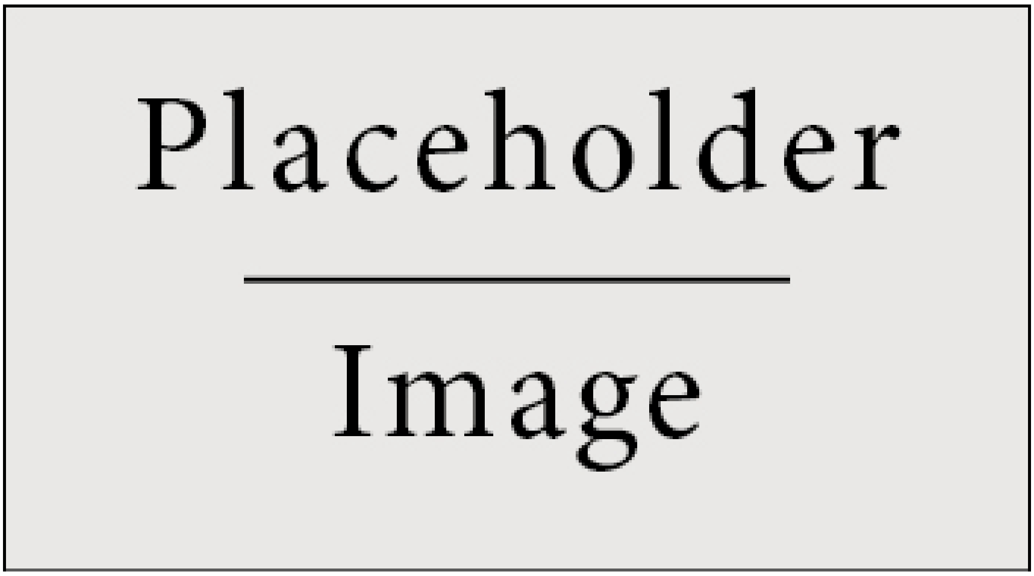

Figure 42: Correlation matrix for nuisance parameters for non-resonance with a fit to observed data.

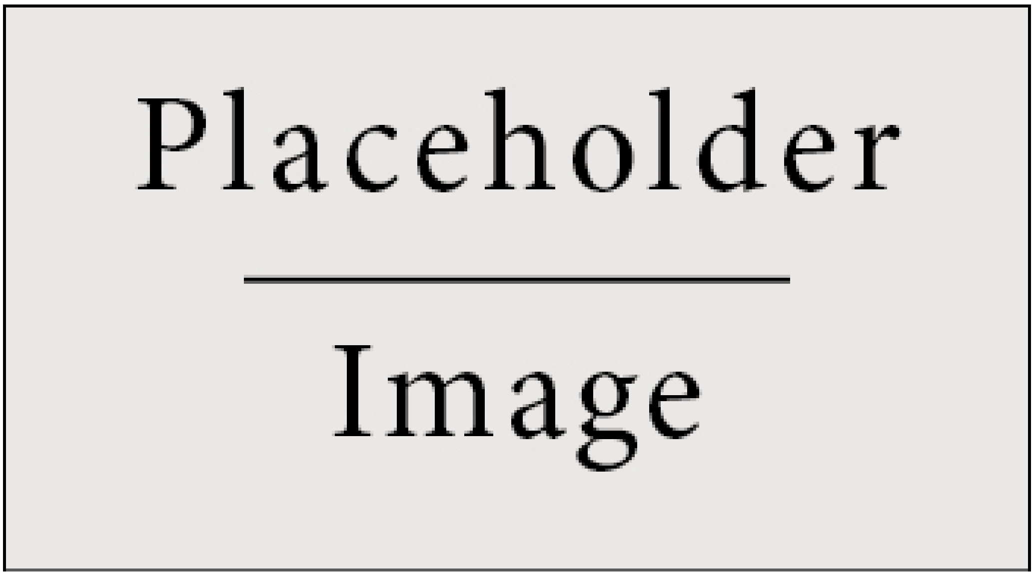

Figure 43: Correlation matrix for nuisance parameters for resonance $m_H = 260$ GeV with a fit to observed data.

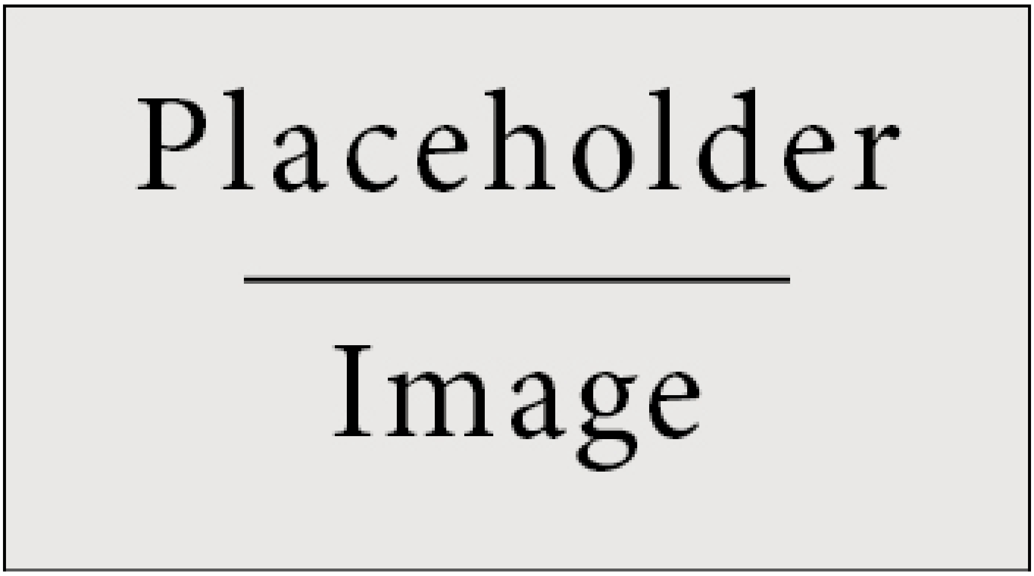

Figure 44: Correlation matrix for nuisance parameters for resonance $m_H = 300$ GeV with a fit to observed data.

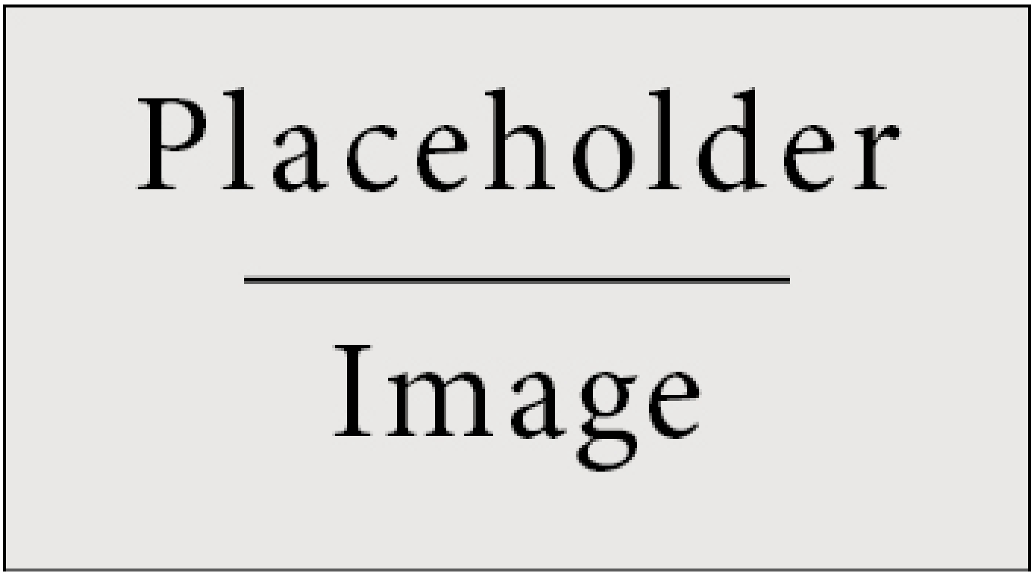

Figure 45: Correlation matrix for nuisance parameters for resonance $m_H = 400$ GeV with a fit to observed data.

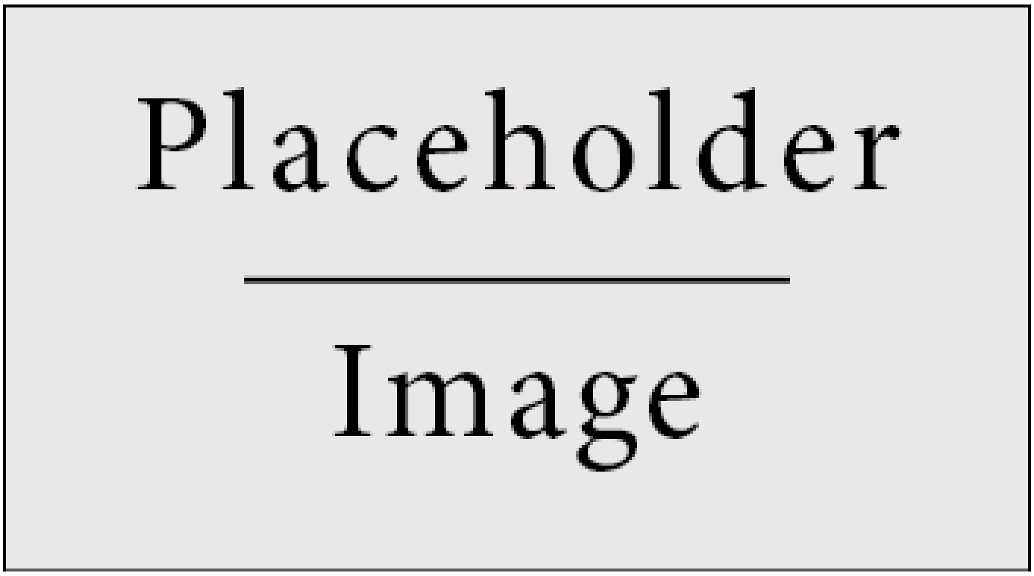

Figure 46: Correlation matrix for nuisance parameters for resonance $m_H = 500$ GeV with a fit to observed data.

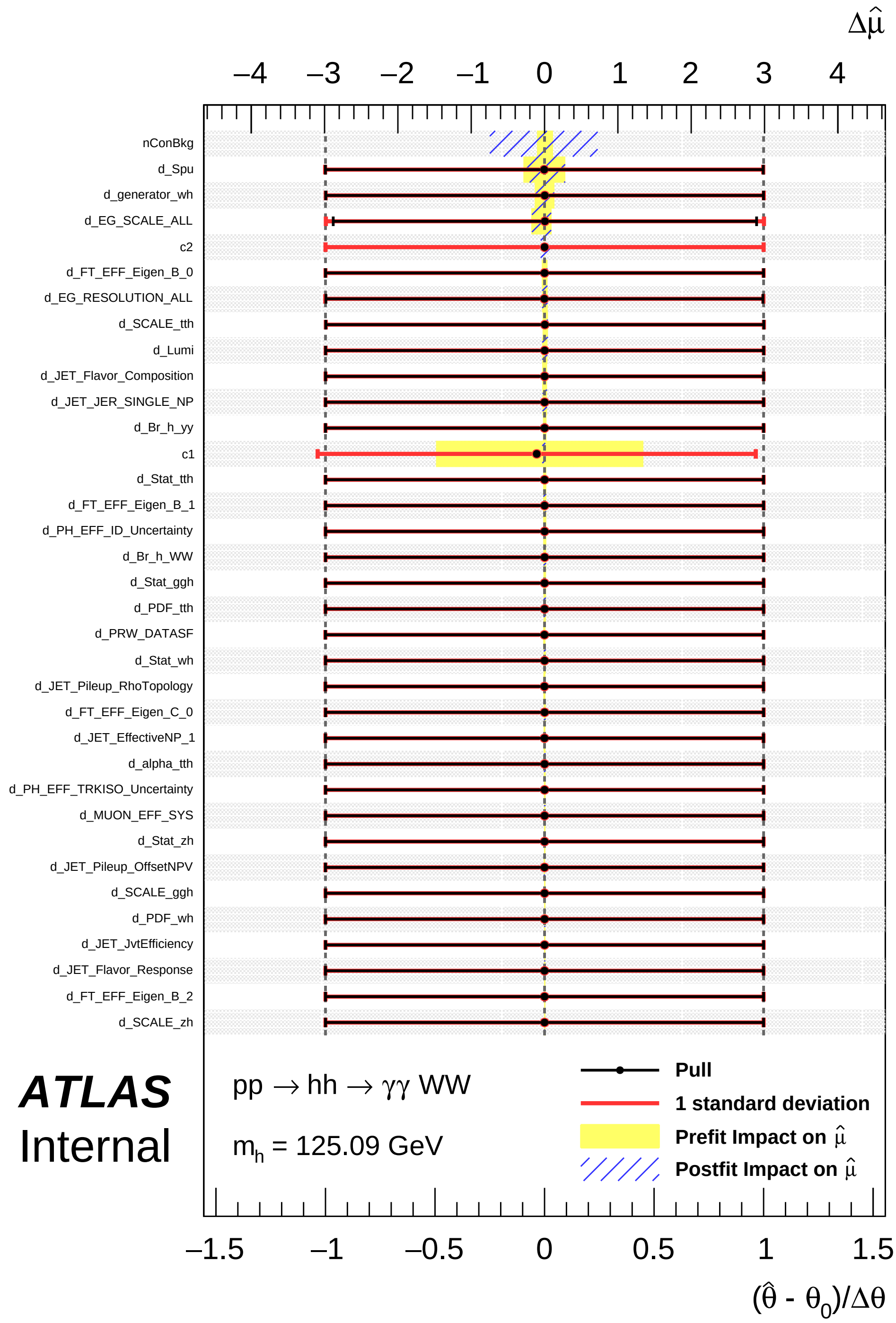

(a)

Figure 47: Nuisance parameters ranking and pulls for non-resonance on (a) asimov data

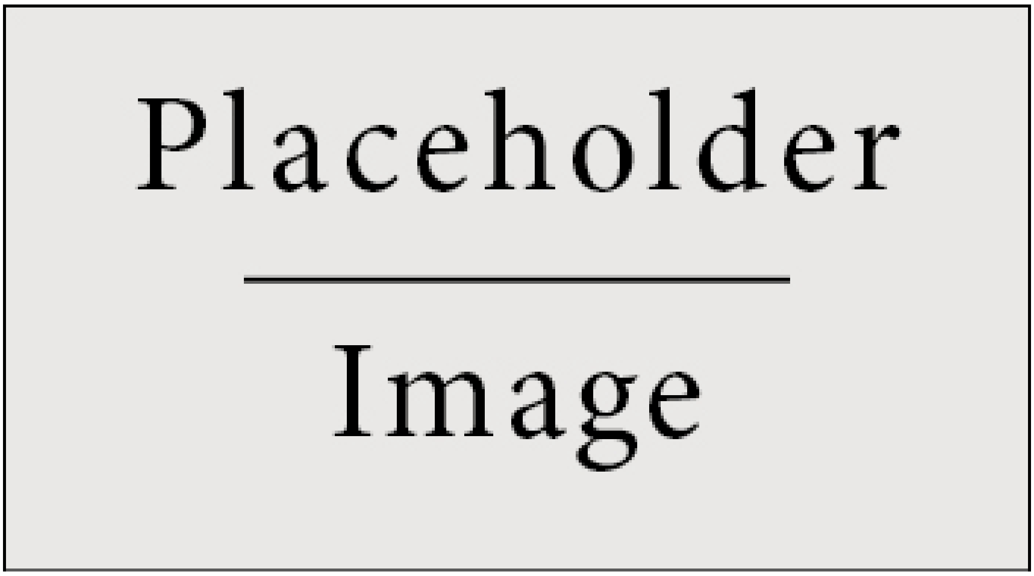

(a)

Figure 48: Nuisance parameters ranking and pulls for non-resonance on data

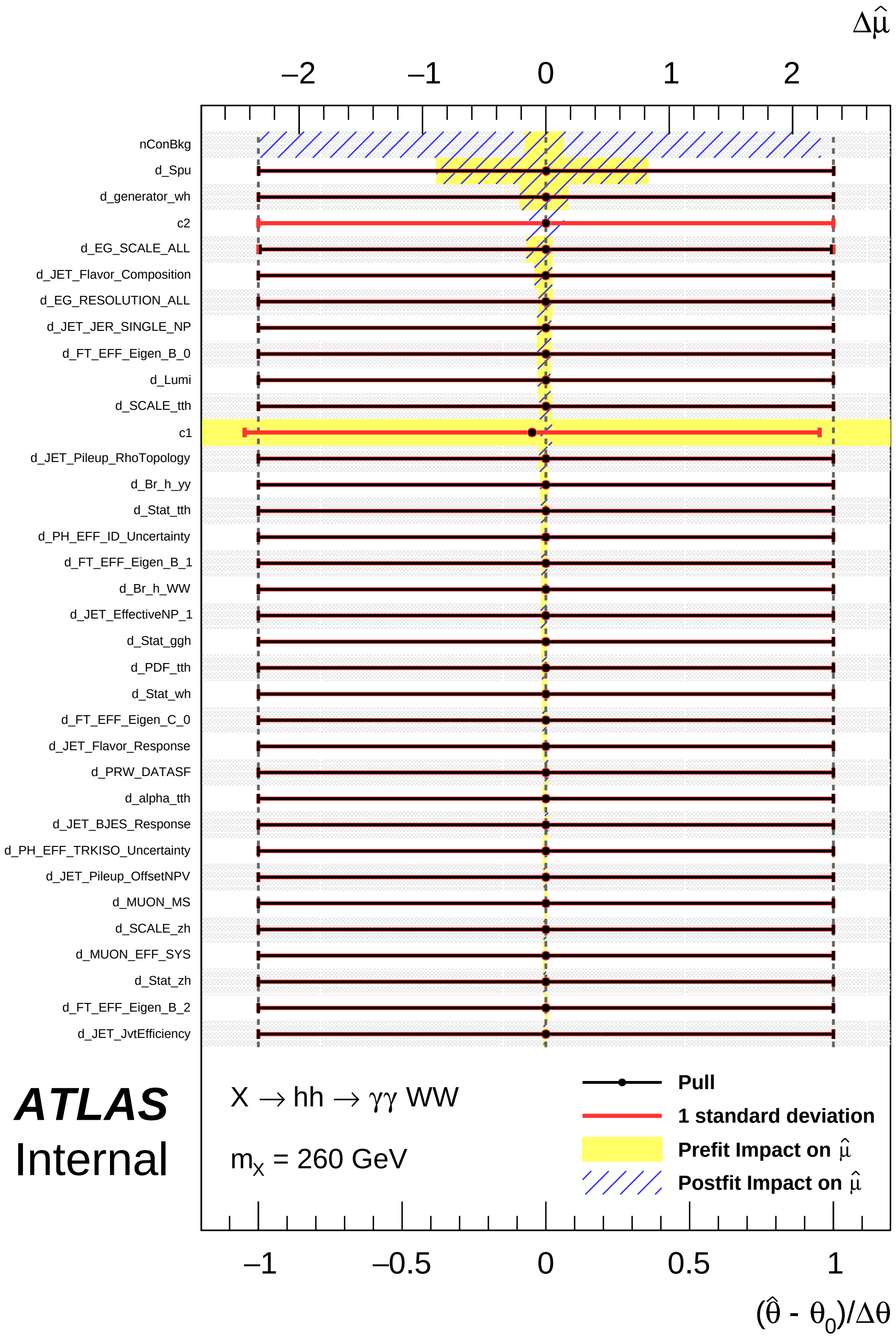

(a)

Figure 49: Nuisance parameters ranking and pulls for m_H =260 GeV on (a) asimov data

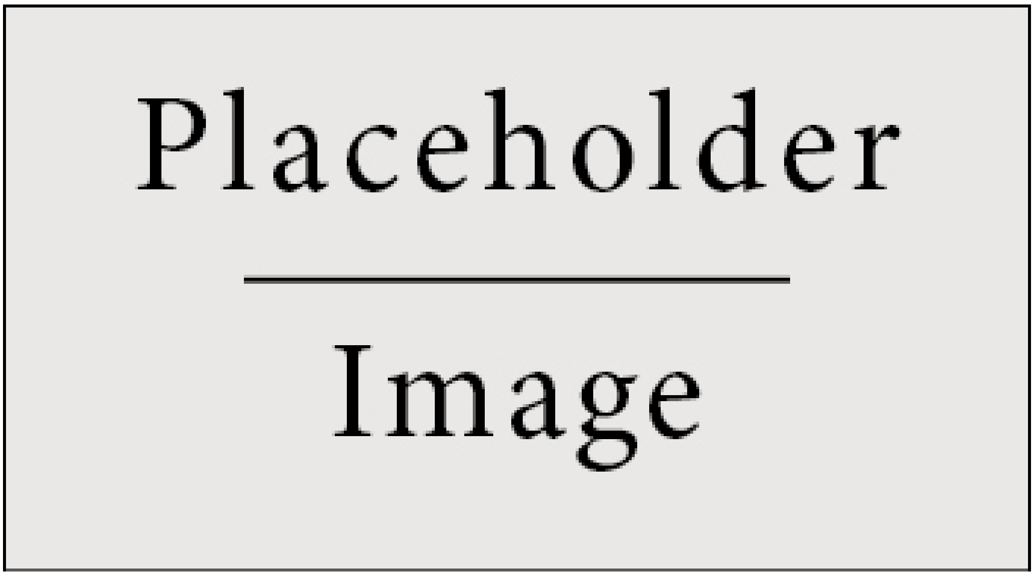

(a)

Figure 50: Nuisance parameters ranking and pulls for m_H =260 GeV on data

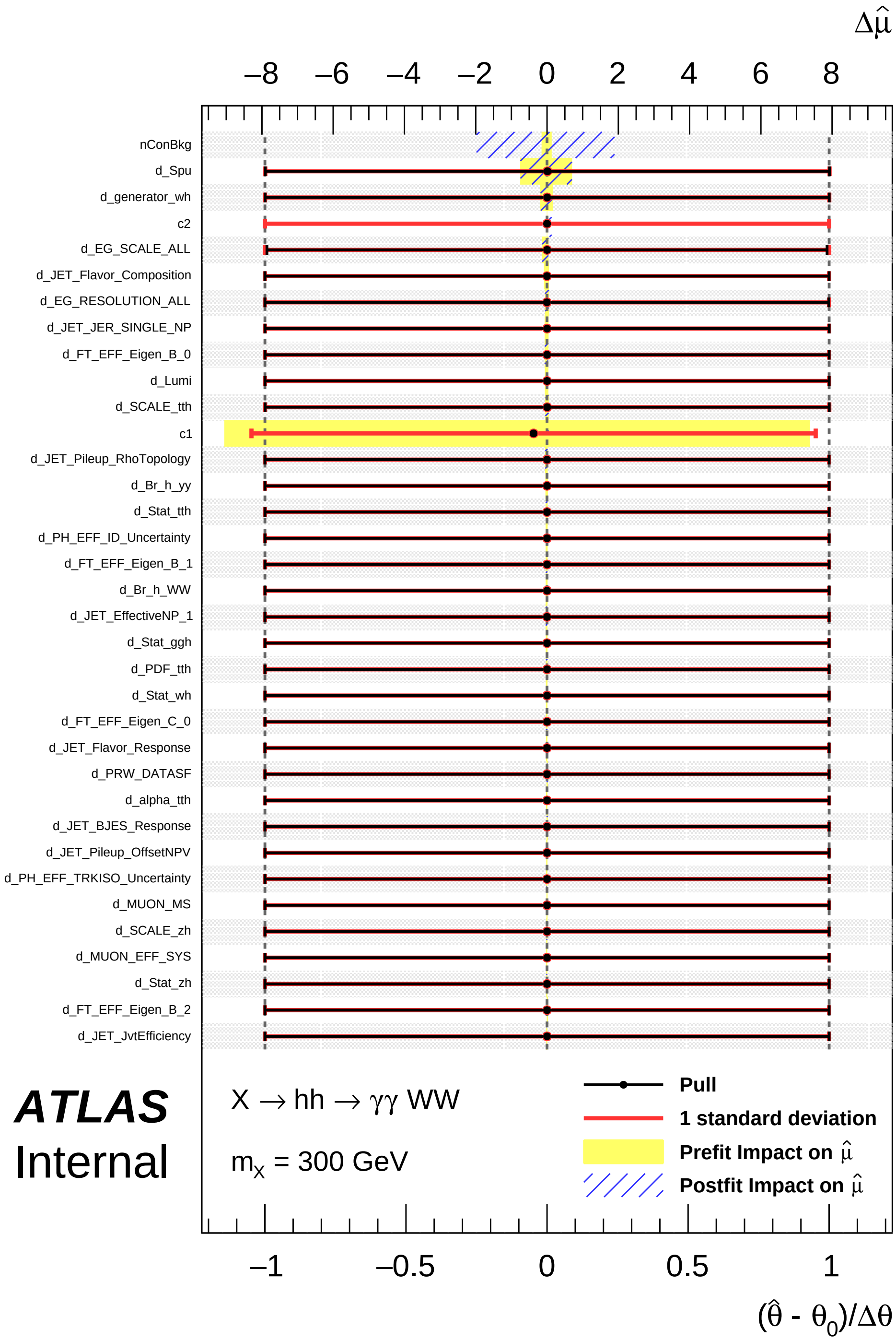

(a)

Figure 51: Nuisance parameters ranking and pulls for m_H =300 GeV on (a) asimov data

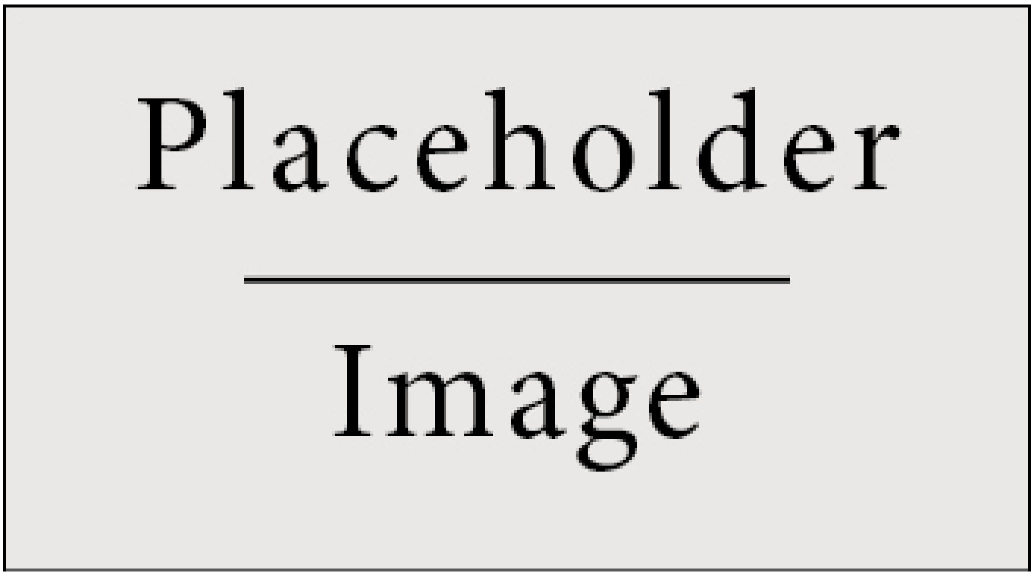

(a)

Figure 52: Nuisance parameters ranking and pulls for m_H =300 GeV on data

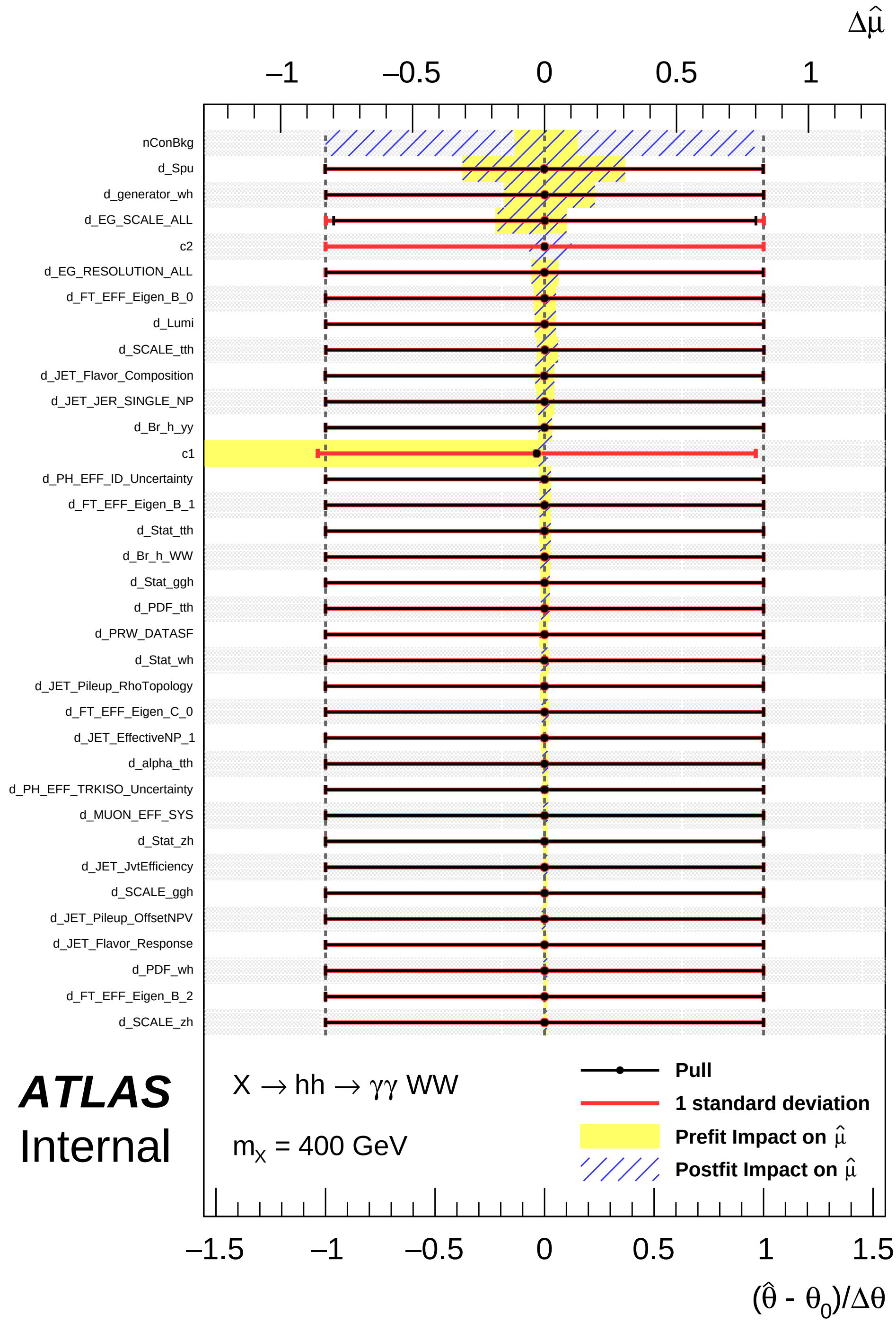

(a)

Figure 53: Nuisance parameters ranking and pulls for m_H =400 GeV on (a) asimov data

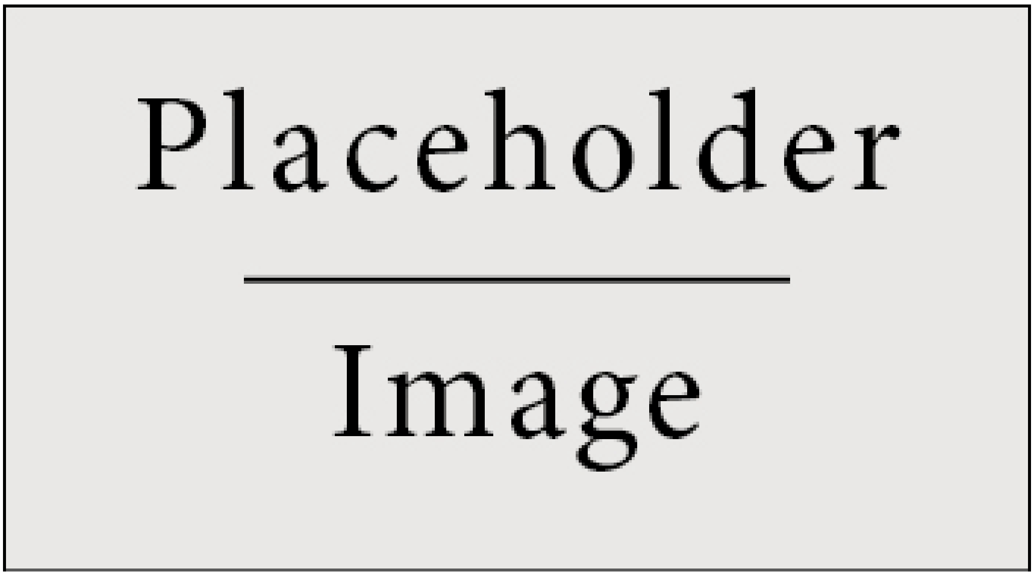

(a)

Figure 54: Nuisance parameters ranking and pulls for m_H =400 GeV on data

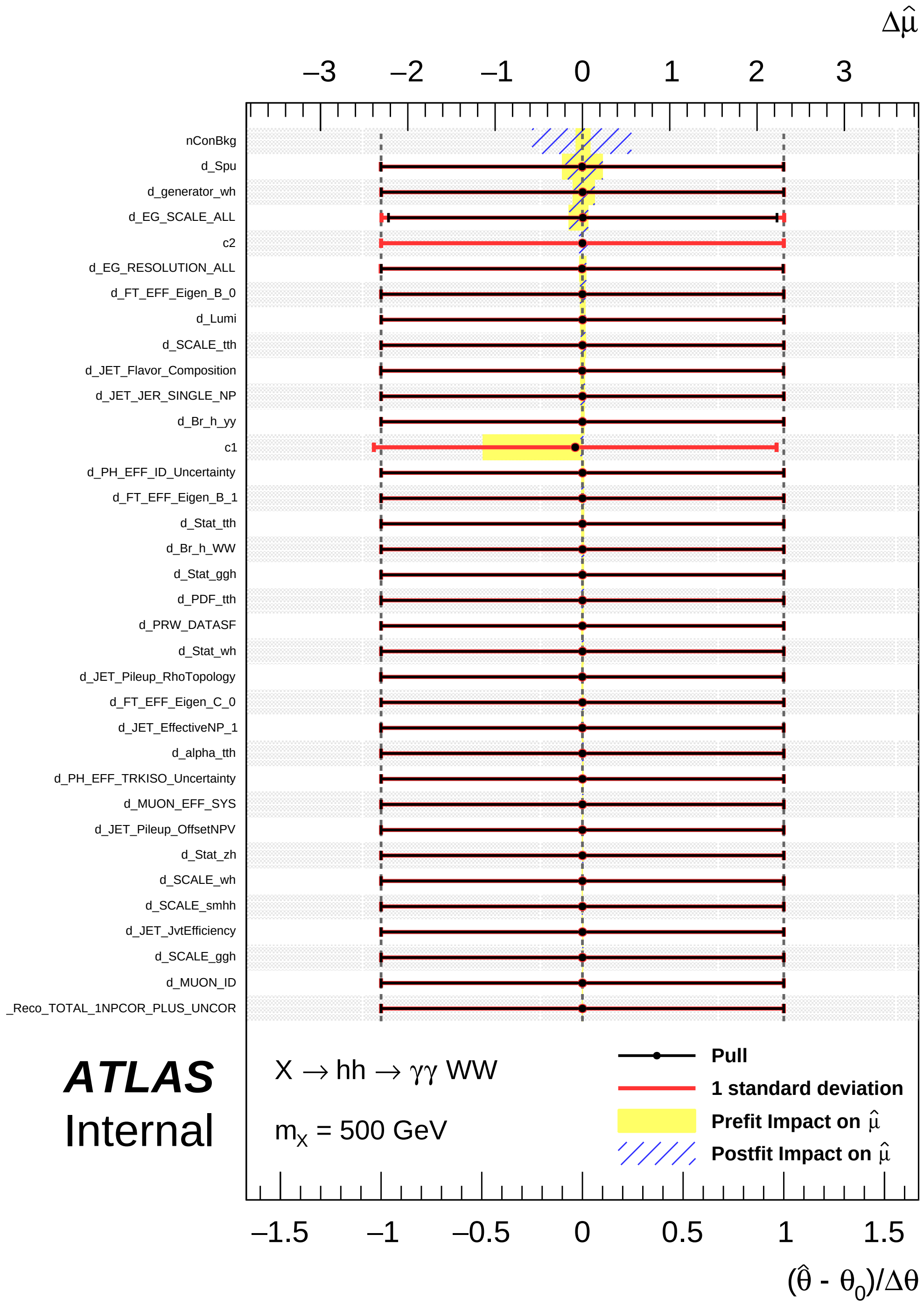

(a)

Figure 55: Nuisance parameters ranking and pulls for m_H =500 GeV on (a) asimov data

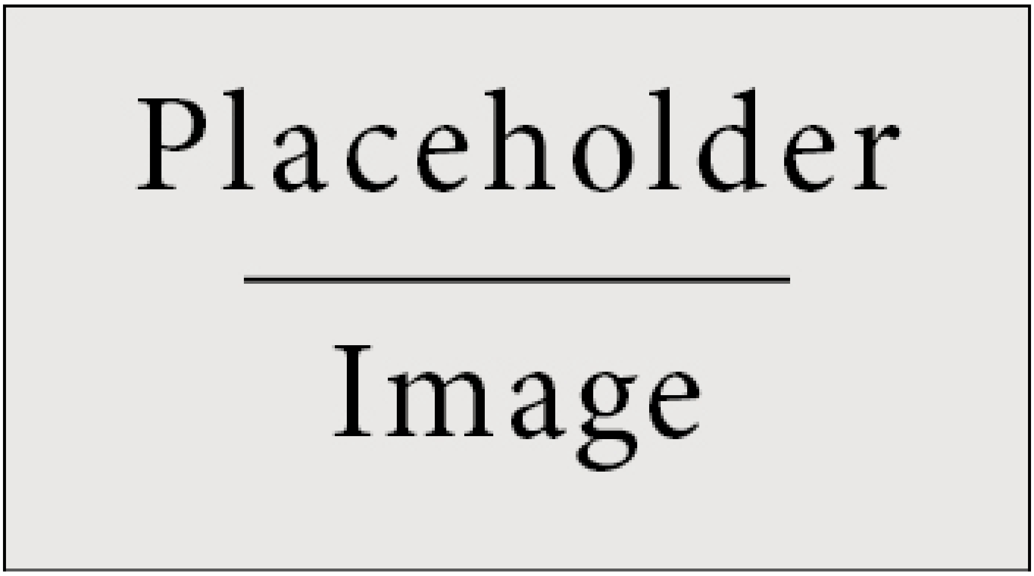

(a)

Figure 56: Nuisance parameters ranking and pulls for m_H =500 GeV on data

9.3 Upper limit setting

A likelihood ratio based test statistic is used in the statistical analysis. It is defined as follows:

$$\tilde{q}_\mu = \begin{cases} -2\ln\frac{\mathcal{L}(\mu,\hat{\hat{\theta}}(\mu))}{\mathcal{L}(0,\hat{\hat{\theta}}(0))} & \text{if } \hat{\mu} < 0 \\ -2\ln\frac{\mathcal{L}(\mu,\hat{\hat{\theta}}(\mu))}{\mathcal{L}(\hat{\mu},\hat{\theta})} & \text{if } 0 \leq \hat{\mu} \leq \mu \\ 0 & \text{if } \hat{\mu} > \mu \end{cases} \tag{4}$$

where $\mathcal{L}$ stands for the likelihood function for the statisticl model of the analysis, θ a set of nuisance parameters through which the systematic uncertainties are introduced, and the parameter of interest (POI) μ the cross section of non-resonant production or the cross section of resonant production times the branching ratio of $X \to hh$. Single hat stands for unconditional fit and double hat for conditional fit, i.e., POI μ is fixed to a certain value. With this test statistic, one derives the upper limits of the cross section for non-resonant production and the cross section times the branching ratio of $X \to hh$ for resonant production at 95% confidence level by using the CL_s method [33] under the asymptotic approximation [34]. The results are shown in Figure 57 and the numbers are summarized in Table 30.

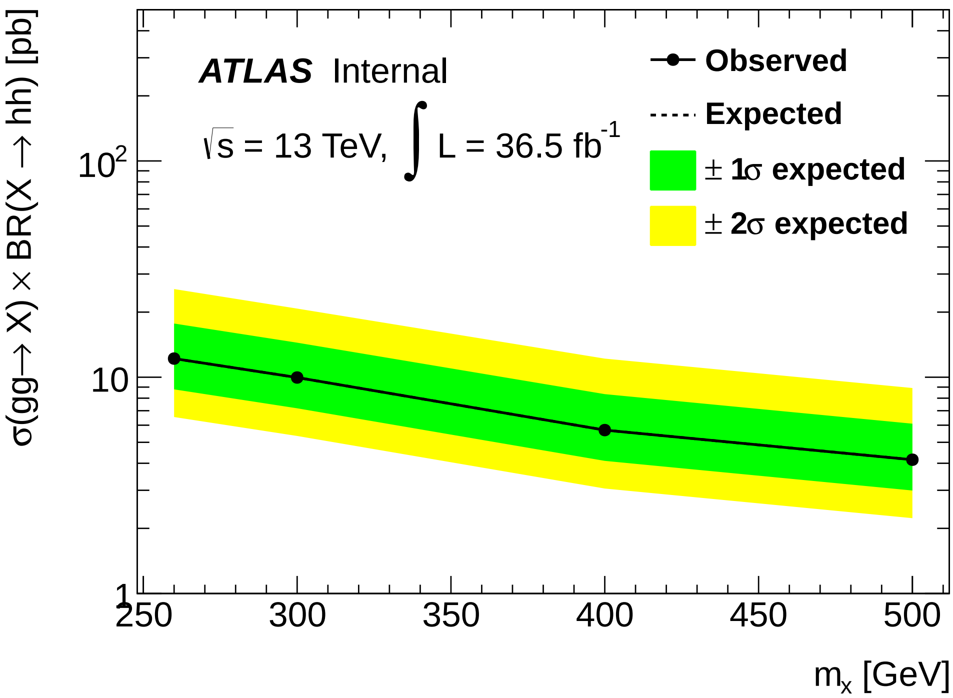

Figure 57: Upper limits at the 95% confidence level for resonance as a function of the mass of the heavy scalar.

	non-resonance	260 GeV	300 GeV	400 GeV	500 GeV
$+2\sigma$	11.78	29.86	25.13	13.28	9.73
$+1\sigma$	8.11	20.89	17.67	9.14	6.69
-1σ	4.01	10.44	8.86	4.52	3.30
-2σ	2.99	7.78	6.60	3.37	2.46
Median	5.57	14.49	12.30	6.27	4.58

Table 30: Upper limits at the 95% confidence level for the cross section of the gluon fusion production of the non-resonance and the cross section of the gluon fusion production of the resonance times the branching ratio of $X \to hh$.

10 Summary

In this note, a search is performed for non-resonant and resonant Higgs pair production with the one Higgs boson decaying to semi-leptonic WW and the other to $\gamma\gamma$. For the non-resonant Higgs pair production, the observed (expected) upper limit $gg \to hh$ is XXX pb (5.57 pb). For resonant Higgs pair production, the observed (expected) upper limits range from XXX pb (14.49 pb) to XXX pb (4.59 pb) as a function of the resonant mass under the assumption of the narrow-width approximation. The expected limits are compared to RUN I results [11] under 8 TeV in Table 31. Comparing the limit of Run1 and Run2, if the same parameter space is setup, the expected cross section from 8 TeV to 13 TeV should be 2 3 times larger. However, the current expected limit in Run2 is similar with Run1. This means that we have better exclusion power in Run2. A rough estimation of upper limit could be $\frac{\sqrt{N_b}}{eff_S*L}$. The yields in data sideband in [120, 130] GeV is 9 in Run1 [35] and 119 in Run2 and the signal efficiency is from 3.9% to 7.4% in Run1 and from 6.56% to 12.0% in Run2 for different mass point. As a result, for instance the ratio of limit in Run2 over Run1 could be $\frac{sqrt119/9}{(6.56/3.9)\times(36.1/20.3)} = 1.22$ for $m_H = 260GeV$, which is comparable with the expectation in the table.

	Non-resonance	260 GeV	300 GeV	400 GeV	500 GeV
RUN II limits (36.1 fb^{-1})	5.57	14.49	12.30	6.27	4.58
RUN II limits (13.3 fb^{-1})	13.8	24.30	20.6	15.0	12.7
RUN I limits (20.3 fb^{-1})	6.7	11.2	9.3	6.9	5.9

Table 31: The expected limits obtained in this analysis (RUN II 13 TeV) compared to RUN I 8 TeV. The SM non-resonant production is expected to increase by a factor of 3.3 from 8 TeV to 13 TeV.

References

[1] ATLAS Collaboration, *Observation of a new particle in the search for the Standard Model Higgs boson with the ATLAS detector at the LHC*, Phys. Lett. B **716** (2012) 1–29. http://www.sciencedirect.com/science/article/pii/S037026931200857X.

[2] CMS Collaboration, *Observation of a new boson at a mass of 125 GeV with the CMS experiment at the LHC*, Phys. Lett. B **716** (2012) 30–61. http://www.sciencedirect.com/science/article/pii/S0370269312008581.

[3] ATLAS Collaboration, *Measurements of Higgs boson production and couplings in diboson final states with the ATLAS detector at the LHC*, Phys.Lett. **B726** (2013) 88–119.

[4] The CMS Collaboration, *Combination of standard model Higgs boson searches and measurements of the properties of the new boson with a mass near 125 GeV*, CMS-PAS-HIG-13-005, CERN, Geneva, 2013. http://cdsweb.cern.ch/record/1542387.

[5] ATLAS and CMS Collaborations ATLAS-CONF-2015-044, Sep, 2015. https://atlas.web.cern.ch/Atlas/GROUPS/PHYSICS/CONFNOTES/ATLAS-CONF-2015-044/.

[6] *LHC Higgs Cross Section HH Sub-group*, https://twiki.cern.ch/twiki/bin/view/LHCPhysics/LHCHXSWGHH.

[7] J. Baglio, A. Djouadi, R. Gröber, M.M. Mühlleitner, J. Quevillon et al., *The measurement of the Higgs self-coupling at the LHC: theoretical status*, JHEP **1304** (2013) 151.

[8] G. C. Branco, P. M. Ferreira, L. Lavoura, M. N. Rebelo, M. Sher, and J. P. Silva, *Theory and phenomenology of two-Higgs-doublet models*, Phys. Rept. **516** (2012) 1–102, arXiv:1106.0034 [hep-ph].

[9] ATLAS Collaboration, G. Aad et al., *Search For Higgs Boson Pair Production in the $\gamma\gamma b\bar{b}$ Final State using pp Collision Data at $\sqrt{s} = 8$ TeV from the ATLAS Detector*, Phys. Rev. Lett. **114** (2015) no. 8, 081802, arXiv:1406.5053 [hep-ex].

[10] ATLAS Collaboration, G. Aad et al., *Search for Higgs boson pair production in the $b\bar{b}b\bar{b}$ final state from pp collisions at $\sqrt{s} = 8$ TeVwith the ATLAS detector*, Eur. Phys. J. **C75** (2015) no. 9, 412, arXiv:1506.00285 [hep-ex].

[11] ATLAS Collaboration, G. Aad et al., *Searches for Higgs boson pair production in the $hh \to bb\tau\tau, \gamma\gamma WW^*, \gamma\gamma bb, bbbb$ channels with the ATLAS detector*, Phys. Rev. **D92** (2015) 092004, arXiv:1509.04670 [hep-ex].

[12] T. A. collaboration, *Search for Higgs boson pair production in the $b\bar{b}\gamma\gamma$ final state using pp collision data at $\sqrt{s} = 13$ TeV with the ATLAS detector*, .

[13] ATLAS Collaboration, T. A. collaboration, *Search for pair production of Higgs bosons in the $b\bar{b}b\bar{b}$ final state using proton–proton collisions at $\sqrt{s} = 13$ TeV with the ATLAS detector*, .

[14] ATLAS Collaboration, T. A. collaboration, *Search for Higgs boson pair production in the final state of $\gamma\gamma WW^*(\to l\nu jj)$ using 13.3 fb^{-1} of pp collision data recorded at $\sqrt{s} = 13$ TeV with the ATLAS detector*, .

[15] J. Alwall, M. Herquet, F. Maltoni, O. Mattelaer, and T. Stelzer, *MadGraph 5 : Going Beyond*, JHEP **06** (2011) 128, arXiv:1106.0522 [hep-ph].

[16] Web pages. F. Maltoni, Higgs pair production. https://cp3.irmp.ucl.ac.be/projects/madgraph/wiki/HiggsPairProduction, Dec 2013.

[17] S. Frixione and B. R. Webber, *Matching NLO QCD computations and parton shower simulations*, JHEP **06** (2002) 029, arXiv:hep-ph/0204244 [hep-ph].

[18] J. Grigo, J. Hoff, and M. Steinhauser, *Higgs boson pair production: top quark mass effects at NLO and NNLO*, Nucl. Phys. **B900** (2015) 412–430, arXiv:1508.00909 [hep-ph].

[19] J. Bellm et al., *Herwig++ 2.7 Release Note*, arXiv:1310.6877 [hep-ph].

[20] S. Gieseke, C. Rohr, and A. Siodmok, *Colour reconnections in Herwig++*, Eur. Phys. J. **C72** (2012) 2225, arXiv:1206.0041 [hep-ph].

[21] P. M. Nadolsky, H.-L. Lai, Q.-H. Cao, J. Huston, J. Pumplin, D. Stump, W.-K. Tung, and C. P. Yuan, *Implications of CTEQ global analysis for collider observables*, Phys. Rev. **D78** (2008) 013004, arXiv:0802.0007 [hep-ph].

[22] A. Collaboration, *Measurement of fiducial and differential cross sections in the $H \to \gamma\gamma$ decay channel with 36.1 fb^{-1} of 13 TeV proton-proton collision data with the ATLAS detector*, ATL-COM-PHYS-2017-145, CERN, 2017. https://cds.cern.ch/record/2252597.

[23] LHC Higgs Cross Section Working Group Collaboration, D. de Florian et al., *Handbook of LHC Higgs Cross Sections: 4. Deciphering the Nature of the Higgs Sector*, arXiv:1610.07922 [hep-ph].

[24] M. Cacciari, G. P. Salam, and G. Soyez, *The anti- k t jet clustering algorithm*, Journal of High Energy Physics **2008** (2008) no. 04, 063.

[25] *Performance of missing transverse momentum reconstruction for the ATLAS detector in the first proton-proton collisions at $\sqrt{s}$= 13 TeV*, ATL-PHYS-PUB-2015-027, CERN, Geneva, Jul, 2015. https://cds.cern.ch/record/2037904.

[26] T. J. Khoo, M. H. Klein, H. Okawa, D. Schaefer, S. Williams, M. Begel, D. Cavalli, P. Francavilla, F. Hariri, C. A. Lee, T.-H. Lin, B. Liu, P. Loch, D. Lopez Mateos, R. Mazini, C. Pizio, S. Resconi, R. Simoniello, M. Smith, M. Testa, and I. Vichou, *Performance of algorithms that reconstruct missing transverse momentum in $\sqrt{s}$ = 8 TeV proton–proton collisions in the ATLAS detector*, ATL-COM-PHYS-2015-341, CERN, Geneva, Apr, 2015. https://cds.cern.ch/record/2012749.

[27] D. Cavalli, P. Francavilla, F. Hariri, T. J. Khoo, M. H. Klein, C. A. Lee, T.-h. Lin, B. Liu, R. Mazini, C. Pizio, S. Resconi, D. Schaefer, M. Smith, and M. Testa, *Reconstruction of Soft Missing Transverse Momentum with Inner Detector Tracks*, ATL-COM-PHYS-2015-209, CERN, Geneva, Mar, 2015. https://cds.cern.ch/record/2002888. Intended as backup for MET paper.

[28] ATLAS Collaboration, *Supporting Note: Selection and performance for the $H \to \gamma\gamma$ and $H \to Z\gamma$ analyses*, ATL-COM-PHYS-2016-862 (2015) . https://cds.cern.ch/record/2196102.

[29] L. C. et al., *Measurement of the isolated di-photon cross section in 4.9 fb1 of pp collisions at ps = 7 TeV with the ATLAS detecto*, ATL-COM-PHYS-2012-592, CERN, 2012. https://cds.cern.ch/record/1450063.

[30] ATLAS Collaboration, M. Aaboud et al., *Luminosity determination in pp collisions at* $\sqrt{s} = 8$ *TeV using the ATLAS detector at the LHC*, Eur. Phys. J. **C76** (2016) no. 12, 653, arXiv:1608.03953 [hep-ex].

[31] *CERN Yellow Report 4*, https://twiki.cern.ch/twiki/bin/view/LHCPhysics/CERNYellowReportPageAt13TeV.

[32] *LHC Higgs Cross Section HH Sub-group*, https://twiki.cern.ch/twiki/bin/view/LHCPhysics/LHCHXSWGHH#Current_recommendations_for_di_H.

[33] A. L. Read, *Presentation of search results: The CL(s) technique*, J.Phys. **G28** (2002) 2693–2704.

[34] G. Cowan et al., *Asymptotic formulae for likelihood-based tests of new physics*, Eur. Phys. J. **C71** (2011) 1554, arXiv:1007.1727 [physics.data-an].

[35] X. Sun, H. Zhang, and Y. Fang, *Search for Higgs pair production with decays to WW and* $\gamma\gamma$ *in 20.3* fb^{-1} *proton-proton data at 8 TeV*, ATL-COM-PHYS-2014-1446, CERN, Geneva, Nov, 2014. https://cds.cern.ch/record/1967498.

[36] *Isolation working points*, https://twiki.cern.ch/twiki/bin/view/AtlasProtected/IsolationSelectionTool#Leptons.

Appendices

A MadGraphs5 cards used for signals

Here, the cards used for generating heavy scalar resonant at the mass point of 300 GeV are given. The cards for other mass points are basically the same except the mass setting.

```
#***********************************************************************
#                        MadGraph5_aMC@NLO                             *
#                                                                      *
#                      run_card.dat aMC@NLO                            *
#                                                                      *
#  This file is used to set the parameters of the run.                 *
#                                                                      *
#  Some notation/conventions:                                          *
#                                                                      *
#   Lines starting with a hash (#) are info or comments                *
#                                                                      *
#   mind the format:   value    = variable     ! comment               *
#***********************************************************************
#
#*******************
# Running parameters
#*******************
#
#***********************************************************************
# Tag name for the run (one word)                                      *
#***********************************************************************
  tag_1     = run_tag ! name of the run
#***********************************************************************
# Number of LHE events (and their normalization) and the required      *
# (relative) accuracy on the Xsec.                                     *
# These values are ignored for fixed order runs                        *
#***********************************************************************
  15000       = nevents ! Number of unweighted events requested
    -1 = req_acc ! Required accuracy (-1=auto determined from nevents)
    -1 = nevt_job! Max number of events per job in event generation.
                 !  (-1= no split).
#***********************************************************************
# Normalize the weights of LHE events such that they sum or average to *
# the total cross section                                              *
#***********************************************************************
 average = event_norm      ! average or sum
#***********************************************************************
# Number of points per itegration channel (ignored for aMC@NLO runs)   *
#***********************************************************************
 0.01   = req_acc_FO       ! Required accuracy (-1=ignored, and use the
                           ! number of points and iter. below)
```

```
# These numbers are ignored except if req_acc_FO is equal to -1
 5000   = npoints_FO_grid  ! number of points to setup grids
 4      = niters_FO_grid   ! number of iter. to setup grids
 10000  = npoints_FO       ! number of points to compute Xsec
 6      = niters_FO        ! number of iter. to compute Xsec
#***********************************************************************
# Random number seed                                                   *
#***********************************************************************
   234      = iseed   ! rnd seed (0=assigned automatically=default))
#***********************************************************************
# Collider type and energy                                             *
#***********************************************************************
    1   = lpp1    ! beam 1 type (0 = no PDF)
    1   = lpp2    ! beam 2 type (0 = no PDF)
   6500      = ebeam1  ! beam 1 energy in GeV
   6500      = ebeam2  ! beam 2 energy in GeV
#***********************************************************************
# PDF choice: this automatically fixes also alpha_s(MZ) and its evol.  *
#***********************************************************************
 lhapdf    = pdlabel   ! PDF set
 11000    = lhaid     ! if pdlabel=lhapdf, this is the lhapdf number
#***********************************************************************
# Include the NLO Monte Carlo subtr. terms for the following parton    *
# shower (HERWIG6 | HERWIGPP | PYTHIA6Q | PYTHIA6PT | PYTHIA8)         *
# WARNING: PYTHIA6PT works only for processes without FSR!!!!          *
#***********************************************************************
 HERWIGPP    = parton_shower
#***********************************************************************
# Renormalization and factorization scales                             *
# (Default functional form for the non-fixed scales is the sum of      *
# the transverse masses of all final state particles and partons. This *
# can be changed in SubProcesses/set_scales.f)                         *
#***********************************************************************
 .true.   = fixed_ren_scale  ! if .true. use fixed ren scale
 .true.   = fixed_fac_scale  ! if .true. use fixed fac scale
 150.0    = muR_ref_fixed    ! fixed ren reference scale
 150.0    = muF1_ref_fixed   ! fixed fact reference scale for pdf1
 150.0    = muF2_ref_fixed   ! fixed fact reference scale for pdf2
#***********************************************************************
# Renormalization and factorization scales (advanced and NLO options)  *
#***********************************************************************
 .true.   = fixed_QES_scale  ! if .true. use fixed Ellis-Sexton scale
 150.0    = QES_ref_fixed    ! fixed Ellis-Sexton reference scale
 1        = muR_over_ref     ! ratio of current muR over reference muR
 1        = muF1_over_ref    ! ratio of current muF1 over reference muF1
 1        = muF2_over_ref    ! ratio of current muF2 over reference muF2
 1        = QES_over_ref     ! ratio of current QES over reference QES
#***********************************************************************
```

```
# Reweight flags to get scale dependence and PDF uncertainty              *
# For scale dependence: factor rw_scale_up/down around central scale      *
# For PDF uncertainty: use LHAPDF with supported set                       *
#***************************************************************************
 .true.   = reweight_scale   ! reweight to get scale dependence
  0.5     = rw_Rscale_down   ! lower bound for ren scale variations
  2.0     = rw_Rscale_up     ! upper bound for ren scale variations
  0.5     = rw_Fscale_down   ! lower bound for fact scale variations
  2.0     = rw_Fscale_up     ! upper bound for fact scale variations
 .false.  = reweight_PDF     ! reweight to get PDF uncertainty
 11001    = PDF_set_min      ! First of the error PDF sets
 11052    = PDF_set_max      ! Last of the error PDF sets
#***************************************************************************
# Merging - WARNING! Applies merging only at the hard-event level.         *
# After showering an MLM-type merging should be applied as well.           *
# See http://amcatnlo.cern.ch/FxFx_merging.htm for more details.           *
#***************************************************************************
 0        = ickkw            ! 0 no merging, 3 FxFx merging, 4 UNLOPS
#***************************************************************************
#
#***************************************************************************
# BW cutoff (M+/-bwcutoff*Gamma)                                           *
#***************************************************************************
 15  = bwcutoff
#***************************************************************************
# Cuts on the jets                                                         *
# Jet clustering is performed by FastJet.
# When matching to a parton shower, these generation cuts should be        *
# considerably softer than the analysis cuts.                              *
# (more specific cuts can be specified in SubProcesses/cuts.f)             *
#***************************************************************************
  -1  = jetalgo   ! FastJet jet algorithm (1=kT, 0=C/A, -1=anti-kT)
 0.4  = jetradius ! The radius parameter for the jet algorithm
  10  = ptj       ! Min jet transverse momentum
  -1  = etaj      ! Max jet abs(pseudo-rap) (a value .lt.0 means no cut)
#***************************************************************************
# Cuts on the charged leptons (e+, e-, mu+, mu-, tau+ and tau-)            *
# (more specific gen cuts can be specified in SubProcesses/cuts.f)         *
#***************************************************************************
   0  = ptl     ! Min lepton transverse momentum
  -1  = etal    ! Max lepton abs(pseudo-rap) (a value .lt.0 means no cut)
   0  = drll    ! Min distance between opposite sign lepton pairs
   0  = drll_sf ! Min distance between opp. sign same-flavor lepton pairs
   0  = mll     ! Min inv. mass of all opposite sign lepton pairs
  30  = mll_sf  ! Min inv. mass of all opp. sign same-flavor lepton pairs
#***************************************************************************
# Photon-isolation cuts, according to hep-ph/9801442                       *
# When ptgmin=0, all the other parameters are ignored                      *
```

```
#***********************************************************************
  20  = ptgmin    ! Min photon transverse momentum
  -1  = etagamma  ! Max photon abs(pseudo-rap)
 0.4  = R0gamma   ! Radius of isolation code
 1.0  = xn        ! n parameter of eq.(3.4) in hep-ph/9801442
 1.0  = epsgamma  ! epsilon_gamma parameter of eq.(3.4) in hep-ph/9801442
 .true.  = isoEM  ! isolate photons from EM energy (photons and leptons)
#***********************************************************************
# Maximal PDG code for quark to be considered a jet when applying cuts.*
# At least all massless quarks of the model should be included here.   *
#***********************************************************************
 4 = maxjetflavor
#***********************************************************************
# For aMCfast+APPLGRID use in PDF fitting (http://amcfast.hepforge.org)*
#***********************************************************************
 0 = iappl   ! aMCfast switch (0=OFF, 1=prepare APPLgrids, 2=fill grids)
#***********************************************************************
```

B Systematic uncertainties in details for one lepton region

Uncertainty Source	Relative Variations
$EL\_EFF\_ID\_TOTAL\_1NPCOR\_PLUS\_UNCOR\_\_1down$	-0.451016
$EL\_EFF\_ID\_TOTAL\_1NPCOR\_PLUS\_UNCOR\_\_1up$	0.451016
$EL\_EFF\_Iso\_TOTAL\_1NPCOR\_PLUS\_UNCOR\_\_1down$	-0.133728
$EL\_EFF\_Iso\_TOTAL\_1NPCOR\_PLUS\_UNCOR\_\_1up$	0.133728
$EL\_EFF\_Reco\_TOTAL\_1NPCOR\_PLUS\_UNCOR\_\_1down$	-0.129689
$EL\_EFF\_Reco\_TOTAL\_1NPCOR\_PLUS\_UNCOR\_\_1up$	0.129689
$MUON\_EFF\_STAT\_\_1down$	-0.106279
$MUON\_EFF\_STAT\_\_1up$	0.106279
$MUON\_EFF\_SYS\_\_1down$	-0.370158
$MUON\_EFF\_SYS\_\_1up$	0.37089
$MUON\_ID\_\_1down$	0.000119605
$MUON\_ID\_\_1up$	0.000733227
$MUON\_ISO\_STAT\_\_1down$	-0.0389021
$MUON\_ISO\_STAT\_\_1up$	0.0389024
$MUON\_ISO\_SYS\_\_1down$	-0.108095
$MUON\_ISO\_SYS\_\_1up$	0.108094
$MUON\_MS\_\_1down$	-0.000245242
$MUON\_MS\_\_1up$	0.000212413
$MUON\_SAGITTA\_RESBIAS\_\_1down$	0
$MUON\_SAGITTA\_RESBIAS\_\_1up$	0
$MUON\_SAGITTA\_RHO\_\_1down$	0
$MUON\_SAGITTA\_RHO\_\_1up$	0
$MUON\_SCALE\_\_1down$	0.000220205
$MUON\_SCALE\_\_1up$	8.1122e-05
$MUON\_TTVA\_STAT\_\_1down$	-0.0859512
$MUON\_TTVA\_STAT\_\_1up$	0.0859513
$MUON\_TTVA\_SYS\_\_1down$	-0.0475225
$MUON\_TTVA\_SYS\_\_1up$	0.0475225
$PH\_EFF\_ID\_Uncertainty\_\_1down$	-1.60531
$PH\_EFF\_ID\_Uncertainty\_\_1up$	1.61899
$PH\_EFF\_TRKISO\_Uncertainty\_\_1down$	-0.793959
$PH\_EFF\_TRKISO\_Uncertainty\_\_1up$	0.797364
$PH\_Iso\_DDonoff$	0
$PRW\_DATASF\_\_1down$	2.01762
$PRW\_DATASF\_\_1up$	-0.754502

Table 32: Systematic uncertainties for tth in percent in one lepton region without $p_T(\gamma\gamma)$ cut applied.

Uncertainty Source	Relative Variations
JET_BJES_Response__1up	-0.157433
JET_BJES_Response__1down	1.04427
JET_EffectiveNP_1__1up	0.193596
JET_EffectiveNP_1__1down	0.798998
JET_EffectiveNP_2__1up	0.247317
JET_EffectiveNP_2__1down	-0.0860637
JET_EffectiveNP_3__1up	-0.00955768
JET_EffectiveNP_3__1down	0.231497
JET_EffectiveNP_4__1up	0.108658
JET_EffectiveNP_4__1down	-0.0105294
JET_EffectiveNP_5__1up	0.0996838
JET_EffectiveNP_5__1down	0.000330823
JET_EffectiveNP_6__1up	-4.77404e-05
JET_EffectiveNP_6__1down	0.110949
JET_EffectiveNP_7__1up	0.11223
JET_EffectiveNP_7__1down	-0.00443503
JET_EffectiveNP_8restTerm__1up	0.00571768
JET_EffectiveNP_8restTerm__1down	0.0947025
JET_EtaIntercalibration_Modelling__1up	0.121217
JET_EtaIntercalibration_Modelling__1down	0.129124
JET_EtaIntercalibration_NonClosure__1up	0.0589713
JET_EtaIntercalibration_NonClosure__1down	0.172692
JET_EtaIntercalibration_TotalStat__1up	-0.000765441
JET_EtaIntercalibration_TotalStat__1down	0.219402
JET_Flavor_Composition__1up	0.611893
JET_Flavor_Composition__1down	-0.632818
JET_Flavor_Response__1up	-0.416163
JET_Flavor_Response__1down	0.0937692
JET_JER_SINGLE_NP__1up	1.94117
JET_JvtEfficiency__1down	-0.637365
JET_JvtEfficiency__1up	0.641024
JET_Pileup_OffsetMu__1up	-0.0895751
JET_Pileup_OffsetMu__1down	0.00392801
JET_Pileup_OffsetNPV__1up	0.186438
JET_Pileup_OffsetNPV__1down	0.168446
JET_Pileup_PtTerm__1up	0.0266119
JET_Pileup_PtTerm__1down	-0.0192852
JET_Pileup_RhoTopology__1up	-0.41469
JET_Pileup_RhoTopology__1down	1.2558
JET_PunchThrough_MC15__1up	-7.46248e-06
JET_PunchThrough_MC15__1down	7.74158e-06
JET_SingleParticle_HighPt__1up	0
JET_SingleParticle_HighPt__1down	0

Table 33: Systematic uncertainties for tth in percent in one lepton region without $p_T(\gamma\gamma)$ cut applied.

Uncertainty Source	Relative Variations
$FT\_EFF\_Eigen\_B\_0\_\_1down$	-7.70771
$FT\_EFF\_Eigen\_B\_0\_\_1up$	8.00219
$FT\_EFF\_Eigen\_B\_1\_\_1down$	-3.48614
$FT\_EFF\_Eigen\_B\_1\_\_1up$	3.54596
$FT\_EFF\_Eigen\_B\_2\_\_1down$	1.28256
$FT\_EFF\_Eigen\_B\_2\_\_1up$	-1.271
$FT\_EFF\_Eigen\_C\_0\_\_1down$	-1.53147
$FT\_EFF\_Eigen\_C\_0\_\_1up$	1.53868
$FT\_EFF\_Eigen\_C\_1\_\_1down$	-0.308604
$FT\_EFF\_Eigen\_C\_1\_\_1up$	0.308658
$FT\_EFF\_Eigen\_C\_2\_\_1down$	-0.0429205
$FT\_EFF\_Eigen\_C\_2\_\_1up$	0.042953
$FT\_EFF\_Eigen\_C\_3\_\_1down$	0.0677539
$FT\_EFF\_Eigen\_C\_3\_\_1up$	-0.0677471
$FT\_EFF\_Eigen\_Light\_0\_\_1down$	-0.258585
$FT\_EFF\_Eigen\_Light\_0\_\_1up$	0.259169
$FT\_EFF\_Eigen\_Light\_1\_\_1down$	0.034444
$FT\_EFF\_Eigen\_Light\_1\_\_1up$	-0.0344342
$FT\_EFF\_Eigen\_Light\_2\_\_1down$	0.00771715
$FT\_EFF\_Eigen\_Light\_2\_\_1up$	-0.00771943
$FT\_EFF\_Eigen\_Light\_3\_\_1down$	-0.00525147
$FT\_EFF\_Eigen\_Light\_3\_\_1up$	0.00525617
$FT\_EFF\_Eigen\_Light\_4\_\_1down$	0.0406427
$FT\_EFF\_Eigen\_Light\_4\_\_1up$	-0.0406249
$FT\_EFF\_extrapolation\_\_1down$	0.285664
$FT\_EFF\_extrapolation\_\_1up$	-0.28172
$FT\_EFF\_extrapolation\_from\_charm\_\_1down$	0.0187249
$FT\_EFF\_extrapolation\_from\_charm\_\_1up$	-0.0187249

Table 34: Systematic uncertainties for tth in percent in one lepton region without $p_T(\gamma\gamma)$ cut applied.

Uncertainty Source	Relative Variations
EL_EFF_ID_TOTAL_1NPCOR_PLUS_UNCOR__1down	-0.429647
EL_EFF_ID_TOTAL_1NPCOR_PLUS_UNCOR__1up	0.429647
EL_EFF_Iso_TOTAL_1NPCOR_PLUS_UNCOR__1down	-0.125978
EL_EFF_Iso_TOTAL_1NPCOR_PLUS_UNCOR__1up	0.125978
EL_EFF_Reco_TOTAL_1NPCOR_PLUS_UNCOR__1down	-0.111956
EL_EFF_Reco_TOTAL_1NPCOR_PLUS_UNCOR__1up	0.111956
MUON_EFF_STAT__1down	-0.266439
MUON_EFF_STAT__1up	0.266439
MUON_EFF_SYS__1down	-0.533756
MUON_EFF_SYS__1up	0.534663
MUON_ID__1down	0.000102204
MUON_ID__1up	0.000120072
MUON_ISO_STAT__1down	-0.0340592
MUON_ISO_STAT__1up	0.0340595
MUON_ISO_SYS__1down	-0.107535
MUON_ISO_SYS__1up	0.107534
MUON_MS__1down	0.0820036
MUON_MS__1up	-0.000151071
MUON_SAGITTA_RESBIAS__1down	0
MUON_SAGITTA_RESBIAS__1up	0
MUON_SAGITTA_RHO__1down	0
MUON_SAGITTA_RHO__1up	0
MUON_SCALE__1down	0.000269336
MUON_SCALE__1up	-0.000151427
MUON_TTVA_STAT__1down	-0.0829736
MUON_TTVA_STAT__1up	0.0829736
MUON_TTVA_SYS__1down	-0.0442062
MUON_TTVA_SYS__1up	0.0442062
PH_EFF_ID_Uncertainty__1down	-1.61419
PH_EFF_ID_Uncertainty__1up	1.62741
PH_EFF_TRKISO_Uncertainty__1down	-0.81737
PH_EFF_TRKISO_Uncertainty__1up	0.821081
PH_Iso_DDonoff	0.135907
PRW_DATASF__1down	0.786437
PRW_DATASF__1up	0.259293

Table 35: Systematic uncertainties for Wh in percent in one lepton region without $p_T(\gamma\gamma)$ cut applied.

Uncertainty Source	Relative Variations
$JET\_BJES\_Response\_\_1up$	-0.0231078
$JET\_BJES\_Response\_\_1down$	0.0572327
$JET\_EffectiveNP\_1\_\_1up$	3.36971
$JET\_EffectiveNP\_1\_\_1down$	-2.68823
$JET\_EffectiveNP\_2\_\_1up$	-0.881462
$JET\_EffectiveNP\_2\_\_1down$	0.796042
$JET\_EffectiveNP\_3\_\_1up$	0.199223
$JET\_EffectiveNP\_3\_\_1down$	-0.405274
$JET\_EffectiveNP\_4\_\_1up$	-0.324853
$JET\_EffectiveNP\_4\_\_1down$	-0.00144804
$JET\_EffectiveNP\_5\_\_1up$	-0.25006
$JET\_EffectiveNP\_5\_\_1down$	0.00252444
$JET\_EffectiveNP\_6\_\_1up$	0.174614
$JET\_EffectiveNP\_6\_\_1down$	-0.407023
$JET\_EffectiveNP\_7\_\_1up$	-0.486339
$JET\_EffectiveNP\_7\_\_1down$	0.167234
$JET\_EffectiveNP\_8restTerm\_\_1up$	0.00133669
$JET\_EffectiveNP\_8restTerm\_\_1down$	-0.328113
$JET\_EtaIntercalibration\_Modelling\_\_1up$	0.742413
$JET\_EtaIntercalibration\_Modelling\_\_1down$	-1.48479
$JET\_EtaIntercalibration\_NonClosure\_\_1up$	-0.372728
$JET\_EtaIntercalibration\_NonClosure\_\_1down$	0.150208
$JET\_EtaIntercalibration\_TotalStat\_\_1up$	0.408175
$JET\_EtaIntercalibration\_TotalStat\_\_1down$	-0.712647
$JET\_Flavor\_Composition\_\_1up$	8.16721
$JET\_Flavor\_Composition\_\_1down$	-7.1441
$JET\_Flavor\_Response\_\_1up$	-1.97008
$JET\_Flavor\_Response\_\_1down$	1.72342
$JET\_JER\_SINGLE\_NP\_\_1up$	5.20475
$JET\_JvtEfficiency\_\_1down$	-0.538754
$JET\_JvtEfficiency\_\_1up$	0.540548
$JET\_Pileup\_OffsetMu\_\_1up$	-0.43289
$JET\_Pileup\_OffsetMu\_\_1down$	0.0941849
$JET\_Pileup\_OffsetNPV\_\_1up$	0.980575
$JET\_Pileup\_OffsetNPV\_\_1down$	-0.507806
$JET\_Pileup\_PtTerm\_\_1up$	0.0112159
$JET\_Pileup\_PtTerm\_\_1down$	0.0248859
$JET\_Pileup\_RhoTopology\_\_1up$	4.79589
$JET\_Pileup\_RhoTopology\_\_1down$	-3.90133
$JET\_PunchThrough\_MC15\_\_1up$	-2.36746e-07
$JET\_PunchThrough\_MC15\_\_1down$	9.09924e-06
$JET\_SingleParticle\_HighPt\_\_1up$	0
$JET\_SingleParticle\_HighPt\_\_1down$	0

Table 36: Systematic uncertainties for Wh in percent in one lepton region without $p_T(\gamma\gamma)$ cut applied.

Uncertainty Source	Relative Variations
$FT\_EFF\_Eigen\_B\_0\_\_1down$	-0.0899175
$FT\_EFF\_Eigen\_B\_0\_\_1up$	0.0927434
$FT\_EFF\_Eigen\_B\_1\_\_1down$	-0.0113505
$FT\_EFF\_Eigen\_B\_1\_\_1up$	0.0113367
$FT\_EFF\_Eigen\_B\_2\_\_1down$	0.00236481
$FT\_EFF\_Eigen\_B\_2\_\_1up$	-0.00237557
$FT\_EFF\_Eigen\_C\_0\_\_1down$	-0.565789
$FT\_EFF\_Eigen\_C\_0\_\_1up$	0.569621
$FT\_EFF\_Eigen\_C\_1\_\_1down$	-0.0488319
$FT\_EFF\_Eigen\_C\_1\_\_1up$	0.0488954
$FT\_EFF\_Eigen\_C\_2\_\_1down$	-0.0345158
$FT\_EFF\_Eigen\_C\_2\_\_1up$	0.0344119
$FT\_EFF\_Eigen\_C\_3\_\_1down$	0.0292769
$FT\_EFF\_Eigen\_C\_3\_\_1up$	-0.0292754
$FT\_EFF\_Eigen\_Light\_0\_\_1down$	-0.283082
$FT\_EFF\_Eigen\_Light\_0\_\_1up$	0.283586
$FT\_EFF\_Eigen\_Light\_1\_\_1down$	0.0466426
$FT\_EFF\_Eigen\_Light\_1\_\_1up$	-0.0466286
$FT\_EFF\_Eigen\_Light\_2\_\_1down$	-0.00889927
$FT\_EFF\_Eigen\_Light\_2\_\_1up$	0.00890185
$FT\_EFF\_Eigen\_Light\_3\_\_1down$	0.0170021
$FT\_EFF\_Eigen\_Light\_3\_\_1up$	-0.0169984
$FT\_EFF\_Eigen\_Light\_4\_\_1down$	0.0197891
$FT\_EFF\_Eigen\_Light\_4\_\_1up$	-0.0197856
$FT\_EFF\_extrapolation\_\_1down$	0.0120396
$FT\_EFF\_extrapolation\_\_1up$	-0.0120397
$FT\_EFF\_extrapolation\_from\_charm\_\_1down$	0
$FT\_EFF\_extrapolation\_from\_charm\_\_1up$	0

Table 37: Systematic uncertainties for Wh in percent in one lepton region without $p_T(\gamma\gamma)$ cut applied.

Uncertainty Source	Relative Variations
EL_EFF_ID_TOTAL_1NPCOR_PLUS_UNCOR__1down	-0.414868
EL_EFF_ID_TOTAL_1NPCOR_PLUS_UNCOR__1up	0.414867
EL_EFF_Iso_TOTAL_1NPCOR_PLUS_UNCOR__1down	-0.115012
EL_EFF_Iso_TOTAL_1NPCOR_PLUS_UNCOR__1up	0.115012
EL_EFF_Reco_TOTAL_1NPCOR_PLUS_UNCOR__1down	-0.1248
EL_EFF_Reco_TOTAL_1NPCOR_PLUS_UNCOR__1up	0.1248
MUON_EFF_STAT__1down	-0.103181
MUON_EFF_STAT__1up	0.103181
MUON_EFF_SYS__1down	-0.372604
MUON_EFF_SYS__1up	0.373514
MUON_ID__1down	-0.000281855
MUON_ID__1up	-0.000269726
MUON_ISO_STAT__1down	-0.046463
MUON_ISO_STAT__1up	0.0464629
MUON_ISO_SYS__1down	-0.111914
MUON_ISO_SYS__1up	0.111913
MUON_MS__1down	0.0910969
MUON_MS__1up	-0.000299612
MUON_SAGITTA_RESBIAS__1down	0
MUON_SAGITTA_RESBIAS__1up	0
MUON_SAGITTA_RHO__1down	0
MUON_SAGITTA_RHO__1up	0
MUON_SCALE__1down	-3.37733e-05
MUON_SCALE__1up	7.05483e-06
MUON_TTVA_STAT__1down	-0.0949855
MUON_TTVA_STAT__1up	0.0949854
MUON_TTVA_SYS__1down	-0.055563
MUON_TTVA_SYS__1up	0.055563
PH_EFF_ID_Uncertainty__1down	-1.58318
PH_EFF_ID_Uncertainty__1up	1.59573
PH_EFF_TRKISO_Uncertainty__1down	-0.809736
PH_EFF_TRKISO_Uncertainty__1up	0.813497
PH_Iso_DDonoff	0
PRW_DATASF__1down	-1.20557
PRW_DATASF__1up	2.07656

Table 38: Systematic uncertainties for Zh in percent in one lepton region without $p_T(\gamma\gamma)$ cut applied.

Uncertainty Source	Relative Variations
$JET\_BJES\_Response\_\_1up$	0.00104824
$JET\_BJES\_Response\_\_1down$	0.113495
$JET\_EffectiveNP\_1\_\_1up$	3.0441
$JET\_EffectiveNP\_1\_\_1down$	-2.31258
$JET\_EffectiveNP\_2\_\_1up$	-0.324077
$JET\_EffectiveNP\_2\_\_1down$	0.280546
$JET\_EffectiveNP\_3\_\_1up$	0.036392
$JET\_EffectiveNP\_3\_\_1down$	0.185793
$JET\_EffectiveNP\_4\_\_1up$	0.185825
$JET\_EffectiveNP\_4\_\_1down$	0.0330047
$JET\_EffectiveNP\_5\_\_1up$	-0.000989775
$JET\_EffectiveNP\_5\_\_1down$	0.221169
$JET\_EffectiveNP\_6\_\_1up$	0.0356397
$JET\_EffectiveNP\_6\_\_1down$	0.0049169
$JET\_EffectiveNP\_7\_\_1up$	0.165148
$JET\_EffectiveNP\_7\_\_1down$	0.0281939
$JET\_EffectiveNP\_8restTerm\_\_1up$	0.200961
$JET\_EffectiveNP\_8restTerm\_\_1down$	-0.000877335
$JET\_EtaIntercalibration\_Modelling\_\_1up$	0.578097
$JET\_EtaIntercalibration\_Modelling\_\_1down$	-0.522543
$JET\_EtaIntercalibration\_NonClosure\_\_1up$	-0.220832
$JET\_EtaIntercalibration\_NonClosure\_\_1down$	0.477048
$JET\_EtaIntercalibration\_TotalStat\_\_1up$	0.344507
$JET\_EtaIntercalibration\_TotalStat\_\_1down$	-0.361741
$JET\_Flavor\_Composition\_\_1up$	8.31211
$JET\_Flavor\_Composition\_\_1down$	-5.43258
$JET\_Flavor\_Response\_\_1up$	-1.39873
$JET\_Flavor\_Response\_\_1down$	1.0571
$JET\_JER\_SINGLE\_NP\_\_1up$	3.86087
$JET\_JvtEfficiency\_\_1down$	-0.535541
$JET\_JvtEfficiency\_\_1up$	0.537396
$JET\_Pileup\_OffsetMu\_\_1up$	-0.208226
$JET\_Pileup\_OffsetMu\_\_1down$	0.131217
$JET\_Pileup\_OffsetNPV\_\_1up$	0.980307
$JET\_Pileup\_OffsetNPV\_\_1down$	-0.748568
$JET\_Pileup\_PtTerm\_\_1up$	0.248664
$JET\_Pileup\_PtTerm\_\_1down$	-0.0163349
$JET\_Pileup\_RhoTopology\_\_1up$	4.60248
$JET\_Pileup\_RhoTopology\_\_1down$	-3.16769
$JET\_PunchThrough\_MC15\_\_1up$	-1.88973e-05
$JET\_PunchThrough\_MC15\_\_1down$	0
$JET\_SingleParticle\_HighPt\_\_1up$	0
$JET\_SingleParticle\_HighPt\_\_1down$	0

Table 39: Systematic uncertainties for Zh in percent in one lepton region without $p_T(\gamma\gamma)$ cut applied.

Uncertainty Source	Relative Variations
$FT\_EFF\_Eigen\_B\_0\_\_1down$	-0.425695
$FT\_EFF\_Eigen\_B\_0\_\_1up$	0.427555
$FT\_EFF\_Eigen\_B\_1\_\_1down$	-0.0986619
$FT\_EFF\_Eigen\_B\_1\_\_1up$	0.0985928
$FT\_EFF\_Eigen\_B\_2\_\_1down$	0.0817472
$FT\_EFF\_Eigen\_B\_2\_\_1up$	-0.0817576
$FT\_EFF\_Eigen\_C\_0\_\_1down$	-0.634753
$FT\_EFF\_Eigen\_C\_0\_\_1up$	0.641572
$FT\_EFF\_Eigen\_C\_1\_\_1down$	0.00426713
$FT\_EFF\_Eigen\_C\_1\_\_1up$	-0.00396342
$FT\_EFF\_Eigen\_C\_2\_\_1down$	-0.0166689
$FT\_EFF\_Eigen\_C\_2\_\_1up$	0.0167306
$FT\_EFF\_Eigen\_C\_3\_\_1down$	0.027708
$FT\_EFF\_Eigen\_C\_3\_\_1up$	-0.0276889
$FT\_EFF\_Eigen\_Light\_0\_\_1down$	-0.26381
$FT\_EFF\_Eigen\_Light\_0\_\_1up$	0.264258
$FT\_EFF\_Eigen\_Light\_1\_\_1down$	0.0416827
$FT\_EFF\_Eigen\_Light\_1\_\_1up$	-0.0416709
$FT\_EFF\_Eigen\_Light\_2\_\_1down$	0.00335586
$FT\_EFF\_Eigen\_Light\_2\_\_1up$	-0.00335263
$FT\_EFF\_Eigen\_Light\_3\_\_1down$	0.0248221
$FT\_EFF\_Eigen\_Light\_3\_\_1up$	-0.0248169
$FT\_EFF\_Eigen\_Light\_4\_\_1down$	0.019197
$FT\_EFF\_Eigen\_Light\_4\_\_1up$	-0.019194
$FT\_EFF\_extrapolation\_\_1down$	0.00881996
$FT\_EFF\_extrapolation\_\_1up$	-0.00881999
$FT\_EFF\_extrapolation\_from\_charm\_\_1down$	0.0795361
$FT\_EFF\_extrapolation\_from\_charm\_\_1up$	-0.0795184

Table 40: Systematic uncertainties for Zh in percent in one lepton region without $p_T(\gamma\gamma)$ cut applied.

Uncertainty Source	Relative Variations
nominal	0
EG_RESOLUTION_ALL__1down	0.953526
EG_RESOLUTION_ALL__1up	-0.0170817
EG_SCALE_ALL__1down	-0.0081652
EG_SCALE_ALL__1up	0.017471
EL_EFF_ID_TOTAL_1NPCOR_PLUS_UNCOR__1down	-0.460155
EL_EFF_ID_TOTAL_1NPCOR_PLUS_UNCOR__1up	0.460155
EL_EFF_Iso_TOTAL_1NPCOR_PLUS_UNCOR__1down	-0.0205882
EL_EFF_Iso_TOTAL_1NPCOR_PLUS_UNCOR__1up	0.0205883
EL_EFF_Reco_TOTAL_1NPCOR_PLUS_UNCOR__1down	-0.125262
EL_EFF_Reco_TOTAL_1NPCOR_PLUS_UNCOR__1up	0.125262
MUON_EFF_STAT__1down	-1.1394
MUON_EFF_STAT__1up	1.1394
MUON_EFF_SYS__1down	-1.16159
MUON_EFF_SYS__1up	1.16159
MUON_ID__1down	0.00185505
MUON_ID__1up	0
MUON_ISO_STAT__1down	-0.242427
MUON_ISO_STAT__1up	0.242427
MUON_ISO_SYS__1down	-0.129533
MUON_ISO_SYS__1up	0.12953
MUON_MS__1down	0
MUON_MS__1up	0
MUON_SAGITTA_RESBIAS__1down	0
MUON_SAGITTA_RESBIAS__1up	0
MUON_SAGITTA_RHO__1down	0
MUON_SAGITTA_RHO__1up	0
MUON_SCALE__1down	0
MUON_SCALE__1up	0
MUON_TTVA_STAT__1down	-0.348912
MUON_TTVA_STAT__1up	0.348912
MUON_TTVA_SYS__1down	-0.134795
MUON_TTVA_SYS__1up	0.134795
PH_EFF_ID_Uncertainty__1down	-1.44564
PH_EFF_ID_Uncertainty__1up	1.45674
PH_EFF_TRKISO_Uncertainty__1down	-0.778027
PH_EFF_TRKISO_Uncertainty__1up	0.781359
PH_Iso_DDonoff	1.84745
PRW_DATASF__1down	-5.42056
PRW_DATASF__1up	0.0998584

Table 41: Systematic uncertainties for VBF in percent in one lepton region without $p_T(\gamma\gamma)$ cut applied.

Uncertainty Source	Relative Variations
JET_BJES_Response__1up	-0.00115359
JET_BJES_Response__1down	0.000674515
JET_EffectiveNP_1__1up	1.7242
JET_EffectiveNP_1__1down	-0.852597
JET_EffectiveNP_2__1up	0.0911839
JET_EffectiveNP_2__1down	0.0188812
JET_EffectiveNP_3__1up	-0.000429948
JET_EffectiveNP_3__1down	0.0395022
JET_EffectiveNP_4__1up	0.0396718
JET_EffectiveNP_4__1down	-0.000422317
JET_EffectiveNP_5__1up	0.0390791
JET_EffectiveNP_5__1down	1.6845e-05
JET_EffectiveNP_6__1up	-5.81832e-05
JET_EffectiveNP_6__1down	0.0397225
JET_EffectiveNP_7__1up	0.0396621
JET_EffectiveNP_7__1down	-1.18535e-05
JET_EffectiveNP_8restTerm__1up	-9.21712e-05
JET_EffectiveNP_8restTerm__1down	0.039757
JET_EtaIntercalibration_Modelling__1up	0.0375552
JET_EtaIntercalibration_Modelling__1down	0.0275318
JET_EtaIntercalibration_NonClosure__1up	0.0917713
JET_EtaIntercalibration_NonClosure__1down	-0.00113144
JET_EtaIntercalibration_TotalStat__1up	0.0172232
JET_EtaIntercalibration_TotalStat__1down	0.0912086
JET_Flavor_Composition__1up	2.90203
JET_Flavor_Composition__1down	-3.49921
JET_Flavor_Response__1up	0.0839987
JET_Flavor_Response__1down	0.69675
JET_JER_SINGLE_NP__1up	3.29864
JET_JvtEfficiency__1down	-0.353969
JET_JvtEfficiency__1up	0.355176
JET_Pileup_OffsetMu__1up	0.0933344
JET_Pileup_OffsetMu__1down	0.0167256
JET_Pileup_OffsetNPV__1up	0.0659938
JET_Pileup_OffsetNPV__1down	0.0271697
JET_Pileup_PtTerm__1up	0.0162876
JET_Pileup_PtTerm__1down	0.000520467
JET_Pileup_RhoTopology__1up	0.807597
JET_Pileup_RhoTopology__1down	-1.22965
JET_PunchThrough_MC15__1up	0
JET_PunchThrough_MC15__1down	0
JET_SingleParticle_HighPt__1up	0
JET_SingleParticle_HighPt__1down	0

Table 42: Systematic uncertainties for VBF in percent in one lepton region without $p_T(\gamma\gamma)$ cut applied.

Uncertainty Source	Relative Variations
$FT\_EFF\_Eigen\_B\_0\_\_1down$	-0.422985
$FT\_EFF\_Eigen\_B\_0\_\_1up$	0.422985
$FT\_EFF\_Eigen\_B\_1\_\_1down$	-0.0615609
$FT\_EFF\_Eigen\_B\_1\_\_1up$	0.0615609
$FT\_EFF\_Eigen\_B\_2\_\_1down$	0.0764919
$FT\_EFF\_Eigen\_B\_2\_\_1up$	-0.0764918
$FT\_EFF\_Eigen\_C\_0\_\_1down$	-1.14275
$FT\_EFF\_Eigen\_C\_0\_\_1up$	1.14302
$FT\_EFF\_Eigen\_C\_1\_\_1down$	-0.358197
$FT\_EFF\_Eigen\_C\_1\_\_1up$	0.358184
$FT\_EFF\_Eigen\_C\_2\_\_1down$	-0.09607
$FT\_EFF\_Eigen\_C\_2\_\_1up$	0.0960775
$FT\_EFF\_Eigen\_C\_3\_\_1down$	0.0704578
$FT\_EFF\_Eigen\_C\_3\_\_1up$	-0.070459
$FT\_EFF\_Eigen\_Light\_0\_\_1down$	-0.269741
$FT\_EFF\_Eigen\_Light\_0\_\_1up$	0.270273
$FT\_EFF\_Eigen\_Light\_1\_\_1down$	0.0333681
$FT\_EFF\_Eigen\_Light\_1\_\_1up$	-0.0333578
$FT\_EFF\_Eigen\_Light\_2\_\_1down$	0.0400058
$FT\_EFF\_Eigen\_Light\_2\_\_1up$	-0.0399928
$FT\_EFF\_Eigen\_Light\_3\_\_1down$	0.0249126
$FT\_EFF\_Eigen\_Light\_3\_\_1up$	-0.0249168
$FT\_EFF\_Eigen\_Light\_4\_\_1down$	0.0339202
$FT\_EFF\_Eigen\_Light\_4\_\_1up$	-0.0339144
$FT\_EFF\_extrapolation\_\_1down$	0.0419485
$FT\_EFF\_extrapolation\_\_1up$	-0.041949
$FT\_EFF\_extrapolation\_from\_charm\_\_1down$	0
$FT\_EFF\_extrapolation\_from\_charm\_\_1up$	0

Table 43: Systematic uncertainties for VBF in percent in one lepton region without $p_T(\gamma\gamma)$ cut applied.

Uncertainty Source	Relative Variations
nominal	0
EG_RESOLUTION_ALL__1down	-1.52823
EG_RESOLUTION_ALL__1up	1.4768
EG_SCALE_ALL__1down	1.48157
EG_SCALE_ALL__1up	-1.53195
EL_EFF_ID_TOTAL_1NPCOR_PLUS_UNCOR__1down	-0.409569
EL_EFF_ID_TOTAL_1NPCOR_PLUS_UNCOR__1up	0.409569
EL_EFF_Iso_TOTAL_1NPCOR_PLUS_UNCOR__1down	-0.0170324
EL_EFF_Iso_TOTAL_1NPCOR_PLUS_UNCOR__1up	0.0170323
EL_EFF_Reco_TOTAL_1NPCOR_PLUS_UNCOR__1down	-0.121956
EL_EFF_Reco_TOTAL_1NPCOR_PLUS_UNCOR__1up	0.121955
MUON_EFF_STAT__1down	-3.66996
MUON_EFF_STAT__1up	3.66996
MUON_EFF_SYS__1down	-3.68086
MUON_EFF_SYS__1up	3.68086
MUON_ID__1down	0
MUON_ID__1up	0
MUON_ISO_STAT__1down	-0.242024
MUON_ISO_STAT__1up	0.242025
MUON_ISO_SYS__1down	-0.128764
MUON_ISO_SYS__1up	0.12876
MUON_MS__1down	0
MUON_MS__1up	2.03383
MUON_SAGITTA_RESBIAS__1down	0
MUON_SAGITTA_RESBIAS__1up	0
MUON_SAGITTA_RHO__1down	0
MUON_SAGITTA_RHO__1up	0
MUON_SCALE__1down	0
MUON_SCALE__1up	0
MUON_TTVA_STAT__1down	-0.369052
MUON_TTVA_STAT__1up	0.369052
MUON_TTVA_SYS__1down	-0.120652
MUON_TTVA_SYS__1up	0.120651
PH_EFF_ID_Uncertainty__1down	-1.55782
PH_EFF_ID_Uncertainty__1up	1.57051
PH_EFF_TRKISO_Uncertainty__1down	-0.743886
PH_EFF_TRKISO_Uncertainty__1up	0.7468
PH_Iso_DDonoff	0
PRW_DATASF__1down	-4.58649
PRW_DATASF__1up	-1.10324

Table 44: Systematic uncertainties for ggh in percent in one lepton region without $p_T(\gamma\gamma)$ cut applied.

Uncertainty Source	Relative Variations
JET_BJES_Response__1up	-0.00631053
JET_BJES_Response__1down	0.00433381
JET_EffectiveNP_1__1up	3.23323
JET_EffectiveNP_1__1down	-1.54428
JET_EffectiveNP_2__1up	-0.0278767
JET_EffectiveNP_2__1down	0.012819
JET_EffectiveNP_3__1up	0.000246504
JET_EffectiveNP_3__1down	-0.0004208
JET_EffectiveNP_4__1up	-0.000422317
JET_EffectiveNP_4__1down	0.00119528
JET_EffectiveNP_5__1up	0.000955996
JET_EffectiveNP_5__1down	0.0127971
JET_EffectiveNP_6__1up	0.0128347
JET_EffectiveNP_6__1down	-4.27755e-06
JET_EffectiveNP_7__1up	-7.39217e-05
JET_EffectiveNP_7__1down	-0.000100238
JET_EffectiveNP_8restTerm__1up	-0.000232008
JET_EffectiveNP_8restTerm__1down	0.000166624
JET_EtaIntercalibration_Modelling__1up	1.46294
JET_EtaIntercalibration_Modelling__1down	0.00627484
JET_EtaIntercalibration_NonClosure__1up	0.00547038
JET_EtaIntercalibration_NonClosure__1down	-0.0415511
JET_EtaIntercalibration_TotalStat__1up	0.0124268
JET_EtaIntercalibration_TotalStat__1down	-0.026268
JET_Flavor_Composition__1up	15.3552
JET_Flavor_Composition__1down	-5.95582
JET_Flavor_Response__1up	-0.0376125
JET_Flavor_Response__1down	1.46414
JET_JER_SINGLE_NP__1up	7.44641
JET_JvtEfficiency__1down	-0.592277
JET_JvtEfficiency__1up	0.594901
JET_Pileup_OffsetMu__1up	0.0136958
JET_Pileup_OffsetMu__1down	0.00419188
JET_Pileup_OffsetNPV__1up	0.0113038
JET_Pileup_OffsetNPV__1down	-0.0301702
JET_Pileup_PtTerm__1up	0.0117992
JET_Pileup_PtTerm__1down	-0.0387644
JET_Pileup_RhoTopology__1up	9.71342
JET_Pileup_RhoTopology__1down	-4.01986
JET_PunchThrough_MC15__1up	-1.42016e-07
JET_PunchThrough_MC15__1down	0
JET_SingleParticle_HighPt__1up	0
JET_SingleParticle_HighPt__1down	0

Table 45: Systematic uncertainties for *ggh* in percent in one lepton region without $p_T(\gamma\gamma)$ cut applied.

Uncertainty Source	Relative Variations
$FT\_EFF\_Eigen\_B\_0\_\_1down$	-0.931471
$FT\_EFF\_Eigen\_B\_0\_\_1up$	0.941972
$FT\_EFF\_Eigen\_B\_1\_\_1down$	-0.131991
$FT\_EFF\_Eigen\_B\_1\_\_1up$	0.131921
$FT\_EFF\_Eigen\_B\_2\_\_1down$	0.118169
$FT\_EFF\_Eigen\_B\_2\_\_1up$	-0.118099
$FT\_EFF\_Eigen\_C\_0\_\_1down$	-0.372185
$FT\_EFF\_Eigen\_C\_0\_\_1up$	0.372185
$FT\_EFF\_Eigen\_C\_1\_\_1down$	0.0345223
$FT\_EFF\_Eigen\_C\_1\_\_1up$	-0.0345222
$FT\_EFF\_Eigen\_C\_2\_\_1down$	0.00270721
$FT\_EFF\_Eigen\_C\_2\_\_1up$	-0.00270707
$FT\_EFF\_Eigen\_C\_3\_\_1down$	0.0306874
$FT\_EFF\_Eigen\_C\_3\_\_1up$	-0.0306873
$FT\_EFF\_Eigen\_Light\_0\_\_1down$	-0.297775
$FT\_EFF\_Eigen\_Light\_0\_\_1up$	0.298343
$FT\_EFF\_Eigen\_Light\_1\_\_1down$	0.0559665
$FT\_EFF\_Eigen\_Light\_1\_\_1up$	-0.0559454
$FT\_EFF\_Eigen\_Light\_2\_\_1down$	-0.0223491
$FT\_EFF\_Eigen\_Light\_2\_\_1up$	0.022373
$FT\_EFF\_Eigen\_Light\_3\_\_1down$	0.0294458
$FT\_EFF\_Eigen\_Light\_3\_\_1up$	-0.0294438
$FT\_EFF\_Eigen\_Light\_4\_\_1down$	0.0149886
$FT\_EFF\_Eigen\_Light\_4\_\_1up$	-0.0149892
$FT\_EFF\_extrapolation\_\_1down$	0
$FT\_EFF\_extrapolation\_\_1up$	0
$FT\_EFF\_extrapolation\_from\_charm\_\_1down$	0
$FT\_EFF\_extrapolation\_from\_charm\_\_1up$	0

Table 46: Systematic uncertainties for ggh in percent in one lepton region without $p_T(\gamma\gamma)$ cut applied.

Uncertainty Source	Relative Variations
nominal	0
EG_RESOLUTION_ALL__1down	-0.0556198
EG_RESOLUTION_ALL__1up	0.0406091
EG_SCALE_ALL__1down	0.0494382
EG_SCALE_ALL__1up	0.012464
EL_EFF_ID_TOTAL_1NPCOR_PLUS_UNCOR__1down	-0.512883
EL_EFF_ID_TOTAL_1NPCOR_PLUS_UNCOR__1up	0.512883
EL_EFF_Iso_TOTAL_1NPCOR_PLUS_UNCOR__1down	-0.0738717
EL_EFF_Iso_TOTAL_1NPCOR_PLUS_UNCOR__1up	0.0738716
EL_EFF_Reco_TOTAL_1NPCOR_PLUS_UNCOR__1down	-0.14291
EL_EFF_Reco_TOTAL_1NPCOR_PLUS_UNCOR__1up	0.14291
MUON_EFF_STAT__1down	-0.23046
MUON_EFF_STAT__1up	0.23046
MUON_EFF_SYS__1down	-0.439572
MUON_EFF_SYS__1up	0.440034
MUON_ID__1down	-0.050929
MUON_ID__1up	-0.0265046
MUON_ISO_STAT__1down	-0.0484389
MUON_ISO_STAT__1up	0.0484395
MUON_ISO_SYS__1down	-0.100503
MUON_ISO_SYS__1up	0.100502
MUON_MS__1down	-0.0613195
MUON_MS__1up	-0.00824064
MUON_SAGITTA_RESBIAS__1down	0
MUON_SAGITTA_RESBIAS__1up	0
MUON_SAGITTA_RHO__1down	0
MUON_SAGITTA_RHO__1up	0
MUON_SCALE__1down	0.0181895
MUON_SCALE__1up	-0.0112826
MUON_TTVA_STAT__1down	-0.103894
MUON_TTVA_STAT__1up	0.103894
MUON_TTVA_SYS__1down	-0.0530074
MUON_TTVA_SYS__1up	0.0530074
PH_EFF_ID_Uncertainty__1down	-1.61819
PH_EFF_ID_Uncertainty__1up	1.6315
PH_EFF_TRKISO_Uncertainty__1down	-0.765879
PH_EFF_TRKISO_Uncertainty__1up	0.769051
PH_Iso_DDonoff	0.0178505
PRW_DATASF__1down	0.272447
PRW_DATASF__1up	0.836547

Table 47: Systematic uncertainties for SM Higgs pair process in percent in one lepton region without $p_T(\gamma\gamma)$ cut applied.

Uncertainty Source	Relative Variations
$JET\_BJES\_Response\_\_1up$	-0.00634441
$JET\_BJES\_Response\_\_1down$	0.00742968
$JET\_EffectiveNP\_1\_\_1up$	1.47043
$JET\_EffectiveNP\_1\_\_1down$	-1.35102
$JET\_EffectiveNP\_2\_\_1up$	-0.382535
$JET\_EffectiveNP\_2\_\_1down$	0.280547
$JET\_EffectiveNP\_3\_\_1up$	0.076654
$JET\_EffectiveNP\_3\_\_1down$	-0.0544159
$JET\_EffectiveNP\_4\_\_1up$	-0.0256944
$JET\_EffectiveNP\_4\_\_1down$	0.0320802
$JET\_EffectiveNP\_5\_\_1up$	-0.0357717
$JET\_EffectiveNP\_5\_\_1down$	0.0426226
$JET\_EffectiveNP\_6\_\_1up$	0.102353
$JET\_EffectiveNP\_6\_\_1down$	-0.0615842
$JET\_EffectiveNP\_7\_\_1up$	-0.0567163
$JET\_EffectiveNP\_7\_\_1down$	0.137102
$JET\_EffectiveNP\_8restTerm\_\_1up$	0.0382057
$JET\_EffectiveNP\_8restTerm\_\_1down$	-0.0367334
$JET\_EtaIntercalibration\_Modelling\_\_1up$	0.658323
$JET\_EtaIntercalibration\_Modelling\_\_1down$	-0.485387
$JET\_EtaIntercalibration\_NonClosure\_\_1up$	-0.275345
$JET\_EtaIntercalibration\_NonClosure\_\_1down$	0.210464
$JET\_EtaIntercalibration\_TotalStat\_\_1up$	0.226605
$JET\_EtaIntercalibration\_TotalStat\_\_1down$	-0.312316
$JET\_Flavor\_Composition\_\_1up$	2.98393
$JET\_Flavor\_Composition\_\_1down$	-3.28335
$JET\_Flavor\_Response\_\_1up$	-0.982917
$JET\_Flavor\_Response\_\_1down$	0.920792
$JET\_JER\_SINGLE\_NP\_\_1up$	-0.23153
$JET\_JvtEfficiency\_\_1down$	-0.636952
$JET\_JvtEfficiency\_\_1up$	0.640118
$JET\_Pileup\_OffsetMu\_\_1up$	-0.131008
$JET\_Pileup\_OffsetMu\_\_1down$	0.151986
$JET\_Pileup\_OffsetNPV\_\_1up$	0.327895
$JET\_Pileup\_OffsetNPV\_\_1down$	-0.386444
$JET\_Pileup\_PtTerm\_\_1up$	0.0752004
$JET\_Pileup\_PtTerm\_\_1down$	0.0128304
$JET\_Pileup\_RhoTopology\_\_1up$	2.05416
$JET\_Pileup\_RhoTopology\_\_1down$	-2.12867
$JET\_PunchThrough\_MC15\_\_1up$	6.6676e-07
$JET\_PunchThrough\_MC15\_\_1down$	1.59135e-07
$JET\_SingleParticle\_HighPt\_\_1up$	0
$JET\_SingleParticle\_HighPt\_\_1down$	0

Table 48: Systematic uncertainties for SM Higgs pair process in percent in one lepton region without $p_T(\gamma\gamma)$ cut applied.

Uncertainty Source	Relative Variations
$FT\_EFF\_Eigen\_B\_0\_\_1down$	-0.0532314
$FT\_EFF\_Eigen\_B\_0\_\_1up$	0.0537035
$FT\_EFF\_Eigen\_B\_1\_\_1down$	-0.0146869
$FT\_EFF\_Eigen\_B\_1\_\_1up$	0.014721
$FT\_EFF\_Eigen\_B\_2\_\_1down$	0.00851813
$FT\_EFF\_Eigen\_B\_2\_\_1up$	-0.00855245
$FT\_EFF\_Eigen\_C\_0\_\_1down$	-1.49871
$FT\_EFF\_Eigen\_C\_0\_\_1up$	1.50474
$FT\_EFF\_Eigen\_C\_1\_\_1down$	-0.0293429
$FT\_EFF\_Eigen\_C\_1\_\_1up$	0.0293359
$FT\_EFF\_Eigen\_C\_2\_\_1down$	0.0139937
$FT\_EFF\_Eigen\_C\_2\_\_1up$	-0.0139421
$FT\_EFF\_Eigen\_C\_3\_\_1down$	0.0469302
$FT\_EFF\_Eigen\_C\_3\_\_1up$	-0.0469171
$FT\_EFF\_Eigen\_Light\_0\_\_1down$	-0.287233
$FT\_EFF\_Eigen\_Light\_0\_\_1up$	0.287862
$FT\_EFF\_Eigen\_Light\_1\_\_1down$	0.0484868
$FT\_EFF\_Eigen\_Light\_1\_\_1up$	-0.0484688
$FT\_EFF\_Eigen\_Light\_2\_\_1down$	-0.00950244
$FT\_EFF\_Eigen\_Light\_2\_\_1up$	0.00950951
$FT\_EFF\_Eigen\_Light\_3\_\_1down$	0.00915347
$FT\_EFF\_Eigen\_Light\_3\_\_1up$	-0.00915217
$FT\_EFF\_Eigen\_Light\_4\_\_1down$	0.0345496
$FT\_EFF\_Eigen\_Light\_4\_\_1up$	-0.0345427
$FT\_EFF\_extrapolation\_\_1down$	0.0154917
$FT\_EFF\_extrapolation\_\_1up$	-0.015497
$FT\_EFF\_extrapolation\_from\_charm\_\_1down$	0.000400323
$FT\_EFF\_extrapolation\_from\_charm\_\_1up$	-0.000400322

Table 49: Systematic uncertainties for SM Higgs pair process in percent in one lepton region without $p_T(\gamma\gamma)$ cut applied.

Uncertainty Source	Relative Variations
EL_EFF_ID_TOTAL_1NPCOR_PLUS_UNCOR__1down	-0.675097
EL_EFF_ID_TOTAL_1NPCOR_PLUS_UNCOR__1up	0.675097
EL_EFF_Iso_TOTAL_1NPCOR_PLUS_UNCOR__1down	-0.0340512
EL_EFF_Iso_TOTAL_1NPCOR_PLUS_UNCOR__1up	0.0340511
EL_EFF_Reco_TOTAL_1NPCOR_PLUS_UNCOR__1down	-0.211155
EL_EFF_Reco_TOTAL_1NPCOR_PLUS_UNCOR__1up	0.211155
MUON_EFF_STAT__1down	-0.357493
MUON_EFF_STAT__1up	0.357493
MUON_EFF_SYS__1down	-0.526677
MUON_EFF_SYS__1up	0.526877
MUON_ID__1down	-0.0117811
MUON_ID__1up	0.218636
MUON_ISO_STAT__1down	-0.0823346
MUON_ISO_STAT__1up	0.0823355
MUON_ISO_SYS__1down	-0.10736
MUON_ISO_SYS__1up	0.107358
MUON_MS__1down	0.146137
MUON_MS__1up	-0.0591802
MUON_SAGITTA_RESBIAS__1down	0
MUON_SAGITTA_RESBIAS__1up	0
MUON_SAGITTA_RHO__1down	0
MUON_SAGITTA_RHO__1up	0
MUON_SCALE__1down	0.151976
MUON_SCALE__1up	-0.044551
MUON_TTVA_STAT__1down	-0.154042
MUON_TTVA_STAT__1up	0.154042
MUON_TTVA_SYS__1down	-0.0595999
MUON_TTVA_SYS__1up	0.0595998
PH_EFF_ID_Uncertainty__1down	-1.44218
PH_EFF_ID_Uncertainty__1up	1.45227
PH_EFF_TRKISO_Uncertainty__1down	-0.745629
PH_EFF_TRKISO_Uncertainty__1up	0.748551
PH_Iso_DDonoff	0.0364698
PRW_DATASF__1down	0.581876
PRW_DATASF__1up	-0.846425

Table 50: Systematic uncertainties for m_H = 260 GeV in percent in one lepton region without $p_T(\gamma\gamma)$ cut applied.

Uncertainty Source	Relative Variations
JET_BJES_Response__1up	0.0364481
JET_BJES_Response__1down	0.0298853
JET_EffectiveNP_1__1up	3.90888
JET_EffectiveNP_1__1down	-2.81555
JET_EffectiveNP_2__1up	-1.01169
JET_EffectiveNP_2__1down	0.885465
JET_EffectiveNP_3__1up	0.0867493
JET_EffectiveNP_3__1down	-0.276057
JET_EffectiveNP_4__1up	-0.140511
JET_EffectiveNP_4__1down	0.115769
JET_EffectiveNP_5__1up	-0.0796343
JET_EffectiveNP_5__1down	0.111172
JET_EffectiveNP_6__1up	0.131941
JET_EffectiveNP_6__1down	-0.238467
JET_EffectiveNP_7__1up	-0.318684
JET_EffectiveNP_7__1down	0.155867
JET_EffectiveNP_8restTerm__1up	0.108097
JET_EffectiveNP_8restTerm__1down	-0.116121
JET_EtaIntercalibration_Modelling__1up	1.66683
JET_EtaIntercalibration_Modelling__1down	-1.48712
JET_EtaIntercalibration_NonClosure__1up	-0.593932
JET_EtaIntercalibration_NonClosure__1down	0.459304
JET_EtaIntercalibration_TotalStat__1up	0.746444
JET_EtaIntercalibration_TotalStat__1down	-0.914741
JET_Flavor_Composition__1up	7.67199
JET_Flavor_Composition__1down	-6.94799
JET_Flavor_Response__1up	-2.07578
JET_Flavor_Response__1down	2.67387
JET_JER_SINGLE_NP__1up	1.4945
JET_JvtEfficiency__1down	-0.812107
JET_JvtEfficiency__1up	0.816614
JET_Pileup_OffsetMu__1up	-0.232676
JET_Pileup_OffsetMu__1down	0.0576072
JET_Pileup_OffsetNPV__1up	0.982825
JET_Pileup_OffsetNPV__1down	-0.229665
JET_Pileup_PtTerm__1up	0.107061
JET_Pileup_PtTerm__1down	-0.0323359
JET_Pileup_RhoTopology__1up	5.07353
JET_Pileup_RhoTopology__1down	-3.97922
JET_PunchThrough_MC15__1up	-7.99705e-07
JET_PunchThrough_MC15__1down	-5.90278e-06
JET_SingleParticle_HighPt__1up	0
JET_SingleParticle_HighPt__1down	0

Table 51: Systematic uncertainties for m_H = 260 GeV in percent in one lepton region without $p_T(\gamma\gamma)$ cut applied.

Uncertainty Source	Relative Variations
$FT\_EFF\_Eigen\_B\_0\_\_1down$	-0.0879983
$FT\_EFF\_Eigen\_B\_0\_\_1up$	0.0880971
$FT\_EFF\_Eigen\_B\_1\_\_1down$	-0.00363612
$FT\_EFF\_Eigen\_B\_1\_\_1up$	0.00363082
$FT\_EFF\_Eigen\_B\_2\_\_1down$	0.0115458
$FT\_EFF\_Eigen\_B\_2\_\_1up$	-0.0115437
$FT\_EFF\_Eigen\_C\_0\_\_1down$	-1.00556
$FT\_EFF\_Eigen\_C\_0\_\_1up$	1.00861
$FT\_EFF\_Eigen\_C\_1\_\_1down$	0.275929
$FT\_EFF\_Eigen\_C\_1\_\_1up$	-0.275868
$FT\_EFF\_Eigen\_C\_2\_\_1down$	-0.0328963
$FT\_EFF\_Eigen\_C\_2\_\_1up$	0.0329065
$FT\_EFF\_Eigen\_C\_3\_\_1down$	0.0675572
$FT\_EFF\_Eigen\_C\_3\_\_1up$	-0.0675511
$FT\_EFF\_Eigen\_Light\_0\_\_1down$	-0.300506
$FT\_EFF\_Eigen\_Light\_0\_\_1up$	0.301124
$FT\_EFF\_Eigen\_Light\_1\_\_1down$	0.0595976
$FT\_EFF\_Eigen\_Light\_1\_\_1up$	-0.0595734
$FT\_EFF\_Eigen\_Light\_2\_\_1down$	-0.0408728
$FT\_EFF\_Eigen\_Light\_2\_\_1up$	0.0408841
$FT\_EFF\_Eigen\_Light\_3\_\_1down$	0.0194861
$FT\_EFF\_Eigen\_Light\_3\_\_1up$	-0.0194826
$FT\_EFF\_Eigen\_Light\_4\_\_1down$	0.00791545
$FT\_EFF\_Eigen\_Light\_4\_\_1up$	-0.00791426
$FT\_EFF\_extrapolation\_\_1down$	0.000959514
$FT\_EFF\_extrapolation\_\_1up$	-0.00095951
$FT\_EFF\_extrapolation\_from\_charm\_\_1down$	0.000281282
$FT\_EFF\_extrapolation\_from\_charm\_\_1up$	-0.000281283

Table 52: Systematic uncertainties for m_H = 260 GeV in percent in one lepton region without $p_T(\gamma\gamma)$ cut applied.

Uncertainty Source	Relative Variations
EL_EFF_ID_TOTAL_1NPCOR_PLUS_UNCOR__1down	-0.598587
EL_EFF_ID_TOTAL_1NPCOR_PLUS_UNCOR__1up	0.598586
EL_EFF_Iso_TOTAL_1NPCOR_PLUS_UNCOR__1down	-0.0346488
EL_EFF_Iso_TOTAL_1NPCOR_PLUS_UNCOR__1up	0.0346487
EL_EFF_Reco_TOTAL_1NPCOR_PLUS_UNCOR__1down	-0.178384
EL_EFF_Reco_TOTAL_1NPCOR_PLUS_UNCOR__1up	0.178383
MUON_EFF_STAT__1down	-0.311864
MUON_EFF_STAT__1up	0.311864
MUON_EFF_SYS__1down	-0.494398
MUON_EFF_SYS__1up	0.494666
MUON_ID__1down	0.0558797
MUON_ID__1up	-0.0513436
MUON_ISO_STAT__1down	-0.0697496
MUON_ISO_STAT__1up	0.0697505
MUON_ISO_SYS__1down	-0.107505
MUON_ISO_SYS__1up	0.107503
MUON_MS__1down	0.0522322
MUON_MS__1up	0.0337712
MUON_SAGITTA_RESBIAS__1down	0
MUON_SAGITTA_RESBIAS__1up	0
MUON_SAGITTA_RHO__1down	0
MUON_SAGITTA_RHO__1up	0
MUON_SCALE__1down	-0.000712263
MUON_SCALE__1up	0.0763127
MUON_TTVA_STAT__1down	-0.137214
MUON_TTVA_STAT__1up	0.137214
MUON_TTVA_SYS__1down	-0.0588281
MUON_TTVA_SYS__1up	0.058828
PH_EFF_ID_Uncertainty__1down	-1.4338
PH_EFF_ID_Uncertainty__1up	1.44397
PH_EFF_TRKISO_Uncertainty__1down	-0.736472
PH_EFF_TRKISO_Uncertainty__1up	0.73942
PH_Iso_DDonoff	0.1021
PRW_DATASF__1down	-0.491422
PRW_DATASF__1up	0.848256

Table 53: Systematic uncertainties for m_H = 300 GeV in percent in one lepton region without $p_T(\gamma\gamma)$ cut applied.

Uncertainty Source	Relative Variations
JET_BJES_Response__1up	0.0421141
JET_BJES_Response__1down	0.000190441
JET_EffectiveNP_1__1up	2.45987
JET_EffectiveNP_1__1down	-2.46367
JET_EffectiveNP_2__1up	-0.493623
JET_EffectiveNP_2__1down	0.790901
JET_EffectiveNP_3__1up	0.0550125
JET_EffectiveNP_3__1down	-0.0746209
JET_EffectiveNP_4__1up	-0.0382735
JET_EffectiveNP_4__1down	-0.0255607
JET_EffectiveNP_5__1up	-0.000960952
JET_EffectiveNP_5__1down	-0.00316738
JET_EffectiveNP_6__1up	0.0719043
JET_EffectiveNP_6__1down	-0.08383
JET_EffectiveNP_7__1up	-0.11911
JET_EffectiveNP_7__1down	0.0918789
JET_EffectiveNP_8restTerm__1up	-0.0229668
JET_EffectiveNP_8restTerm__1down	-0.0117085
JET_EtaIntercalibration_Modelling__1up	0.828874
JET_EtaIntercalibration_Modelling__1down	-0.760503
JET_EtaIntercalibration_NonClosure__1up	-0.316261
JET_EtaIntercalibration_NonClosure__1down	0.209625
JET_EtaIntercalibration_TotalStat__1up	0.592365
JET_EtaIntercalibration_TotalStat__1down	-0.37779
JET_Flavor_Composition__1up	5.00248
JET_Flavor_Composition__1down	-5.61561
JET_Flavor_Response__1up	-1.48493
JET_Flavor_Response__1down	1.56974
JET_JER_SINGLE_NP__1up	-0.228524
JET_JvtEfficiency__1down	-0.766822
JET_JvtEfficiency__1up	0.771121
JET_Pileup_OffsetMu__1up	-0.0958275
JET_Pileup_OffsetMu__1down	0.160604
JET_Pileup_OffsetNPV__1up	0.600908
JET_Pileup_OffsetNPV__1down	-0.214525
JET_Pileup_PtTerm__1up	-0.00156443
JET_Pileup_PtTerm__1down	-0.0104321
JET_Pileup_RhoTopology__1up	3.50705
JET_Pileup_RhoTopology__1down	-3.87193
JET_PunchThrough_MC15__1up	8.09011e-05
JET_PunchThrough_MC15__1down	8.0908e-05
JET_SingleParticle_HighPt__1up	8.09055e-05
JET_SingleParticle_HighPt__1down	8.09055e-05

Table 54: Systematic uncertainties for m_H = 300 GeV in percent in one lepton region without $p_T(\gamma\gamma)$ cut applied.

Uncertainty Source	Relative Variations
$FT\_EFF\_Eigen\_B\_0\_\_1down$	-0.0553237
$FT\_EFF\_Eigen\_B\_0\_\_1up$	0.056147
$FT\_EFF\_Eigen\_B\_1\_\_1down$	-0.00842724
$FT\_EFF\_Eigen\_B\_1\_\_1up$	0.00859039
$FT\_EFF\_Eigen\_B\_2\_\_1down$	0.00826442
$FT\_EFF\_Eigen\_B\_2\_\_1up$	-0.00810305
$FT\_EFF\_Eigen\_C\_0\_\_1down$	-1.16152
$FT\_EFF\_Eigen\_C\_0\_\_1up$	1.16588
$FT\_EFF\_Eigen\_C\_1\_\_1down$	0.25652
$FT\_EFF\_Eigen\_C\_1\_\_1up$	-0.256384
$FT\_EFF\_Eigen\_C\_2\_\_1down$	0.00200085
$FT\_EFF\_Eigen\_C\_2\_\_1up$	-0.00187498
$FT\_EFF\_Eigen\_C\_3\_\_1down$	0.0672032
$FT\_EFF\_Eigen\_C\_3\_\_1up$	-0.0670332
$FT\_EFF\_Eigen\_Light\_0\_\_1down$	-0.29042
$FT\_EFF\_Eigen\_Light\_0\_\_1up$	0.291187
$FT\_EFF\_Eigen\_Light\_1\_\_1down$	0.0575667
$FT\_EFF\_Eigen\_Light\_1\_\_1up$	-0.0573813
$FT\_EFF\_Eigen\_Light\_2\_\_1down$	-0.0363534
$FT\_EFF\_Eigen\_Light\_2\_\_1up$	0.0365251
$FT\_EFF\_Eigen\_Light\_3\_\_1down$	0.0163624
$FT\_EFF\_Eigen\_Light\_3\_\_1up$	-0.0161963
$FT\_EFF\_Eigen\_Light\_4\_\_1down$	0.0168745
$FT\_EFF\_Eigen\_Light\_4\_\_1up$	-0.0167099
$FT\_EFF\_extrapolation\_\_1down$	0.00137358
$FT\_EFF\_extrapolation\_\_1up$	-0.00121176
$FT\_EFF\_extrapolation\_from\_charm\_\_1down$	0.000246475
$FT\_EFF\_extrapolation\_from\_charm\_\_1up$	-8.46635e-05

Table 55: Systematic uncertainties for m_H = 300 GeV in percent in one lepton region without $p_T(\gamma\gamma)$ cut applied.

Uncertainty Source	Relative Variations
$EL\_EFF\_ID\_TOTAL\_1NPCOR\_PLUS\_UNCOR\_\_1down$	-0.468124
$EL\_EFF\_ID\_TOTAL\_1NPCOR\_PLUS\_UNCOR\_\_1up$	0.468123
$EL\_EFF\_Iso\_TOTAL\_1NPCOR\_PLUS\_UNCOR\_\_1down$	-0.159928
$EL\_EFF\_Iso\_TOTAL\_1NPCOR\_PLUS\_UNCOR\_\_1up$	0.159928
$EL\_EFF\_Reco\_TOTAL\_1NPCOR\_PLUS\_UNCOR\_\_1down$	-0.12334
$EL\_EFF\_Reco\_TOTAL\_1NPCOR\_PLUS\_UNCOR\_\_1up$	0.123339
$MUON\_EFF\_STAT\_\_1down$	-0.104575
$MUON\_EFF\_STAT\_\_1up$	0.104574
$MUON\_EFF\_SYS\_\_1down$	-0.364745
$MUON\_EFF\_SYS\_\_1up$	0.365491
$MUON\_ID\_\_1down$	2.38855e-05
$MUON\_ID\_\_1up$	2.95481e-05
$MUON\_ISO\_STAT\_\_1down$	-0.0389071
$MUON\_ISO\_STAT\_\_1up$	0.0389073
$MUON\_ISO\_SYS\_\_1down$	-0.110032
$MUON\_ISO\_SYS\_\_1up$	0.110031
$MUON\_MS\_\_1down$	3.27003e-05
$MUON\_MS\_\_1up$	0.000171115
$MUON\_SAGITTA\_RESBIAS\_\_1down$	0
$MUON\_SAGITTA\_RESBIAS\_\_1up$	0
$MUON\_SAGITTA\_RHO\_\_1down$	0
$MUON\_SAGITTA\_RHO\_\_1up$	0
$MUON\_SCALE\_\_1down$	0.000203282
$MUON\_SCALE\_\_1up$	0.000162128
$MUON\_TTVA\_STAT\_\_1down$	-0.0810245
$MUON\_TTVA\_STAT\_\_1up$	0.0810246
$MUON\_TTVA\_SYS\_\_1down$	-0.0483897
$MUON\_TTVA\_SYS\_\_1up$	0.0483898
$PH\_EFF\_ID\_Uncertainty\_\_1down$	-1.69952
$PH\_EFF\_ID\_Uncertainty\_\_1up$	1.71528
$PH\_EFF\_TRKISO\_Uncertainty\_\_1down$	-0.798445
$PH\_EFF\_TRKISO\_Uncertainty\_\_1up$	0.801916
$PH\_Iso\_DDonoff$	0
$PRW\_DATASF\_\_1down$	0.899056
$PRW\_DATASF\_\_1up$	1.45491

Table 56: Systematic uncertainties for tth in percent in one lepton region with $p_T(\gamma\gamma)$ cut applied.

Uncertainty Source	Relative Variations
$JET\_BJES\_Response\_\_1up$	0.116704
$JET\_BJES\_Response\_\_1down$	1.02055
$JET\_EffectiveNP\_1\_\_1up$	0.0260266
$JET\_EffectiveNP\_1\_\_1down$	1.12423
$JET\_EffectiveNP\_2\_\_1up$	0.554732
$JET\_EffectiveNP\_2\_\_1down$	-0.0121425
$JET\_EffectiveNP\_3\_\_1up$	-0.0097391
$JET\_EffectiveNP\_3\_\_1down$	0.190938
$JET\_EffectiveNP\_4\_\_1up$	0.181098
$JET\_EffectiveNP\_4\_\_1down$	-0.00650626
$JET\_EffectiveNP\_5\_\_1up$	0.17517
$JET\_EffectiveNP\_5\_\_1down$	0.00552037
$JET\_EffectiveNP\_6\_\_1up$	0.00573145
$JET\_EffectiveNP\_6\_\_1down$	0.177531
$JET\_EffectiveNP\_7\_\_1up$	0.177666
$JET\_EffectiveNP\_7\_\_1down$	-0.00470705
$JET\_EffectiveNP\_8restTerm\_\_1up$	0.0082096
$JET\_EffectiveNP\_8restTerm\_\_1down$	0.1718
$JET\_EtaIntercalibration\_Modelling\_\_1up$	0.147767
$JET\_EtaIntercalibration\_Modelling\_\_1down$	0.279977
$JET\_EtaIntercalibration\_NonClosure\_\_1up$	0.297457
$JET\_EtaIntercalibration\_NonClosure\_\_1down$	0.199687
$JET\_EtaIntercalibration\_TotalStat\_\_1up$	0.124901
$JET\_EtaIntercalibration\_TotalStat\_\_1down$	0.531413
$JET\_Flavor\_Composition\_\_1up$	-0.210492
$JET\_Flavor\_Composition\_\_1down$	-0.257702
$JET\_Flavor\_Response\_\_1up$	-0.188936
$JET\_Flavor\_Response\_\_1down$	-0.00456546
$JET\_JER\_SINGLE\_NP\_\_1up$	0.148948
$JET\_JvtEfficiency\_\_1down$	-0.611652
$JET\_JvtEfficiency\_\_1up$	0.614949
$JET\_Pileup\_OffsetMu\_\_1up$	0.365325
$JET\_Pileup\_OffsetMu\_\_1down$	0.00619168
$JET\_Pileup\_OffsetNPV\_\_1up$	0.980268
$JET\_Pileup\_OffsetNPV\_\_1down$	0.292719
$JET\_Pileup\_PtTerm\_\_1up$	0.0248392
$JET\_Pileup\_PtTerm\_\_1down$	-0.0196737
$JET\_Pileup\_RhoTopology\_\_1up$	-0.9715
$JET\_Pileup\_RhoTopology\_\_1down$	1.68904
$JET\_PunchThrough\_MC15\_\_1up$	-1.17779e-05
$JET\_PunchThrough\_MC15\_\_1down$	1.19382e-05
$JET\_SingleParticle\_HighPt\_\_1up$	0
$JET\_SingleParticle\_HighPt\_\_1down$	0

Table 57: Systematic uncertainties for tth in percent in one lepton region with $p_T(\gamma\gamma)$ cut applied.

Uncertainty Source	Relative Variations
$FT\_EFF\_Eigen\_B\_0\_\_1down$	-7.50226
$FT\_EFF\_Eigen\_B\_0\_\_1up$	7.78766
$FT\_EFF\_Eigen\_B\_1\_\_1down$	-3.80002
$FT\_EFF\_Eigen\_B\_1\_\_1up$	3.86351
$FT\_EFF\_Eigen\_B\_2\_\_1down$	1.1075
$FT\_EFF\_Eigen\_B\_2\_\_1up$	-1.0957
$FT\_EFF\_Eigen\_C\_0\_\_1down$	-1.54641
$FT\_EFF\_Eigen\_C\_0\_\_1up$	1.55049
$FT\_EFF\_Eigen\_C\_1\_\_1down$	-0.401379
$FT\_EFF\_Eigen\_C\_1\_\_1up$	0.401753
$FT\_EFF\_Eigen\_C\_2\_\_1down$	-0.0952325
$FT\_EFF\_Eigen\_C\_2\_\_1up$	0.0952413
$FT\_EFF\_Eigen\_C\_3\_\_1down$	0.0809451
$FT\_EFF\_Eigen\_C\_3\_\_1up$	-0.0809383
$FT\_EFF\_Eigen\_Light\_0\_\_1down$	-0.264276
$FT\_EFF\_Eigen\_Light\_0\_\_1up$	0.264882
$FT\_EFF\_Eigen\_Light\_1\_\_1down$	0.0310648
$FT\_EFF\_Eigen\_Light\_1\_\_1up$	-0.0310573
$FT\_EFF\_Eigen\_Light\_2\_\_1down$	0.0127531
$FT\_EFF\_Eigen\_Light\_2\_\_1up$	-0.0127529
$FT\_EFF\_Eigen\_Light\_3\_\_1down$	-0.0109577
$FT\_EFF\_Eigen\_Light\_3\_\_1up$	0.0109615
$FT\_EFF\_Eigen\_Light\_4\_\_1down$	0.0413153
$FT\_EFF\_Eigen\_Light\_4\_\_1up$	-0.0412986
$FT\_EFF\_extrapolation\_\_1down$	0.438676
$FT\_EFF\_extrapolation\_\_1up$	-0.432021
$FT\_EFF\_extrapolation\_from\_charm\_\_1down$	0.0203165
$FT\_EFF\_extrapolation\_from\_charm\_\_1up$	-0.0203165

Table 58: Systematic uncertainties for tth in percent in one lepton region with $p_T(\gamma\gamma)$ cut applied.

Uncertainty Source	Relative Variations
EL_EFF_ID_TOTAL_1NPCOR_PLUS_UNCOR__1down	-0.459169
EL_EFF_ID_TOTAL_1NPCOR_PLUS_UNCOR__1up	0.459169
EL_EFF_Iso_TOTAL_1NPCOR_PLUS_UNCOR__1down	-0.192462
EL_EFF_Iso_TOTAL_1NPCOR_PLUS_UNCOR__1up	0.192461
EL_EFF_Reco_TOTAL_1NPCOR_PLUS_UNCOR__1down	-0.115181
EL_EFF_Reco_TOTAL_1NPCOR_PLUS_UNCOR__1up	0.115181
MUON_EFF_STAT__1down	-0.40472
MUON_EFF_STAT__1up	0.40472
MUON_EFF_SYS__1down	-0.67767
MUON_EFF_SYS__1up	0.678804
MUON_ID__1down	0.000681681
MUON_ID__1up	0.000187764
MUON_ISO_STAT__1down	-0.0298554
MUON_ISO_STAT__1up	0.0298552
MUON_ISO_SYS__1down	-0.103595
MUON_ISO_SYS__1up	0.103594
MUON_MS__1down	0.153027
MUON_MS__1up	6.65609e-07
MUON_SAGITTA_RESBIAS__1down	0
MUON_SAGITTA_RESBIAS__1up	0
MUON_SAGITTA_RHO__1down	0
MUON_SAGITTA_RHO__1up	0
MUON_SCALE__1down	0.000502843
MUON_SCALE__1up	0
MUON_TTVA_STAT__1down	-0.0714486
MUON_TTVA_STAT__1up	0.0714487
MUON_TTVA_SYS__1down	-0.0444063
MUON_TTVA_SYS__1up	0.0444063
PH_EFF_ID_Uncertainty__1down	-1.68313
PH_EFF_ID_Uncertainty__1up	1.69783
PH_EFF_TRKISO_Uncertainty__1down	-0.832118
PH_EFF_TRKISO_Uncertainty__1up	0.835942
PH_Iso_DDonoff	0.0707
PRW_DATASF__1down	0.19209
PRW_DATASF__1up	1.50642

Table 59: Systematic uncertainties for Wh in percent in one lepton region with $p_T(\gamma\gamma)$ cut applied.

Uncertainty Source	Relative Variations
$JET\_BJES\_Response\_\_1up$	-0.000739321
$JET\_BJES\_Response\_\_1down$	0.000607054
$JET\_EffectiveNP\_1\_\_1up$	2.44203
$JET\_EffectiveNP\_1\_\_1down$	-1.59259
$JET\_EffectiveNP\_2\_\_1up$	-0.357732
$JET\_EffectiveNP\_2\_\_1down$	0.612856
$JET\_EffectiveNP\_3\_\_1up$	0.256942
$JET\_EffectiveNP\_3\_\_1down$	-0.243125
$JET\_EffectiveNP\_4\_\_1up$	-0.240448
$JET\_EffectiveNP\_4\_\_1down$	-0.00102691
$JET\_EffectiveNP\_5\_\_1up$	-0.246931
$JET\_EffectiveNP\_5\_\_1down$	0.00476418
$JET\_EffectiveNP\_6\_\_1up$	0.257532
$JET\_EffectiveNP\_6\_\_1down$	-0.246549
$JET\_EffectiveNP\_7\_\_1up$	-0.241363
$JET\_EffectiveNP\_7\_\_1down$	0.250735
$JET\_EffectiveNP\_8restTerm\_\_1up$	0.0025712
$JET\_EffectiveNP\_8restTerm\_\_1down$	-0.246587
$JET\_EtaIntercalibration\_Modelling\_\_1up$	0.268124
$JET\_EtaIntercalibration\_Modelling\_\_1down$	-0.879592
$JET\_EtaIntercalibration\_NonClosure\_\_1up$	-0.237776
$JET\_EtaIntercalibration\_NonClosure\_\_1down$	0.0358525
$JET\_EtaIntercalibration\_TotalStat\_\_1up$	0.307637
$JET\_EtaIntercalibration\_TotalStat\_\_1down$	-0.36696
$JET\_Flavor\_Composition\_\_1up$	7.00842
$JET\_Flavor\_Composition\_\_1down$	-5.13212
$JET\_Flavor\_Response\_\_1up$	-1.04271
$JET\_Flavor\_Response\_\_1down$	1.17845
$JET\_JER\_SINGLE\_NP\_\_1up$	5.95771
$JET\_JvtEfficiency\_\_1down$	-0.503824
$JET\_JvtEfficiency\_\_1up$	0.505436
$JET\_Pileup\_OffsetMu\_\_1up$	-0.315455
$JET\_Pileup\_OffsetMu\_\_1down$	-0.0646503
$JET\_Pileup\_OffsetNPV\_\_1up$	1.67684
$JET\_Pileup\_OffsetNPV\_\_1down$	-0.0911143
$JET\_Pileup\_PtTerm\_\_1up$	0.0150916
$JET\_Pileup\_PtTerm\_\_1down$	-0.0110644
$JET\_Pileup\_RhoTopology\_\_1up$	4.11459
$JET\_Pileup\_RhoTopology\_\_1down$	-2.21226
$JET\_PunchThrough\_MC15\_\_1up$	-4.32844e-07
$JET\_PunchThrough\_MC15\_\_1down$	1.69772e-05
$JET\_SingleParticle\_HighPt\_\_1up$	0
$JET\_SingleParticle\_HighPt\_\_1down$	0

Table 60: Systematic uncertainties for Wh in percent in one lepton region with $p_T(\gamma\gamma)$ cut applied.

Uncertainty Source	Relative Variations
$FT\_EFF\_Eigen\_B\_0\_\_1down$	-0.0928038
$FT\_EFF\_Eigen\_B\_0\_\_1up$	0.0928037
$FT\_EFF\_Eigen\_B\_1\_\_1down$	-0.0260989
$FT\_EFF\_Eigen\_B\_1\_\_1up$	0.0260988
$FT\_EFF\_Eigen\_B\_2\_\_1down$	5.94007e-05
$FT\_EFF\_Eigen\_B\_2\_\_1up$	-5.94302e-05
$FT\_EFF\_Eigen\_C\_0\_\_1down$	-0.572625
$FT\_EFF\_Eigen\_C\_0\_\_1up$	0.576667
$FT\_EFF\_Eigen\_C\_1\_\_1down$	-0.13346
$FT\_EFF\_Eigen\_C\_1\_\_1up$	0.133559
$FT\_EFF\_Eigen\_C\_2\_\_1down$	-0.0635219
$FT\_EFF\_Eigen\_C\_2\_\_1up$	0.0634261
$FT\_EFF\_Eigen\_C\_3\_\_1down$	0.039372
$FT\_EFF\_Eigen\_C\_3\_\_1up$	-0.0393811
$FT\_EFF\_Eigen\_Light\_0\_\_1down$	-0.283136
$FT\_EFF\_Eigen\_Light\_0\_\_1up$	0.283668
$FT\_EFF\_Eigen\_Light\_1\_\_1down$	0.0415218
$FT\_EFF\_Eigen\_Light\_1\_\_1up$	-0.0415106
$FT\_EFF\_Eigen\_Light\_2\_\_1down$	0.00112038
$FT\_EFF\_Eigen\_Light\_2\_\_1up$	-0.00111277
$FT\_EFF\_Eigen\_Light\_3\_\_1down$	0.00767927
$FT\_EFF\_Eigen\_Light\_3\_\_1up$	-0.00767395
$FT\_EFF\_Eigen\_Light\_4\_\_1down$	0.0261144
$FT\_EFF\_Eigen\_Light\_4\_\_1up$	-0.0261089
$FT\_EFF\_extrapolation\_\_1down$	0.0205549
$FT\_EFF\_extrapolation\_\_1up$	-0.0205549
$FT\_EFF\_extrapolation\_from\_charm\_\_1down$	0
$FT\_EFF\_extrapolation\_from\_charm\_\_1up$	0

Table 61: Systematic uncertainties for Wh in percent in one lepton region with $p_T(\gamma\gamma)$ cut applied.

Uncertainty Source	Relative Variations
$EL\_EFF\_ID\_TOTAL\_1NPCOR\_PLUS\_UNCOR\_\_1down$	-0.418701
$EL\_EFF\_ID\_TOTAL\_1NPCOR\_PLUS\_UNCOR\_\_1up$	0.418701
$EL\_EFF\_Iso\_TOTAL\_1NPCOR\_PLUS\_UNCOR\_\_1down$	-0.174594
$EL\_EFF\_Iso\_TOTAL\_1NPCOR\_PLUS\_UNCOR\_\_1up$	0.174593
$EL\_EFF\_Reco\_TOTAL\_1NPCOR\_PLUS\_UNCOR\_\_1down$	-0.123409
$EL\_EFF\_Reco\_TOTAL\_1NPCOR\_PLUS\_UNCOR\_\_1up$	0.123409
$MUON\_EFF\_STAT\_\_1down$	-0.101132
$MUON\_EFF\_STAT\_\_1up$	0.101132
$MUON\_EFF\_SYS\_\_1down$	-0.426728
$MUON\_EFF\_SYS\_\_1up$	0.428032
$MUON\_ID\_\_1down$	-0.000382584
$MUON\_ID\_\_1up$	-0.000456538
$MUON\_ISO\_STAT\_\_1down$	-0.0380428
$MUON\_ISO\_STAT\_\_1up$	0.0380425
$MUON\_ISO\_SYS\_\_1down$	-0.11216
$MUON\_ISO\_SYS\_\_1up$	0.11216
$MUON\_MS\_\_1down$	-0.000272997
$MUON\_MS\_\_1up$	-9.55645e-05
$MUON\_SAGITTA\_RESBIAS\_\_1down$	0
$MUON\_SAGITTA\_RESBIAS\_\_1up$	0
$MUON\_SAGITTA\_RHO\_\_1down$	0
$MUON\_SAGITTA\_RHO\_\_1up$	0
$MUON\_SCALE\_\_1down$	0
$MUON\_SCALE\_\_1up$	0
$MUON\_TTVA\_STAT\_\_1down$	-0.0787769
$MUON\_TTVA\_STAT\_\_1up$	0.0787766
$MUON\_TTVA\_SYS\_\_1down$	-0.055877
$MUON\_TTVA\_SYS\_\_1up$	0.0558768
$PH\_EFF\_ID\_Uncertainty\_\_1down$	-1.6994
$PH\_EFF\_ID\_Uncertainty\_\_1up$	1.71404
$PH\_EFF\_TRKISO\_Uncertainty\_\_1down$	-0.81872
$PH\_EFF\_TRKISO\_Uncertainty\_\_1up$	0.822643
$PH\_Iso\_DDonoff$	0
$PRW\_DATASF\_\_1down$	-0.390702
$PRW\_DATASF\_\_1up$	-0.562202

Table 62: Systematic uncertainties for Zh in percent in one lepton region with $p_T(\gamma\gamma)$ cut applied.

Uncertainty Source	Relative Variations
$JET\_BJES\_Response\_\_1up$	0.000910606
$JET\_BJES\_Response\_\_1down$	0.00131423
$JET\_EffectiveNP\_1\_\_1up$	2.41145
$JET\_EffectiveNP\_1\_\_1down$	-1.64196
$JET\_EffectiveNP\_2\_\_1up$	-0.0603545
$JET\_EffectiveNP\_2\_\_1down$	0.317473
$JET\_EffectiveNP\_3\_\_1up$	0.0779391
$JET\_EffectiveNP\_3\_\_1down$	-0.000160185
$JET\_EffectiveNP\_4\_\_1up$	-8.70834e-05
$JET\_EffectiveNP\_4\_\_1down$	0.0764308
$JET\_EffectiveNP\_5\_\_1up$	-0.0022544
$JET\_EffectiveNP\_5\_\_1down$	0.0798774
$JET\_EffectiveNP\_6\_\_1up$	0.067637
$JET\_EffectiveNP\_6\_\_1down$	-0.000194322
$JET\_EffectiveNP\_7\_\_1up$	-4.56486e-05
$JET\_EffectiveNP\_7\_\_1down$	0.0588003
$JET\_EffectiveNP\_8restTerm\_\_1up$	0.0797736
$JET\_EffectiveNP\_8restTerm\_\_1down$	-0.00213968
$JET\_EtaIntercalibration\_Modelling\_\_1up$	0.666787
$JET\_EtaIntercalibration\_Modelling\_\_1down$	-0.149423
$JET\_EtaIntercalibration\_NonClosure\_\_1up$	-0.00663997
$JET\_EtaIntercalibration\_NonClosure\_\_1down$	0.393235
$JET\_EtaIntercalibration\_TotalStat\_\_1up$	0.0665094
$JET\_EtaIntercalibration\_TotalStat\_\_1down$	-0.0115115
$JET\_Flavor\_Composition\_\_1up$	5.46873
$JET\_Flavor\_Composition\_\_1down$	-4.25065
$JET\_Flavor\_Response\_\_1up$	-0.479069
$JET\_Flavor\_Response\_\_1down$	1.09514
$JET\_JER\_SINGLE\_NP\_\_1up$	1.97601
$JET\_JvtEfficiency\_\_1down$	-0.495114
$JET\_JvtEfficiency\_\_1up$	0.496769
$JET\_Pileup\_OffsetMu\_\_1up$	0.0780539
$JET\_Pileup\_OffsetMu\_\_1down$	0.101962
$JET\_Pileup\_OffsetNPV\_\_1up$	0.332277
$JET\_Pileup\_OffsetNPV\_\_1down$	-0.617625
$JET\_Pileup\_PtTerm\_\_1up$	0.131809
$JET\_Pileup\_PtTerm\_\_1down$	-0.0103645
$JET\_Pileup\_RhoTopology\_\_1up$	3.46397
$JET\_Pileup\_RhoTopology\_\_1down$	-2.22175
$JET\_PunchThrough\_MC15\_\_1up$	-3.94491e-05
$JET\_PunchThrough\_MC15\_\_1down$	0
$JET\_SingleParticle\_HighPt\_\_1up$	0
$JET\_SingleParticle\_HighPt\_\_1down$	0

Table 63: Systematic uncertainties for Zh in percent in one lepton region with $p_T(\gamma\gamma)$ cut applied.

Uncertainty Source	Relative Variations
$FT\_EFF\_Eigen\_B\_0\_\_1down$	-0.241225
$FT\_EFF\_Eigen\_B\_0\_\_1up$	0.241225
$FT\_EFF\_Eigen\_B\_1\_\_1down$	-0.119394
$FT\_EFF\_Eigen\_B\_1\_\_1up$	0.119394
$FT\_EFF\_Eigen\_B\_2\_\_1down$	0.0442263
$FT\_EFF\_Eigen\_B\_2\_\_1up$	-0.0442262
$FT\_EFF\_Eigen\_C\_0\_\_1down$	-0.624151
$FT\_EFF\_Eigen\_C\_0\_\_1up$	0.629149
$FT\_EFF\_Eigen\_C\_1\_\_1down$	-0.0528085
$FT\_EFF\_Eigen\_C\_1\_\_1up$	0.0534747
$FT\_EFF\_Eigen\_C\_2\_\_1down$	-0.0253924
$FT\_EFF\_Eigen\_C\_2\_\_1up$	0.0255068
$FT\_EFF\_Eigen\_C\_3\_\_1down$	0.0293245
$FT\_EFF\_Eigen\_C\_3\_\_1up$	-0.0292885
$FT\_EFF\_Eigen\_Light\_0\_\_1down$	-0.256349
$FT\_EFF\_Eigen\_Light\_0\_\_1up$	0.256777
$FT\_EFF\_Eigen\_Light\_1\_\_1down$	0.0348109
$FT\_EFF\_Eigen\_Light\_1\_\_1up$	-0.0348036
$FT\_EFF\_Eigen\_Light\_2\_\_1down$	0.0107007
$FT\_EFF\_Eigen\_Light\_2\_\_1up$	-0.0106896
$FT\_EFF\_Eigen\_Light\_3\_\_1down$	0.0113036
$FT\_EFF\_Eigen\_Light\_3\_\_1up$	-0.0113024
$FT\_EFF\_Eigen\_Light\_4\_\_1down$	0.0217286
$FT\_EFF\_Eigen\_Light\_4\_\_1up$	-0.0217252
$FT\_EFF\_extrapolation\_\_1down$	0.0137011
$FT\_EFF\_extrapolation\_\_1up$	-0.0137011
$FT\_EFF\_extrapolation\_from\_charm\_\_1down$	0.0944637
$FT\_EFF\_extrapolation\_from\_charm\_\_1up$	-0.0944267

Table 64: Systematic uncertainties for Zh in percent in one lepton region with $p_T(\gamma\gamma)$ cut applied.

Uncertainty Source	Relative Variations
EL_EFF_ID_TOTAL_1NPCOR_PLUS_UNCOR__1down	-0.639214
EL_EFF_ID_TOTAL_1NPCOR_PLUS_UNCOR__1up	0.639214
EL_EFF_Iso_TOTAL_1NPCOR_PLUS_UNCOR__1down	-0.0309921
EL_EFF_Iso_TOTAL_1NPCOR_PLUS_UNCOR__1up	0.0309922
EL_EFF_Reco_TOTAL_1NPCOR_PLUS_UNCOR__1down	-0.19099
EL_EFF_Reco_TOTAL_1NPCOR_PLUS_UNCOR__1up	0.190991
MUON_EFF_STAT__1down	-0.00405988
MUON_EFF_STAT__1up	0.0040597
MUON_EFF_SYS__1down	-0.0155657
MUON_EFF_SYS__1up	0.0155741
MUON_ID__1down	0
MUON_ID__1up	0
MUON_ISO_STAT__1down	-0.218406
MUON_ISO_STAT__1up	0.218405
MUON_ISO_SYS__1down	-0.114691
MUON_ISO_SYS__1up	0.114688
MUON_MS__1down	0
MUON_MS__1up	0
MUON_SAGITTA_RESBIAS__1down	0
MUON_SAGITTA_RESBIAS__1up	0
MUON_SAGITTA_RHO__1down	0
MUON_SAGITTA_RHO__1up	0
MUON_SCALE__1down	0
MUON_SCALE__1up	0
MUON_TTVA_STAT__1down	-0.311455
MUON_TTVA_STAT__1up	0.311456
MUON_TTVA_SYS__1down	-0.146917
MUON_TTVA_SYS__1up	0.146917
PH_EFF_ID_Uncertainty__1down	-1.42756
PH_EFF_ID_Uncertainty__1up	1.43949
PH_EFF_TRKISO_Uncertainty__1down	-0.702767
PH_EFF_TRKISO_Uncertainty__1up	0.705647
PH_Iso_DDonoff	3.36629
PRW_DATASF__1down	-5.24319
PRW_DATASF__1up	0.42167

Table 65: Systematic uncertainties for VBF in percent in one lepton region with $p_T(\gamma\gamma)$ cut applied.

Uncertainty Source	Relative Variations
$JET\_BJES\_Response\_\_1up$	-0.000460298
$JET\_BJES\_Response\_\_1down$	-0.000388933
$JET\_EffectiveNP\_1\_\_1up$	1.22385
$JET\_EffectiveNP\_1\_\_1down$	0.168464
$JET\_EffectiveNP\_2\_\_1up$	0.169763
$JET\_EffectiveNP\_2\_\_1down$	0.000237186
$JET\_EffectiveNP\_3\_\_1up$	-0.000877919
$JET\_EffectiveNP\_3\_\_1down$	0.0720759
$JET\_EffectiveNP\_4\_\_1up$	0.0723827
$JET\_EffectiveNP\_4\_\_1down$	-0.000923619
$JET\_EffectiveNP\_5\_\_1up$	0.0710834
$JET\_EffectiveNP\_5\_\_1down$	0.000153569
$JET\_EffectiveNP\_6\_\_1up$	-1.56119e-05
$JET\_EffectiveNP\_6\_\_1down$	0.072288
$JET\_EffectiveNP\_7\_\_1up$	0.0722906
$JET\_EffectiveNP\_7\_\_1down$	-4.35122e-05
$JET\_EffectiveNP\_8restTerm\_\_1up$	-7.69105e-05
$JET\_EffectiveNP\_8restTerm\_\_1down$	0.0723504
$JET\_EtaIntercalibration\_Modelling\_\_1up$	0.0240121
$JET\_EtaIntercalibration\_Modelling\_\_1down$	0.0709149
$JET\_EtaIntercalibration\_NonClosure\_\_1up$	0.169917
$JET\_EtaIntercalibration\_NonClosure\_\_1down$	-0.00107816
$JET\_EtaIntercalibration\_TotalStat\_\_1up$	-0.0024083
$JET\_EtaIntercalibration\_TotalStat\_\_1down$	0.168846
$JET\_Flavor\_Composition\_\_1up$	1.64423
$JET\_Flavor\_Composition\_\_1down$	-1.84326
$JET\_Flavor\_Response\_\_1up$	0.167798
$JET\_Flavor\_Response\_\_1down$	1.23455
$JET\_JER\_SINGLE\_NP\_\_1up$	-1.56317
$JET\_JvtEfficiency\_\_1down$	-0.262794
$JET\_JvtEfficiency\_\_1up$	0.263482
$JET\_Pileup\_OffsetMu\_\_1up$	0.169375
$JET\_Pileup\_OffsetMu\_\_1down$	-0.000255894
$JET\_Pileup\_OffsetNPV\_\_1up$	0.0954956
$JET\_Pileup\_OffsetNPV\_\_1down$	0.0717925
$JET\_Pileup\_PtTerm\_\_1up$	-0.00386056
$JET\_Pileup\_PtTerm\_\_1down$	0.000362053
$JET\_Pileup\_RhoTopology\_\_1up$	1.63797
$JET\_Pileup\_RhoTopology\_\_1down$	1.51901
$JET\_PunchThrough\_MC15\_\_1up$	0
$JET\_PunchThrough\_MC15\_\_1down$	0
$JET\_SingleParticle\_HighPt\_\_1up$	0
$JET\_SingleParticle\_HighPt\_\_1down$	0

Table 66: Systematic uncertainties for VBF in percent in one lepton region with $p_T(\gamma\gamma)$ cut applied.

Uncertainty Source	Relative Variations
$FT\_EFF\_Eigen\_B\_0\_\_1down$	-0.0939438
$FT\_EFF\_Eigen\_B\_0\_\_1up$	0.0939438
$FT\_EFF\_Eigen\_B\_1\_\_1down$	-0.0364713
$FT\_EFF\_Eigen\_B\_1\_\_1up$	0.0364715
$FT\_EFF\_Eigen\_B\_2\_\_1down$	0.0432793
$FT\_EFF\_Eigen\_B\_2\_\_1up$	-0.0432791
$FT\_EFF\_Eigen\_C\_0\_\_1down$	-1.46633
$FT\_EFF\_Eigen\_C\_0\_\_1up$	1.46633
$FT\_EFF\_Eigen\_C\_1\_\_1down$	-0.736363
$FT\_EFF\_Eigen\_C\_1\_\_1up$	0.736362
$FT\_EFF\_Eigen\_C\_2\_\_1down$	-0.242816
$FT\_EFF\_Eigen\_C\_2\_\_1up$	0.242815
$FT\_EFF\_Eigen\_C\_3\_\_1down$	0.121098
$FT\_EFF\_Eigen\_C\_3\_\_1up$	-0.121099
$FT\_EFF\_Eigen\_Light\_0\_\_1down$	-0.254672
$FT\_EFF\_Eigen\_Light\_0\_\_1up$	0.255253
$FT\_EFF\_Eigen\_Light\_1\_\_1down$	0.0278527
$FT\_EFF\_Eigen\_Light\_1\_\_1up$	-0.0278425
$FT\_EFF\_Eigen\_Light\_2\_\_1down$	0.0450465
$FT\_EFF\_Eigen\_Light\_2\_\_1up$	-0.0450268
$FT\_EFF\_Eigen\_Light\_3\_\_1down$	0.00750237
$FT\_EFF\_Eigen\_Light\_3\_\_1up$	-0.00751386
$FT\_EFF\_Eigen\_Light\_4\_\_1down$	0.0476708
$FT\_EFF\_Eigen\_Light\_4\_\_1up$	-0.0476636
$FT\_EFF\_extrapolation\_\_1down$	0.0764353
$FT\_EFF\_extrapolation\_\_1up$	-0.0764362
$FT\_EFF\_extrapolation\_from\_charm\_\_1down$	0
$FT\_EFF\_extrapolation\_from\_charm\_\_1up$	0

Table 67: Systematic uncertainties for VBF in percent in one lepton region with $p_T(\gamma\gamma)$ cut applied.

Uncertainty Source	Relative Variations
EL_EFF_ID_TOTAL_1NPCOR_PLUS_UNCOR__1down	-0.60799
EL_EFF_ID_TOTAL_1NPCOR_PLUS_UNCOR__1up	0.60799
EL_EFF_Iso_TOTAL_1NPCOR_PLUS_UNCOR__1down	-0.0254989
EL_EFF_Iso_TOTAL_1NPCOR_PLUS_UNCOR__1up	0.0254987
EL_EFF_Reco_TOTAL_1NPCOR_PLUS_UNCOR__1down	-0.19046
EL_EFF_Reco_TOTAL_1NPCOR_PLUS_UNCOR__1up	0.19046
MUON_EFF_STAT__1down	-2.85462
MUON_EFF_STAT__1up	2.85462
MUON_EFF_SYS__1down	-2.85205
MUON_EFF_SYS__1up	2.85206
MUON_ID__1down	0
MUON_ID__1up	0
MUON_ISO_STAT__1down	-0.278197
MUON_ISO_STAT__1up	0.278198
MUON_ISO_SYS__1down	-0.149599
MUON_ISO_SYS__1up	0.149595
MUON_MS__1down	0
MUON_MS__1up	0
MUON_SAGITTA_RESBIAS__1down	0
MUON_SAGITTA_RESBIAS__1up	0
MUON_SAGITTA_RHO__1down	0
MUON_SAGITTA_RHO__1up	0
MUON_SCALE__1down	0
MUON_SCALE__1up	0
MUON_TTVA_STAT__1down	-0.376134
MUON_TTVA_STAT__1up	0.376133
MUON_TTVA_SYS__1down	-0.133891
MUON_TTVA_SYS__1up	0.133891
PH_EFF_ID_Uncertainty__1down	-1.55657
PH_EFF_ID_Uncertainty__1up	1.56905
PH_EFF_TRKISO_Uncertainty__1down	-0.784634
PH_EFF_TRKISO_Uncertainty__1up	0.787542
PH_Iso_DDonoff	0
PRW_DATASF__1down	-12.7763
PRW_DATASF__1up	8.89083

Table 68: Systematic uncertainties for ggh in percent in one lepton region with $p_T(\gamma\gamma)$ cut applied.

Uncertainty Source	Relative Variations
$JET\_BJES\_Response\_\_1up$	-0.00222905
$JET\_BJES\_Response\_\_1down$	-0.00181181
$JET\_EffectiveNP\_1\_\_1up$	1.07105
$JET\_EffectiveNP\_1\_\_1down$	-2.84773
$JET\_EffectiveNP\_2\_\_1up$	-0.000782694
$JET\_EffectiveNP\_2\_\_1down$	0.0246472
$JET\_EffectiveNP\_3\_\_1up$	0.000475847
$JET\_EffectiveNP\_3\_\_1down$	-0.000758017
$JET\_EffectiveNP\_4\_\_1up$	-0.000616538
$JET\_EffectiveNP\_4\_\_1down$	0.000334241
$JET\_EffectiveNP\_5\_\_1up$	-0.000235931
$JET\_EffectiveNP\_5\_\_1down$	0.0243829
$JET\_EffectiveNP\_6\_\_1up$	0.0243882
$JET\_EffectiveNP\_6\_\_1down$	-0.000241805
$JET\_EffectiveNP\_7\_\_1up$	-5.94215e-05
$JET\_EffectiveNP\_7\_\_1down$	-0.000222222
$JET\_EffectiveNP\_8restTerm\_\_1up$	-0.000264645
$JET\_EffectiveNP\_8restTerm\_\_1down$	0.000187633
$JET\_EtaIntercalibration\_Modelling\_\_1up$	0.0355019
$JET\_EtaIntercalibration\_Modelling\_\_1down$	0.0714537
$JET\_EtaIntercalibration\_NonClosure\_\_1up$	-0.000260422
$JET\_EtaIntercalibration\_NonClosure\_\_1down$	0.000498856
$JET\_EtaIntercalibration\_TotalStat\_\_1up$	0.023908
$JET\_EtaIntercalibration\_TotalStat\_\_1down$	0.000372491
$JET\_Flavor\_Composition\_\_1up$	1.20111
$JET\_Flavor\_Composition\_\_1down$	-2.79488
$JET\_Flavor\_Response\_\_1up$	-0.000121379
$JET\_Flavor\_Response\_\_1down$	0.0248079
$JET\_JER\_SINGLE\_NP\_\_1up$	6.19854
$JET\_JvtEfficiency\_\_1down$	-0.718937
$JET\_JvtEfficiency\_\_1up$	0.72248
$JET\_Pileup\_OffsetMu\_\_1up$	0.0240688
$JET\_Pileup\_OffsetMu\_\_1down$	0.000270949
$JET\_Pileup\_OffsetNPV\_\_1up$	0.0247192
$JET\_Pileup\_OffsetNPV\_\_1down$	-0.00666664
$JET\_Pileup\_PtTerm\_\_1up$	0.00984033
$JET\_Pileup\_PtTerm\_\_1down$	-0.00288961
$JET\_Pileup\_RhoTopology\_\_1up$	1.13606
$JET\_Pileup\_RhoTopology\_\_1down$	-2.8482
$JET\_PunchThrough\_MC15\_\_1up$	-2.67278e-07
$JET\_PunchThrough\_MC15\_\_1down$	0
$JET\_SingleParticle\_HighPt\_\_1up$	0
$JET\_SingleParticle\_HighPt\_\_1down$	0

Table 69: Systematic uncertainties for ggh in percent in one lepton region with $p_T(\gamma\gamma)$ cut applied.

Uncertainty Source	Relative Variations
$FT\_EFF\_Eigen\_B\_0\_\_1down$	-0.471003
$FT\_EFF\_Eigen\_B\_0\_\_1up$	0.490767
$FT\_EFF\_Eigen\_B\_1\_\_1down$	-0.261286
$FT\_EFF\_Eigen\_B\_1\_\_1up$	0.261155
$FT\_EFF\_Eigen\_B\_2\_\_1down$	0.0814872
$FT\_EFF\_Eigen\_B\_2\_\_1up$	-0.0813549
$FT\_EFF\_Eigen\_C\_0\_\_1down$	-0.486122
$FT\_EFF\_Eigen\_C\_0\_\_1up$	0.486121
$FT\_EFF\_Eigen\_C\_1\_\_1down$	0.00218374
$FT\_EFF\_Eigen\_C\_1\_\_1up$	-0.00218386
$FT\_EFF\_Eigen\_C\_2\_\_1down$	-0.00577139
$FT\_EFF\_Eigen\_C\_2\_\_1up$	0.00577166
$FT\_EFF\_Eigen\_C\_3\_\_1down$	0.0272647
$FT\_EFF\_Eigen\_C\_3\_\_1up$	-0.0272647
$FT\_EFF\_Eigen\_Light\_0\_\_1down$	-0.277821
$FT\_EFF\_Eigen\_Light\_0\_\_1up$	0.27834
$FT\_EFF\_Eigen\_Light\_1\_\_1down$	0.0537676
$FT\_EFF\_Eigen\_Light\_1\_\_1up$	-0.0537494
$FT\_EFF\_Eigen\_Light\_2\_\_1down$	-0.0300917
$FT\_EFF\_Eigen\_Light\_2\_\_1up$	0.0301266
$FT\_EFF\_Eigen\_Light\_3\_\_1down$	0.00539182
$FT\_EFF\_Eigen\_Light\_3\_\_1up$	-0.00539456
$FT\_EFF\_Eigen\_Light\_4\_\_1down$	0.0343015
$FT\_EFF\_Eigen\_Light\_4\_\_1up$	-0.0343045
$FT\_EFF\_extrapolation\_\_1down$	0
$FT\_EFF\_extrapolation\_\_1up$	0
$FT\_EFF\_extrapolation\_from\_charm\_\_1down$	0
$FT\_EFF\_extrapolation\_from\_charm\_\_1up$	0

Table 70: Systematic uncertainties for *ggh* in percent in one lepton region with $p_T(\gamma\gamma)$ cut applied.

Uncertainty Source	Relative Variations
EL_EFF_ID_TOTAL_1NPCOR_PLUS_UNCOR__1down	-0.505355
EL_EFF_ID_TOTAL_1NPCOR_PLUS_UNCOR__1up	0.505355
EL_EFF_Iso_TOTAL_1NPCOR_PLUS_UNCOR__1down	-0.0784068
EL_EFF_Iso_TOTAL_1NPCOR_PLUS_UNCOR__1up	0.0784067
EL_EFF_Reco_TOTAL_1NPCOR_PLUS_UNCOR__1down	-0.138077
EL_EFF_Reco_TOTAL_1NPCOR_PLUS_UNCOR__1up	0.138077
MUON_EFF_STAT__1down	-0.175946
MUON_EFF_STAT__1up	0.175946
MUON_EFF_SYS__1down	-0.387872
MUON_EFF_SYS__1up	0.388356
MUON_ID__1down	-0.0525174
MUON_ID__1up	-0.0253658
MUON_ISO_STAT__1down	-0.0470025
MUON_ISO_STAT__1up	0.0470031
MUON_ISO_SYS__1down	-0.0996791
MUON_ISO_SYS__1up	0.0996783
MUON_MS__1down	-0.0677144
MUON_MS__1up	-0.00923697
MUON_SAGITTA_RESBIAS__1down	0
MUON_SAGITTA_RESBIAS__1up	0
MUON_SAGITTA_RHO__1down	0
MUON_SAGITTA_RHO__1up	0
MUON_SCALE__1down	0.0225287
MUON_SCALE__1up	-0.0135795
MUON_TTVA_STAT__1down	-0.0999376
MUON_TTVA_STAT__1up	0.0999377
MUON_TTVA_SYS__1down	-0.0530634
MUON_TTVA_SYS__1up	0.0530634
PH_EFF_ID_Uncertainty__1down	-1.65656
PH_EFF_ID_Uncertainty__1up	1.67052
PH_EFF_TRKISO_Uncertainty__1down	-0.763554
PH_EFF_TRKISO_Uncertainty__1up	0.766694
PH_Iso_DDonoff	0.0112794
PRW_DATASF__1down	0.256718
PRW_DATASF__1up	0.731755

Table 71: Systematic uncertainties for SM Higgs pair process and non-resonance in percent in one lepton region with $p_T(\gamma\gamma)$ cut applied.

Uncertainty Source	Relative Variations
$JET\_BJES\_Response\_\_1up$	-0.00759097
$JET\_BJES\_Response\_\_1down$	0.0089667
$JET\_EffectiveNP\_1\_\_1up$	1.36089
$JET\_EffectiveNP\_1\_\_1down$	-1.3476
$JET\_EffectiveNP\_2\_\_1up$	-0.387195
$JET\_EffectiveNP\_2\_\_1down$	0.297416
$JET\_EffectiveNP\_3\_\_1up$	0.114596
$JET\_EffectiveNP\_3\_\_1down$	-0.0735244
$JET\_EffectiveNP\_4\_\_1up$	-0.0339443
$JET\_EffectiveNP\_4\_\_1down$	0.0409822
$JET\_EffectiveNP\_5\_\_1up$	-0.0375898
$JET\_EffectiveNP\_5\_\_1down$	0.0454598
$JET\_EffectiveNP\_6\_\_1up$	0.144392
$JET\_EffectiveNP\_6\_\_1down$	-0.0780871
$JET\_EffectiveNP\_7\_\_1up$	-0.0702508
$JET\_EffectiveNP\_7\_\_1down$	0.175436
$JET\_EffectiveNP\_8restTerm\_\_1up$	0.0463711
$JET\_EffectiveNP\_8restTerm\_\_1down$	-0.0391791
$JET\_EtaIntercalibration\_Modelling\_\_1up$	0.652042
$JET\_EtaIntercalibration\_Modelling\_\_1down$	-0.459222
$JET\_EtaIntercalibration\_NonClosure\_\_1up$	-0.263326
$JET\_EtaIntercalibration\_NonClosure\_\_1down$	0.227977
$JET\_EtaIntercalibration\_TotalStat\_\_1up$	0.231746
$JET\_EtaIntercalibration\_TotalStat\_\_1down$	-0.331224
$JET\_Flavor\_Composition\_\_1up$	2.67167
$JET\_Flavor\_Composition\_\_1down$	-3.14401
$JET\_Flavor\_Response\_\_1up$	-0.97295
$JET\_Flavor\_Response\_\_1down$	0.935043
$JET\_JER\_SINGLE\_NP\_\_1up$	-0.145704
$JET\_JvtEfficiency\_\_1down$	-0.624419
$JET\_JvtEfficiency\_\_1up$	0.627493
$JET\_Pileup\_OffsetMu\_\_1up$	-0.0988886
$JET\_Pileup\_OffsetMu\_\_1down$	0.159764
$JET\_Pileup\_OffsetNPV\_\_1up$	0.332177
$JET\_Pileup\_OffsetNPV\_\_1down$	-0.455123
$JET\_Pileup\_PtTerm\_\_1up$	0.0815124
$JET\_Pileup\_PtTerm\_\_1down$	0.0203146
$JET\_Pileup\_RhoTopology\_\_1up$	1.83787
$JET\_Pileup\_RhoTopology\_\_1down$	-2.01654
$JET\_PunchThrough\_MC15\_\_1up$	8.05837e-07
$JET\_PunchThrough\_MC15\_\_1down$	1.91318e-07
$JET\_SingleParticle\_HighPt\_\_1up$	0
$JET\_SingleParticle\_HighPt\_\_1down$	0

Table 72: Systematic uncertainties for SM Higgs pair process and non-resonance in percent in one lepton region with $p_T(\gamma\gamma)$ cut applied.

Uncertainty Source	Relative Variations
$FT\_EFF\_Eigen\_B\_0\_\_1down$	-0.0554373
$FT\_EFF\_Eigen\_B\_0\_\_1up$	0.0560018
$FT\_EFF\_Eigen\_B\_1\_\_1down$	-0.013626
$FT\_EFF\_Eigen\_B\_1\_\_1up$	0.0136629
$FT\_EFF\_Eigen\_B\_2\_\_1down$	0.00867043
$FT\_EFF\_Eigen\_B\_2\_\_1up$	-0.00871211
$FT\_EFF\_Eigen\_C\_0\_\_1down$	-1.53481
$FT\_EFF\_Eigen\_C\_0\_\_1up$	1.54148
$FT\_EFF\_Eigen\_C\_1\_\_1down$	-0.0764143
$FT\_EFF\_Eigen\_C\_1\_\_1up$	0.0764301
$FT\_EFF\_Eigen\_C\_2\_\_1down$	0.0148855
$FT\_EFF\_Eigen\_C\_2\_\_1up$	-0.0148213
$FT\_EFF\_Eigen\_C\_3\_\_1down$	0.0461933
$FT\_EFF\_Eigen\_C\_3\_\_1up$	-0.0461807
$FT\_EFF\_Eigen\_Light\_0\_\_1down$	-0.285743
$FT\_EFF\_Eigen\_Light\_0\_\_1up$	0.286368
$FT\_EFF\_Eigen\_Light\_1\_\_1down$	0.0479819
$FT\_EFF\_Eigen\_Light\_1\_\_1up$	-0.0479642
$FT\_EFF\_Eigen\_Light\_2\_\_1down$	-0.00930993
$FT\_EFF\_Eigen\_Light\_2\_\_1up$	0.00931658
$FT\_EFF\_Eigen\_Light\_3\_\_1down$	0.00715863
$FT\_EFF\_Eigen\_Light\_3\_\_1up$	-0.00715802
$FT\_EFF\_Eigen\_Light\_4\_\_1down$	0.0363934
$FT\_EFF\_Eigen\_Light\_4\_\_1up$	-0.0363863
$FT\_EFF\_extrapolation\_\_1down$	0.017995
$FT\_EFF\_extrapolation\_\_1up$	-0.0180014
$FT\_EFF\_extrapolation\_from\_charm\_\_1down$	0.00023352
$FT\_EFF\_extrapolation\_from\_charm\_\_1up$	-0.00023352

Table 73: Systematic uncertainties for SM Higgs pair process and non-resonance in percent in one lepton region with $p_T(\gamma\gamma)$ cut applied.

Uncertainty Source	Relative Variations
$EL\_EFF\_ID\_TOTAL\_1NPCOR\_PLUS\_UNCOR\_\_1down$	-0.521683
$EL\_EFF\_ID\_TOTAL\_1NPCOR\_PLUS\_UNCOR\_\_1up$	0.521683
$EL\_EFF\_Iso\_TOTAL\_1NPCOR\_PLUS\_UNCOR\_\_1down$	-0.0402073
$EL\_EFF\_Iso\_TOTAL\_1NPCOR\_PLUS\_UNCOR\_\_1up$	0.0402072
$EL\_EFF\_Reco\_TOTAL\_1NPCOR\_PLUS\_UNCOR\_\_1down$	-0.15132
$EL\_EFF\_Reco\_TOTAL\_1NPCOR\_PLUS\_UNCOR\_\_1up$	0.15132
$MUON\_EFF\_STAT\_\_1down$	-0.278502
$MUON\_EFF\_STAT\_\_1up$	0.278502
$MUON\_EFF\_SYS\_\_1down$	-0.475652
$MUON\_EFF\_SYS\_\_1up$	0.47601
$MUON\_ID\_\_1down$	-0.000213735
$MUON\_ID\_\_1up$	0.00474942
$MUON\_ISO\_STAT\_\_1down$	-0.0564223
$MUON\_ISO\_STAT\_\_1up$	0.056423
$MUON\_ISO\_SYS\_\_1down$	-0.105738
$MUON\_ISO\_SYS\_\_1up$	0.105737
$MUON\_MS\_\_1down$	-0.00745333
$MUON\_MS\_\_1up$	-0.00058199
$MUON\_SAGITTA\_RESBIAS\_\_1down$	0
$MUON\_SAGITTA\_RESBIAS\_\_1up$	0
$MUON\_SAGITTA\_RHO\_\_1down$	0
$MUON\_SAGITTA\_RHO\_\_1up$	0
$MUON\_SCALE\_\_1down$	0.000129398
$MUON\_SCALE\_\_1up$	0.00171644
$MUON\_TTVA\_STAT\_\_1down$	-0.114587
$MUON\_TTVA\_STAT\_\_1up$	0.114587
$MUON\_TTVA\_SYS\_\_1down$	-0.0519702
$MUON\_TTVA\_SYS\_\_1up$	0.0519702
$PH\_EFF\_ID\_Uncertainty\_\_1down$	-1.45643
$PH\_EFF\_ID\_Uncertainty\_\_1up$	1.46732
$PH\_EFF\_TRKISO\_Uncertainty\_\_1down$	-0.747316
$PH\_EFF\_TRKISO\_Uncertainty\_\_1up$	0.750334
$PH\_Iso\_DDonoff$	0.0548131
$PRW\_DATASF\_\_1down$	-0.0417039
$PRW\_DATASF\_\_1up$	-0.0744949

Table 74: Systematic uncertainties for m_H = 400 GeV in percent in one lepton region with $p_T(\gamma\gamma)$ cut applied.

Uncertainty Source	Relative Variations
$JET\_BJES\_Response\_\_1up$	-0.000219829
$JET\_BJES\_Response\_\_1down$	0.000882561
$JET\_EffectiveNP\_1\_\_1up$	1.4722
$JET\_EffectiveNP\_1\_\_1down$	-1.28397
$JET\_EffectiveNP\_2\_\_1up$	-0.251985
$JET\_EffectiveNP\_2\_\_1down$	0.424675
$JET\_EffectiveNP\_3\_\_1up$	0.0803816
$JET\_EffectiveNP\_3\_\_1down$	-0.0582128
$JET\_EffectiveNP\_4\_\_1up$	0.00776763
$JET\_EffectiveNP\_4\_\_1down$	0.0292053
$JET\_EffectiveNP\_5\_\_1up$	-0.00674391
$JET\_EffectiveNP\_5\_\_1down$	0.0207327
$JET\_EffectiveNP\_6\_\_1up$	0.167922
$JET\_EffectiveNP\_6\_\_1down$	-0.12551
$JET\_EffectiveNP\_7\_\_1up$	-0.12348
$JET\_EffectiveNP\_7\_\_1down$	0.179898
$JET\_EffectiveNP\_8restTerm\_\_1up$	0.0405351
$JET\_EffectiveNP\_8restTerm\_\_1down$	-0.0280038
$JET\_EtaIntercalibration\_Modelling\_\_1up$	0.591682
$JET\_EtaIntercalibration\_Modelling\_\_1down$	-0.490423
$JET\_EtaIntercalibration\_NonClosure\_\_1up$	-0.0968161
$JET\_EtaIntercalibration\_NonClosure\_\_1down$	-0.000368866
$JET\_EtaIntercalibration\_TotalStat\_\_1up$	0.356169
$JET\_EtaIntercalibration\_TotalStat\_\_1down$	-0.308682
$JET\_Flavor\_Composition\_\_1up$	3.96798
$JET\_Flavor\_Composition\_\_1down$	-3.14659
$JET\_Flavor\_Response\_\_1up$	-0.964444
$JET\_Flavor\_Response\_\_1down$	1.03409
$JET\_JER\_SINGLE\_NP\_\_1up$	1.00883
$JET\_JvtEfficiency\_\_1down$	-0.683579
$JET\_JvtEfficiency\_\_1up$	0.687055
$JET\_Pileup\_OffsetMu\_\_1up$	-0.148814
$JET\_Pileup\_OffsetMu\_\_1down$	0.185259
$JET\_Pileup\_OffsetNPV\_\_1up$	0.295736
$JET\_Pileup\_OffsetNPV\_\_1down$	-0.0427249
$JET\_Pileup\_PtTerm\_\_1up$	0.0400338
$JET\_Pileup\_PtTerm\_\_1down$	-0.0604664
$JET\_Pileup\_RhoTopology\_\_1up$	2.29413
$JET\_Pileup\_RhoTopology\_\_1down$	-1.87409
$JET\_PunchThrough\_MC15\_\_1up$	-8.26289e-09
$JET\_PunchThrough\_MC15\_\_1down$	1.45012e-08
$JET\_SingleParticle\_HighPt\_\_1up$	0
$JET\_SingleParticle\_HighPt\_\_1down$	0

Table 75: Systematic uncertainties for m_H = 400 GeV in percent in one lepton region with $p_T(\gamma\gamma)$ cut applied.

Uncertainty Source	Relative Variations
FT_EFF_Eigen_B_0__1down	-0.0808276
FT_EFF_Eigen_B_0__1up	0.0811183
FT_EFF_Eigen_B_1__1down	-0.00933067
FT_EFF_Eigen_B_1__1up	0.00933639
FT_EFF_Eigen_B_2__1down	0.00925482
FT_EFF_Eigen_B_2__1up	-0.0092304
FT_EFF_Eigen_C_0__1down	-1.35201
FT_EFF_Eigen_C_0__1up	1.35707
FT_EFF_Eigen_C_1__1down	0.158004
FT_EFF_Eigen_C_1__1up	-0.15806
FT_EFF_Eigen_C_2__1down	0.0577072
FT_EFF_Eigen_C_2__1up	-0.0577019
FT_EFF_Eigen_C_3__1down	0.0450326
FT_EFF_Eigen_C_3__1up	-0.045025
FT_EFF_Eigen_Light_0__1down	-0.285116
FT_EFF_Eigen_Light_0__1up	0.285726
FT_EFF_Eigen_Light_1__1down	0.0532455
FT_EFF_Eigen_Light_1__1up	-0.0532243
FT_EFF_Eigen_Light_2__1down	-0.0214047
FT_EFF_Eigen_Light_2__1up	0.0214102
FT_EFF_Eigen_Light_3__1down	0.0131465
FT_EFF_Eigen_Light_3__1up	-0.013144
FT_EFF_Eigen_Light_4__1down	0.0318171
FT_EFF_Eigen_Light_4__1up	-0.0318105
FT_EFF_extrapolation__1down	0.00365604
FT_EFF_extrapolation__1up	-0.00365604
FT_EFF_extrapolation_from_charm__1down	0.000401627
FT_EFF_extrapolation_from_charm__1up	-0.000401628

Table 76: Systematic uncertainties for m_H = 400 GeV in percent in one lepton region with $p_T(\gamma\gamma)$ cut applied.

Uncertainty Source	Relative Variations
$EL\_EFF\_ID\_TOTAL\_1NPCOR\_PLUS\_UNCOR\_\_1down$	-0.459369
$EL\_EFF\_ID\_TOTAL\_1NPCOR\_PLUS\_UNCOR\_\_1up$	0.459368
$EL\_EFF\_Iso\_TOTAL\_1NPCOR\_PLUS\_UNCOR\_\_1down$	-0.0701366
$EL\_EFF\_Iso\_TOTAL\_1NPCOR\_PLUS\_UNCOR\_\_1up$	0.0701365
$EL\_EFF\_Reco\_TOTAL\_1NPCOR\_PLUS\_UNCOR\_\_1down$	-0.129289
$EL\_EFF\_Reco\_TOTAL\_1NPCOR\_PLUS\_UNCOR\_\_1up$	0.129289
$MUON\_EFF\_STAT\_\_1down$	-0.129765
$MUON\_EFF\_STAT\_\_1up$	0.129765
$MUON\_EFF\_SYS\_\_1down$	-0.351924
$MUON\_EFF\_SYS\_\_1up$	0.352433
$MUON\_ID\_\_1down$	0.00969678
$MUON\_ID\_\_1up$	0.0231123
$MUON\_ISO\_STAT\_\_1down$	-0.0430322
$MUON\_ISO\_STAT\_\_1up$	0.0430326
$MUON\_ISO\_SYS\_\_1down$	-0.100742
$MUON\_ISO\_SYS\_\_1up$	0.100742
$MUON\_MS\_\_1down$	0.0111988
$MUON\_MS\_\_1up$	-0.0190261
$MUON\_SAGITTA\_RESBIAS\_\_1down$	0
$MUON\_SAGITTA\_RESBIAS\_\_1up$	0
$MUON\_SAGITTA\_RHO\_\_1down$	0
$MUON\_SAGITTA\_RHO\_\_1up$	0
$MUON\_SCALE\_\_1down$	0.0232481
$MUON\_SCALE\_\_1up$	0.000121055
$MUON\_TTVA\_STAT\_\_1down$	-0.0925775
$MUON\_TTVA\_STAT\_\_1up$	0.0925776
$MUON\_TTVA\_SYS\_\_1down$	-0.0487003
$MUON\_TTVA\_SYS\_\_1up$	0.0487003
$PH\_EFF\_ID\_Uncertainty\_\_1down$	-1.66286
$PH\_EFF\_ID\_Uncertainty\_\_1up$	1.67695
$PH\_EFF\_TRKISO\_Uncertainty\_\_1down$	-0.724454
$PH\_EFF\_TRKISO\_Uncertainty\_\_1up$	0.727347
$PH\_Iso\_DDonoff$	0.0559
$PRW\_DATASF\_\_1down$	1.17289
$PRW\_DATASF\_\_1up$	-1.61032

Table 77: Systematic uncertainties for m_H = 500 GeV in percent in one lepton region with $p_T(\gamma\gamma)$ cut applied.

Uncertainty Source	Relative Variations
$JET\_BJES\_Response\_\_1up$	-0.00012239
$JET\_BJES\_Response\_\_1down$	-0.00767252
$JET\_EffectiveNP\_1\_\_1up$	1.0447
$JET\_EffectiveNP\_1\_\_1down$	-1.12489
$JET\_EffectiveNP\_2\_\_1up$	-0.244011
$JET\_EffectiveNP\_2\_\_1down$	0.271649
$JET\_EffectiveNP\_3\_\_1up$	0.0225547
$JET\_EffectiveNP\_3\_\_1down$	-0.0318287
$JET\_EffectiveNP\_4\_\_1up$	-0.027783
$JET\_EffectiveNP\_4\_\_1down$	-0.0057468
$JET\_EffectiveNP\_5\_\_1up$	-0.0339831
$JET\_EffectiveNP\_5\_\_1down$	0.0122954
$JET\_EffectiveNP\_6\_\_1up$	0.0292468
$JET\_EffectiveNP\_6\_\_1down$	-0.0331833
$JET\_EffectiveNP\_7\_\_1up$	-0.0277012
$JET\_EffectiveNP\_7\_\_1down$	0.0241323
$JET\_EffectiveNP\_8restTerm\_\_1up$	0.00986801
$JET\_EffectiveNP\_8restTerm\_\_1down$	-0.0325313
$JET\_EtaIntercalibration\_Modelling\_\_1up$	0.309808
$JET\_EtaIntercalibration\_Modelling\_\_1down$	-0.382837
$JET\_EtaIntercalibration\_NonClosure\_\_1up$	-0.0950512
$JET\_EtaIntercalibration\_NonClosure\_\_1down$	0.119662
$JET\_EtaIntercalibration\_TotalStat\_\_1up$	0.227319
$JET\_EtaIntercalibration\_TotalStat\_\_1down$	-0.213015
$JET\_Flavor\_Composition\_\_1up$	2.71082
$JET\_Flavor\_Composition\_\_1down$	-2.57364
$JET\_Flavor\_Response\_\_1up$	-0.461755
$JET\_Flavor\_Response\_\_1down$	0.596197
$JET\_JER\_SINGLE\_NP\_\_1up$	-0.197979
$JET\_JvtEfficiency\_\_1down$	-0.634938
$JET\_JvtEfficiency\_\_1up$	0.63806
$JET\_Pileup\_OffsetMu\_\_1up$	-0.0668627
$JET\_Pileup\_OffsetMu\_\_1down$	0.167656
$JET\_Pileup\_OffsetNPV\_\_1up$	-0.0152505
$JET\_Pileup\_OffsetNPV\_\_1down$	-0.16461
$JET\_Pileup\_PtTerm\_\_1up$	0.0590095
$JET\_Pileup\_PtTerm\_\_1down$	-0.0165964
$JET\_Pileup\_RhoTopology\_\_1up$	1.54238
$JET\_Pileup\_RhoTopology\_\_1down$	-1.4366
$JET\_PunchThrough\_MC15\_\_1up$	-1.27101e-08
$JET\_PunchThrough\_MC15\_\_1down$	2.84316e-08
$JET\_SingleParticle\_HighPt\_\_1up$	0
$JET\_SingleParticle\_HighPt\_\_1down$	0

Table 78: Systematic uncertainties for m_H = 500 GeV in percent in one lepton region with $p_T(\gamma\gamma)$ cut applied.

Uncertainty Source	Relative Variations
$FT\_EFF\_Eigen\_B\_0\_\_1down$	-0.0532437
$FT\_EFF\_Eigen\_B\_0\_\_1up$	0.0532518
$FT\_EFF\_Eigen\_B\_1\_\_1down$	-0.0171535
$FT\_EFF\_Eigen\_B\_1\_\_1up$	0.0171592
$FT\_EFF\_Eigen\_B\_2\_\_1down$	0.00368772
$FT\_EFF\_Eigen\_B\_2\_\_1up$	-0.00368687
$FT\_EFF\_Eigen\_C\_0\_\_1down$	-1.51774
$FT\_EFF\_Eigen\_C\_0\_\_1up$	1.52381
$FT\_EFF\_Eigen\_C\_1\_\_1down$	-0.0510731
$FT\_EFF\_Eigen\_C\_1\_\_1up$	0.0511092
$FT\_EFF\_Eigen\_C\_2\_\_1down$	0.046046
$FT\_EFF\_Eigen\_C\_2\_\_1up$	-0.0460293
$FT\_EFF\_Eigen\_C\_3\_\_1down$	0.0365585
$FT\_EFF\_Eigen\_C\_3\_\_1up$	-0.0365489
$FT\_EFF\_Eigen\_Light\_0\_\_1down$	-0.28397
$FT\_EFF\_Eigen\_Light\_0\_\_1up$	0.284597
$FT\_EFF\_Eigen\_Light\_1\_\_1down$	0.0494979
$FT\_EFF\_Eigen\_Light\_1\_\_1up$	-0.0494789
$FT\_EFF\_Eigen\_Light\_2\_\_1down$	-0.0118591
$FT\_EFF\_Eigen\_Light\_2\_\_1up$	0.0118657
$FT\_EFF\_Eigen\_Light\_3\_\_1down$	0.00859662
$FT\_EFF\_Eigen\_Light\_3\_\_1up$	-0.0085951
$FT\_EFF\_Eigen\_Light\_4\_\_1down$	0.0378742
$FT\_EFF\_Eigen\_Light\_4\_\_1up$	-0.0378652
$FT\_EFF\_extrapolation\_\_1down$	0.00999153
$FT\_EFF\_extrapolation\_\_1up$	-0.00998988
$FT\_EFF\_extrapolation\_from\_charm\_\_1down$	0.000223217
$FT\_EFF\_extrapolation\_from\_charm\_\_1up$	-0.000223217

Table 79: Systematic uncertainties for m_H = 500 GeV in percent in one lepton region with $p_T(\gamma\gamma)$ cut applied.

C Selections optimization

The cuts on the photons side are fully followed the HGam group, and the following optimizations are all on the W boson and its decay products sides. The distributions of the variables are shown in Figure 58 and Figure 59. At the left region for Figure 58(a), 58(c), 59(a), 59(c) and the right region for Figure 58(b), 59(b), the signal statistics will be low if there is a cut on these variables. The significance on the right plots is definded as Z in the Eq 1. Applying a cut on these variables doesn't have significant improvement and will decrise the signal statistics excessively. There is no further cut besides the cuts listed in Section 5.

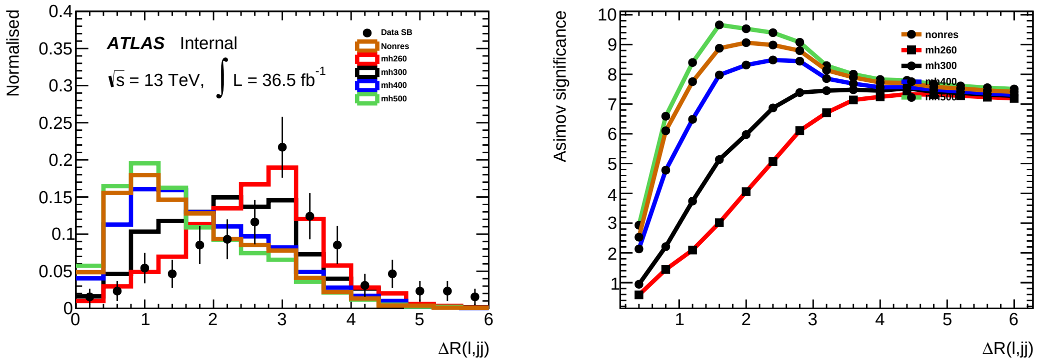

(a)

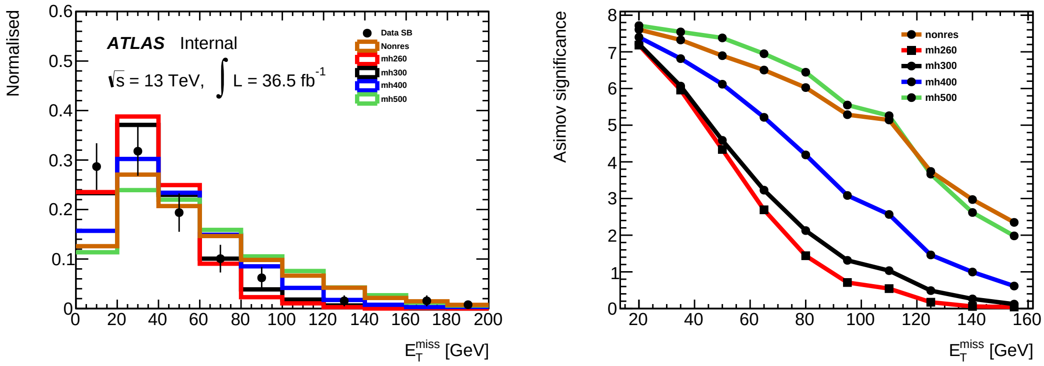

(b)

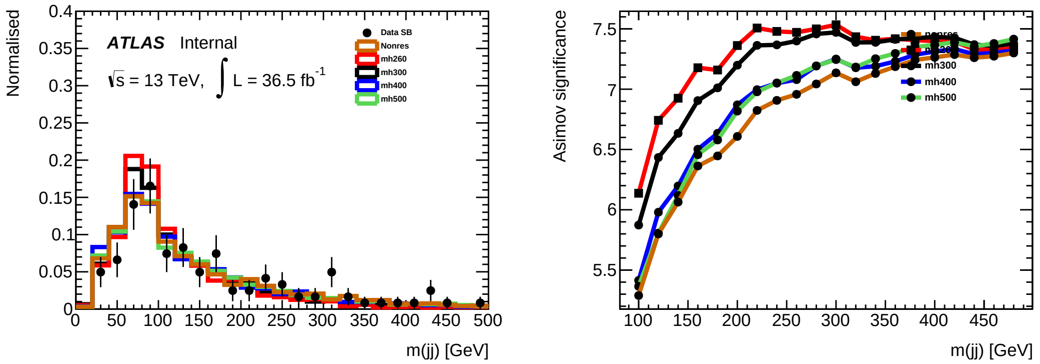

(c)

Figure 58: (a) The ΔR between the leading lepton and the di-jet system, (b) transverse missing energy, (c) the invariant mass of di-jet system.

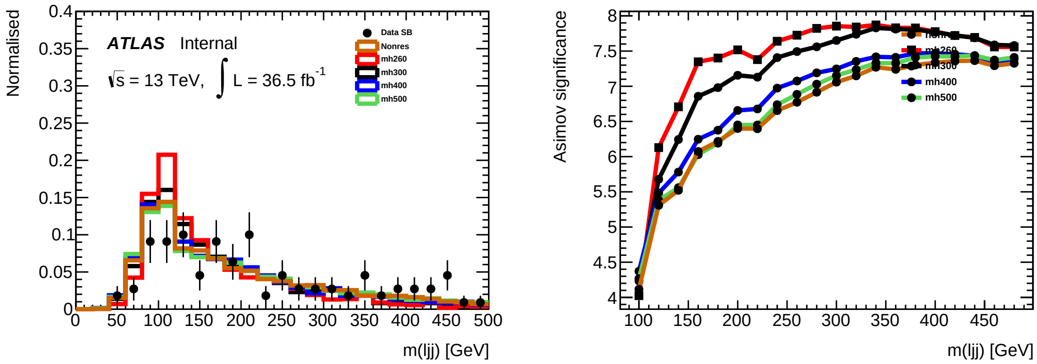

(a)

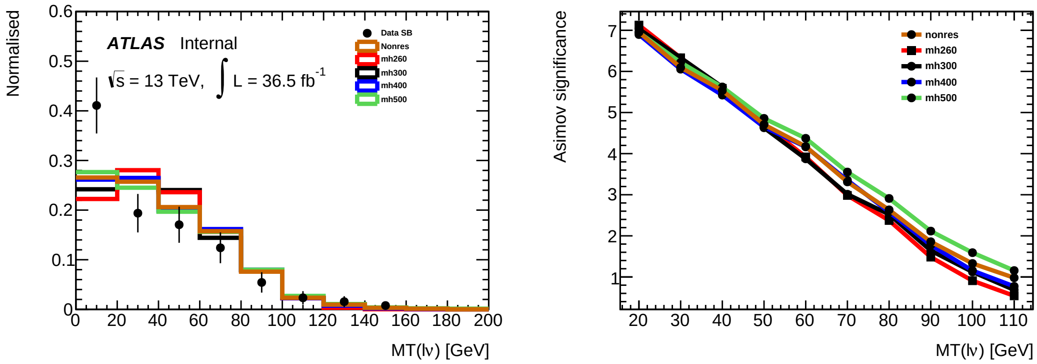

(b)

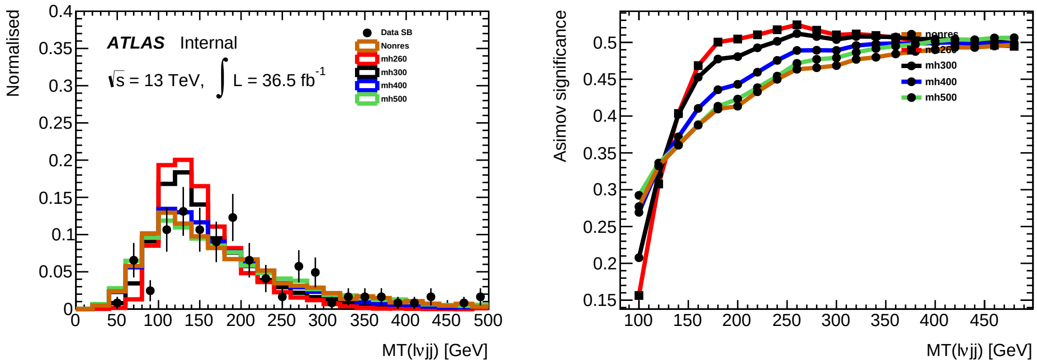

(c)

Figure 59: (a) The invatiant mass of lepton and di-jet, (b) transverse mass of the leading lepton and MET, (c) transverse mass of the leading lepton, MET and di-jet.

Parameter	fit
W1	43.0507±11.2414
W2	23.9493±10.2914
f_{ISO}	0.475728±0.173654
f_{ID}	0.469924±0.166589

Table 80: fit result of one electron channel

fit (real + fake)	FixedCutTight	loose-not-FixedCutTight
tight	35.646±5.35402	3.09965±5.90034
medium-not-tight	3.96067±6.03934	0.344406±6.65559

Table 81: fit result of one electron channel

D Fake lepton estimation

An ABCD method is introduced to estimate fake leptons in electron and muon channel. After the baseline lepton selection, the events are split into 4 regions by two indepent variables. Here tight ID and FixedCutTight[36](current muon isolation variable is not correct) isolation are used. They are supposed to be independent. The correlation factor of these two variables is 0.11 for electron channel and 9e-3 for muon channel in large statistic $l\nu\gamma\gamma jj$ sample. The yield in each region can be calculated by Eq 5, where W1 is real lepton yield and W2 is fake lepton yield,
ϵ_{ID} and ϵ_{ISO} are the efficiency of tight ID and tight ISO for real lepton obtained from background MC,
f_{ID} and f_{ISO} are the efficiency of tight ID and tight ISO for fake lepton.
The minimization of χ^2 in Eq 6 is performed to get the parameter. Table 80 shows the fit result of electron channel and Table 83 shows the fit result of muon channel. Table 86 shows the ID and Isolation efficiency from various sample and it indicates that it is not worthwhile to apply tight ID and tight Isolation cut.

$$\begin{aligned} N_{TI,pred} &= W1 * \epsilon_{ID} * \epsilon_{ISO} + W2 * f_{ID} * f_{ISO}; \\ N_{TnI,pred} &= W1 * \epsilon_{ID} * (1 - \epsilon_{ISO}) + W2 * f_{ID} * (1 - f_{ISO}); \\ N_{nTI,pred} &= W1 * (1 - \epsilon_{ID}) * \epsilon_{ISO} + W2 * (1 - f_{ID}) * f_{ISO}; \\ N_{nTnI,pred} &= W1 * (1 - \epsilon_{ID}) * (1 - \epsilon_{ISO}) + W2 * (1 - f_{ID}) * (1 - f_{ISO}); \end{aligned} \tag{5}$$

$$\begin{aligned} \chi^2 &= \sum_i \frac{(N_i - N_{i,pred})^2}{N_i}, \\ i &= TI(tight - isolated), \\ &TnI(tight - non - isolated), \\ &nTI(non - tight - isolated), \\ &nTnI(non - tight - non - isolated) \end{aligned} \tag{6}$$

data	FixedCutTight	loose-not-FixedCutTight
Tight	41	9
medium-not-tight	10	7

Table 82: data sideband in one electron channel

Parameter	fit
W1	28.1647±14.0766
W2	38.5004±14.6546
f_{ISO}	0.495349±0.172062
f_{ID}	0.8±0.0419173

Table 83: fit result of one muon channel

fit (real + fake)	FixedCutTight	loose-not-FixedCutTight
tight	25.9566+15.2569	1.08152+15.5434
medium-not-tight	1.08152+3.81423	0.0450635+3.88585

Table 84: fit result of one muon channel

data	FixedCutTight	loose-not-FixedCutTight
Tight	41	16
medium-not-tight	5	0

Table 85: data sideband in one muon channel

efficiency/eff_S / $\sqrt{eff_B}$	data	$l\nu jj\gamma\gamma$	WWyy260	WWyy300	WWyy400	WWyy500
electron tight ID	0.75	0.922	0.886/1.023	0.883/1.020	0.906/1.046	0.914/1.055
electron tight ISO	0.76	0.902	0.774/0.888	0.827/0.949	0.847/0.972	0.868/0.996
muon tight ID	0.92	0.960	0.952/0.992	0.949/0.989	0.945/0.985	0.951/0.991
muon tight ISO	0.74	0.960	0.912/1.060	0.924/1.074	0.933/1.085	0.947/1.100

Table 86: This table show the ID and Isolation efficiency for electron and muon channel in different sample. After comparing the $s/\sqrt{b}$, it is not worthwhile to apply tight ID or tight Isolation cut.

Function	Max(S)	Max(S/DeltaS)	Max(S/RefS)	Result
Poly1	-1.93075	-0.486013	-3.7341	fail
Poly2	-0.93036	-0.208244	-1.79933	fail
Exponential	1.05432	0.242821	2.03908	fail
ExpPoly2	0.845848	0.194842	1.6359	pass

Table 87: Spurious signal test for $m_H = 260GeV$

Function	Max(S)	Max(S/DeltaS)	Max(S/RefS)	Result
Poly1	-1.92083	-0.480248	-3.37704	fail
Poly2	-0.95828	-0.213363	-1.68476	fail
Exponential	-2.5556	-0.614349	-4.49304	fail
ExpPoly2	0.826406	0.189248	1.45292	pass

Table 88: Spurious signal test for $m_H = 300GeV$

E Discusssion on continuum background modeling

Table 8788899091 show the spurious signal test for other function. An additional check is performed to make sure the shape difference between 1-lep region and 0-lep region is acceptable. The function used here is the baseline 2nd-exp function, $exp(a1 \times x + a2 \times x^2)$, $x = (m_{\gamma\gamma} - 100)/100$. Table 92939495 show the shape difference in SR and CR in difference samples. The conclusion is that the statistic uncertainty of paramter in SR can cover the difference.

F Parameters extraction for signals and SM backgrounds

In Figures 60, 61, 62, 63, 64, 65, 66 and 67 show the fits to extract the shape parameters which are used to build models of the signals and backgrounds.

Function	Max(S)	Max(S/DeltaS)	Max(S/RefS)	Result
Poly1	0.344039	0.150491	0.44619	pass
Poly2	-0.389102	-0.166955	-0.504633	pass
Exponential	0.411775	0.183332	0.534038	pass
ExpPoly2	-0.398046	-0.169399	-0.516232	pass

Table 89: Spurious signal test for $m_H = 400GeV$

Function	Max(S)	Max(S/DeltaS)	Max(S/RefS)	Result
Poly1	0.352419	0.157594	0.410594	pass
Poly2	-0.385572	-0.169678	-0.449221	pass
Exponential	0.417334	0.189947	0.486226	pass
ExpPoly2	-0.395486	-0.172747	-0.460771	pass

Table 90: Spurious signal test for $m_H = 500GeV$

Function	Max(S)	Max(S/DeltaS)	Max(S/RefS)	Result
Poly1	0.349528	0.15498	0.432416	pass
Poly2	-0.391328	-0.170836	-0.484128	pass
Exponential	0.415397	0.187463	0.513905	pass
ExpPoly2	-0.402366	-0.174128	-0.497784	pass

Table 91: Spurious signal test for non-resonant

MC	parameter	value	error
SR	a1	-2.2482e+00	± 2.30e+00
	a2	3.1279e-01	± 3.64e+00
CR	a1	-2.1722e+00	± 1.22e-01
	a2	-7.0086e-01	± 1.98e-01

Table 92: Shape difference in pure $lvqq\gamma\gamma$ and $\gamma\gamma jjj$ MC sample.

revID	parameter	value	error
SR	a1	-3.3355e+00	+/- 2.96e+00
	a2	1.8383e+00	+/- 4.63e+00
CR	a1	-4.2406e+00	+/- 1.40e-01
	a2	1.4973e+00	+/- 2.33e-01

Table 93: Shape difference in reverse ID region

revISO	parameter	value	error
SR	a1	-4.6782e+00	+/- 1.93e+00
	a2	1.4239e+00	+/- 3.24e+00
CR	a1	-3.5777e+00	+/- 9.78e-02
	a2	8.5102e-01	+/- 1.61e-01

Table 94: Shape difference in reverse isolation region

revID-revISO	parameter	value	error
SR	a1	-3.5107e+00	+/- 7.54e-01
	a2	1.5423e+00	+/- 1.22e+00
CR	a1	-3.5709e+00	+/- 3.23e-02
	a2	1.1725e+00	+/- 5.29e-02

Table 95: Shape difference in reverse both ID and isolation region

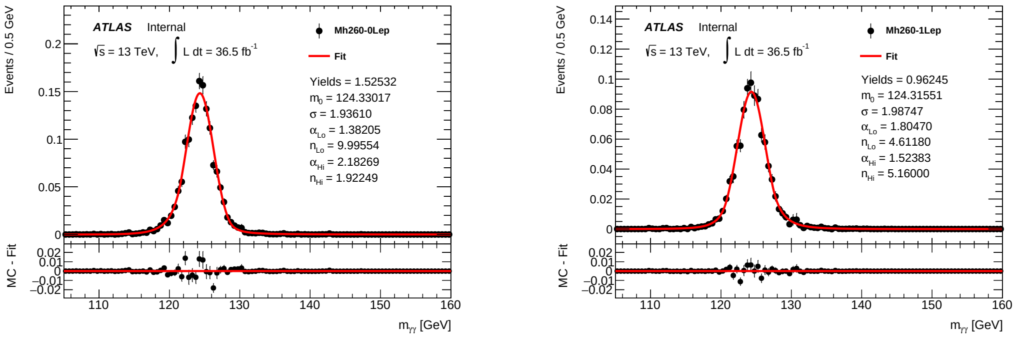

(a) (b)

Figure 60: The fits to obtain the parameters for m_H =260 GeV in (a) zero lepton region, (b) one lepton region.

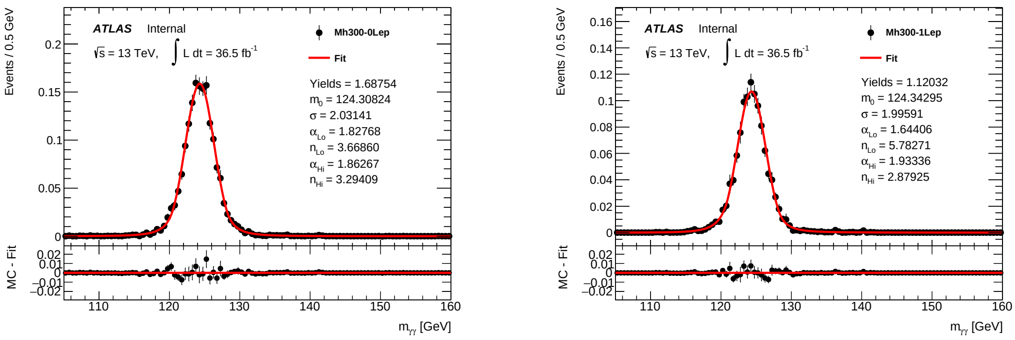

(a) (b)

Figure 61: The fits to obtain the parameters for m_H =300 GeV in (a) zero lepton region, (b) one lepton region.

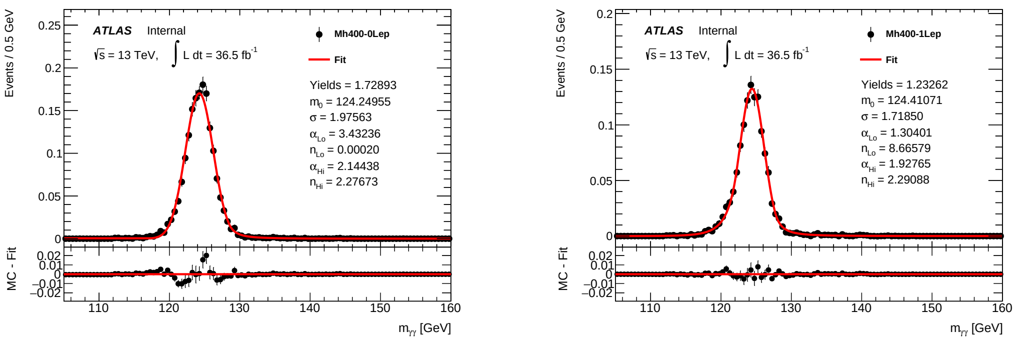

(a) (b)

Figure 62: The fits to obtain the parameters for m_H =400 GeV in (a) zero lepton region, (b) one lepton region.

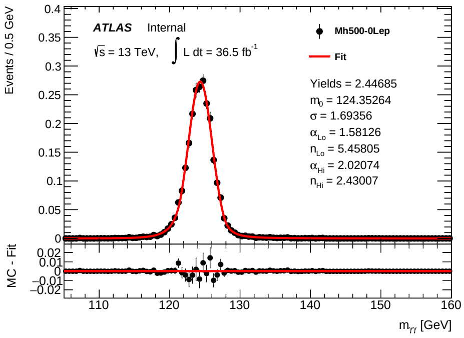

(a)

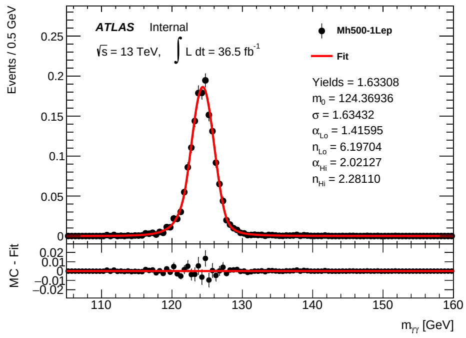

(b)

Figure 63: The fits to obtain the parameters for m_H =500 GeV in (a) zero lepton region, (b) one lepton region.

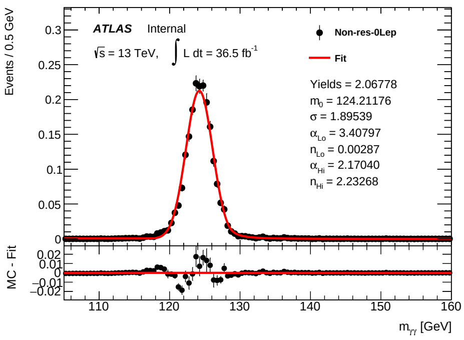

(a)

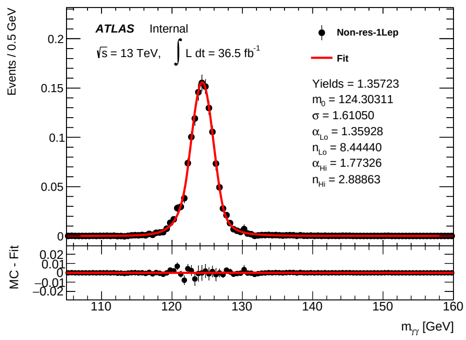

(b)

Figure 64: The fits to obtain the parameters for non-resonance in (a) zero lepton region, (b) one lepton region.

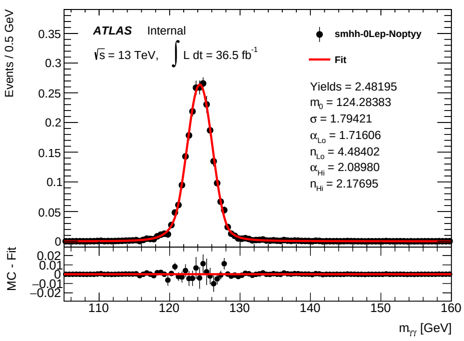

(a)

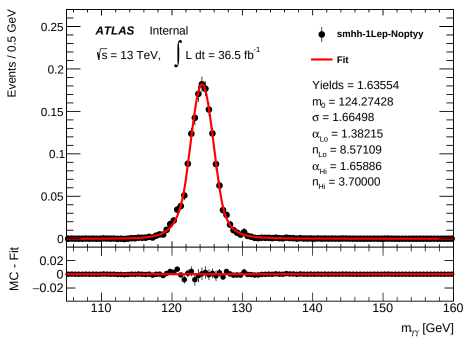

(b)

Figure 65: The fits to obtain the parameters for SM Higgs boson pair in (a) zero lepton region, (b) one lepton region, without $p_T(\gamma\gamma)$ cut applied.

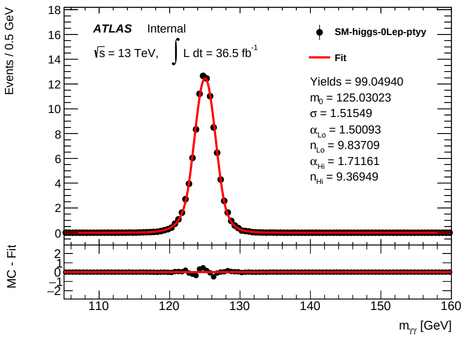

(a)

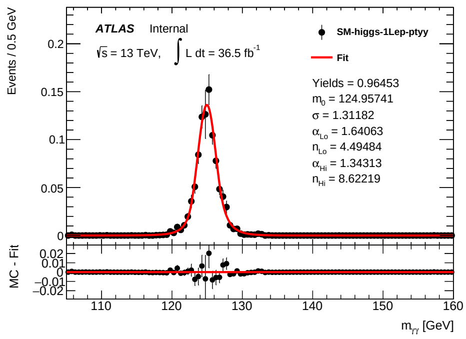

(b)

Figure 66: The fits to obtain the parameters for SM single Higgs background in (a) zero lepton region, (b) one lepton region, with $p_T(\gamma\gamma)$ cut applied.

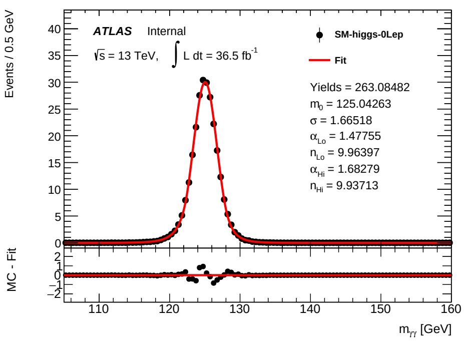

(a)

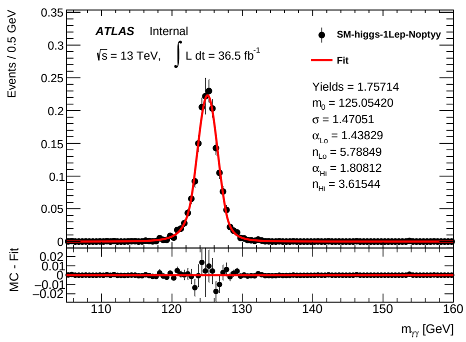

(b)

Figure 67: The fits to obtain the parameters for SM single Higgs background in (a) zero lepton region, (b) one lepton region, without $p_T(\gamma\gamma)$ cut applied.

G Systematics on photon resolution and scale

In the fits, the shape parameters except the m_0 are fixed as those in nominal fits shown in the Section F for extracting the systematics on photon energy scale (EGS). The shape parameters except σ are fixed for photon energy resolution (EGR). All the fits are shown in 68, 69, 70 , 71, 72, 73 , 74 and 75.

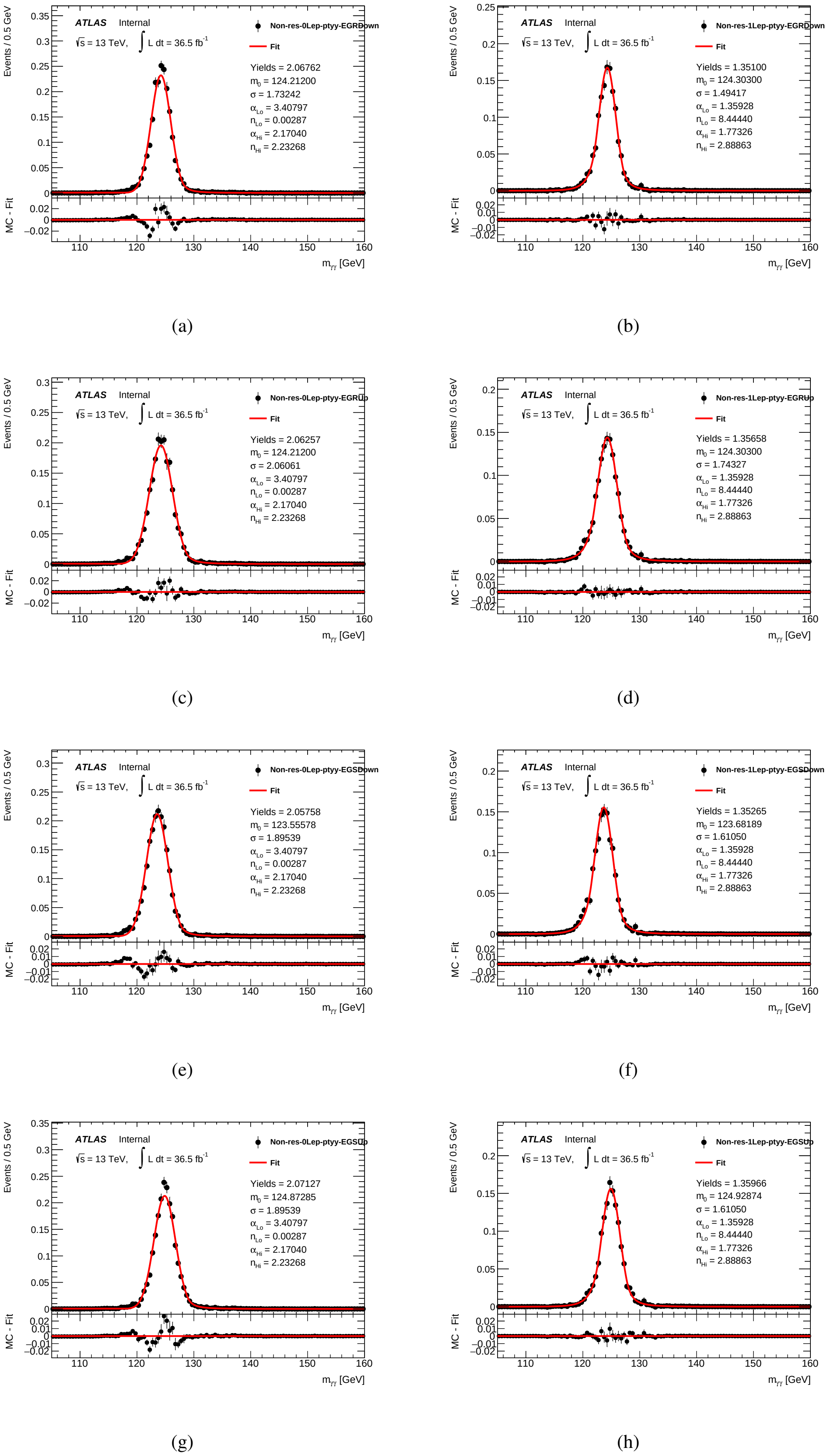

Figure 68: The fits for non-resonance to obtain (a) σ_Down in zero lepton region, (b) σ_Down in one lepton region, (c) σ_Up in zero lepton region, (d) σ_Up in one lepton region, (e) m_0_Down in zero lepton region, (f) m_0_Down in one lepton region, (g) m_0_Up in zero lepton region, (h) m_0_Up in one lepton region.

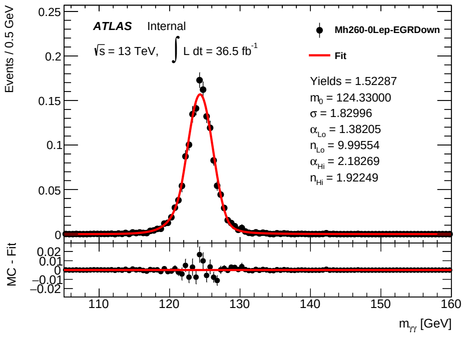

(a)

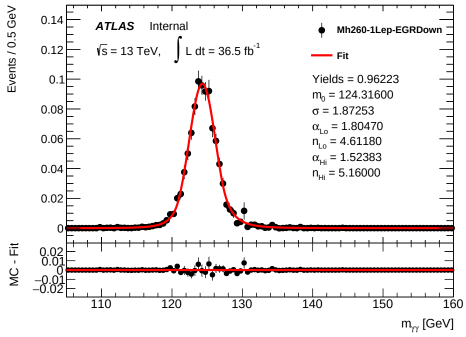

(b)

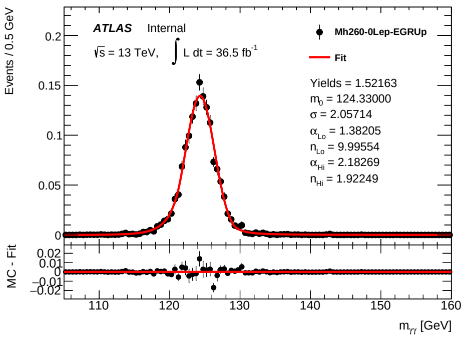

(c)

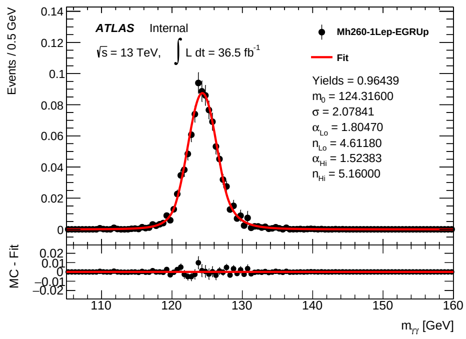

(d)

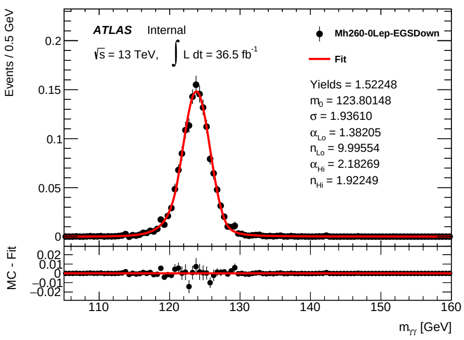

(e)

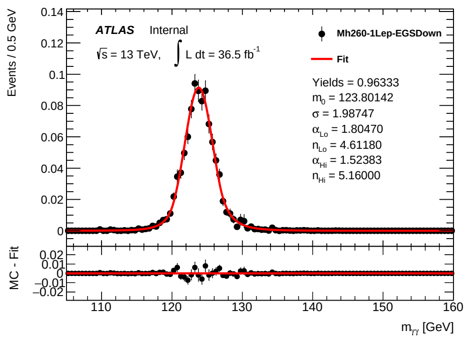

(f)

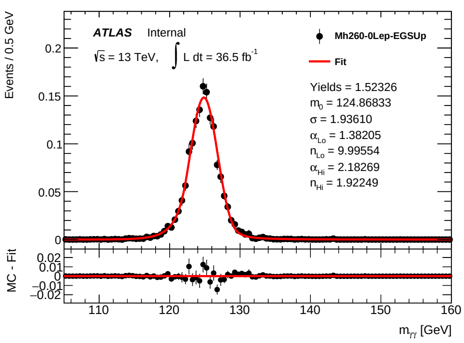

(g)

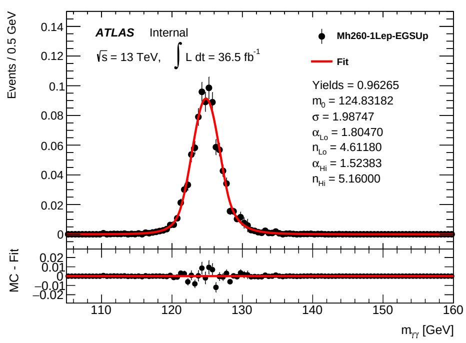

(h)

Figure 69: The fits for m_H = 260 GeV to obtain (a) σ_Down in zero lepton region, (b) σ_Down in one lepton region, (c) σ_Up in zero lepton region, (d) σ_Up in one lepton region, (e) m_0_Down in zero lepton region, (f) m_0_Down in one lepton region, (g) m_0_Up in zero lepton region, (h) m_0_Up in one lepton region.

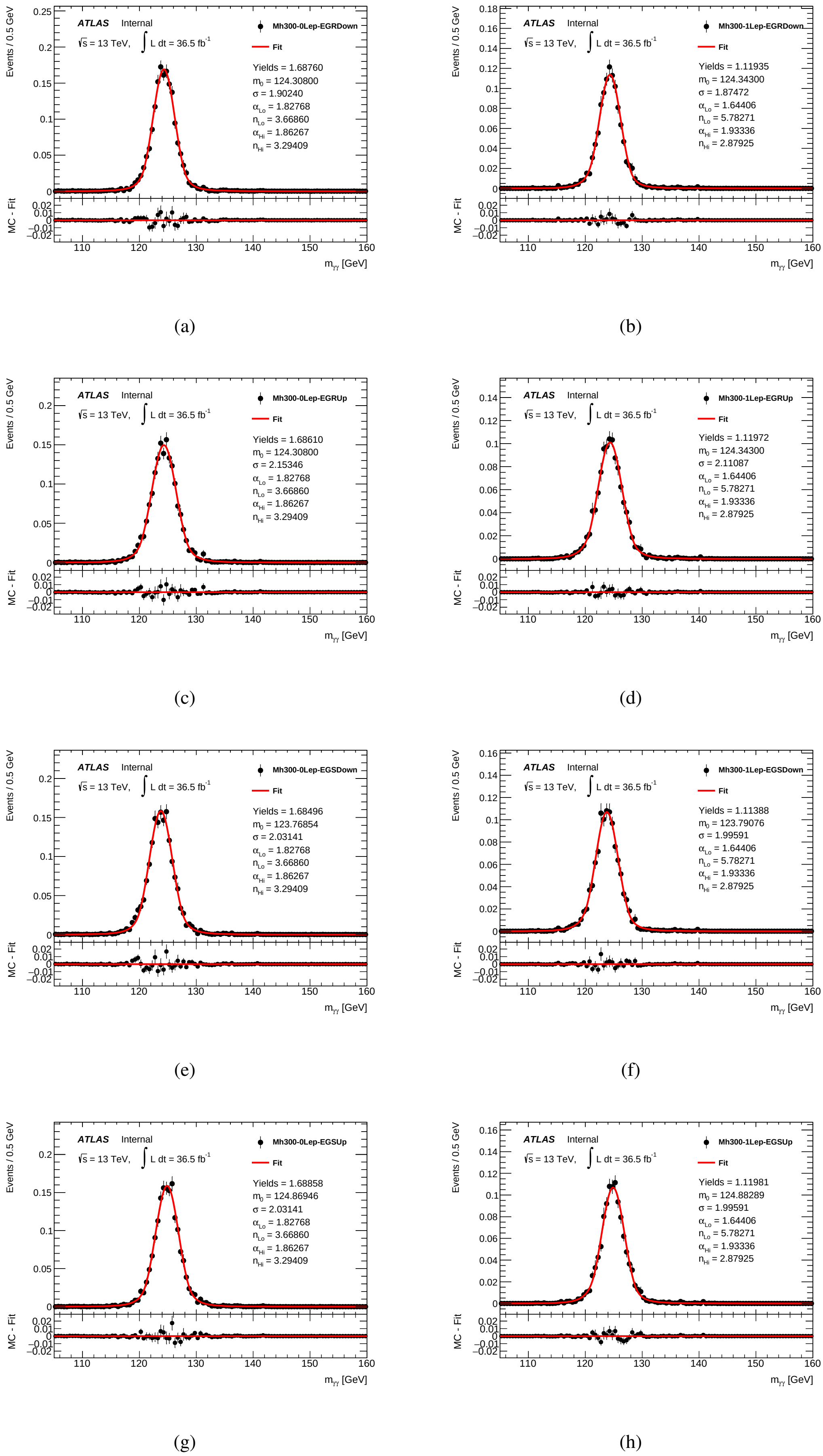

Figure 70: The fits for m_H = 300 GeV to obtain (a) σ_Down in zero lepton region, (b) σ_Down in one lepton region, (c) σ_Up in zero lepton region, (d) σ_Up in one lepton region, (e) m_0_Down in zero lepton region, (f) m_0_Down in one lepton region, (g) m_0_Up in zero lepton region, (h) m_0_Up in one lepton region.

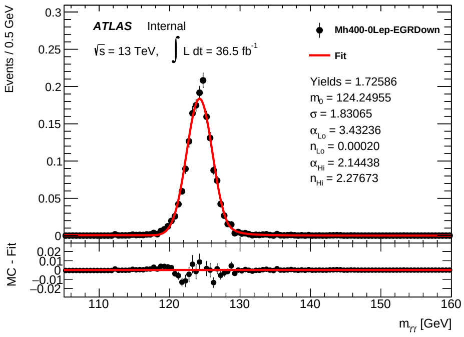

(a)

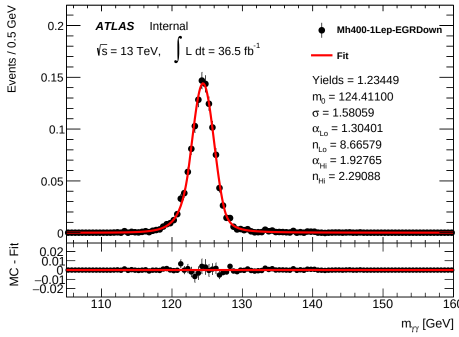

(b)

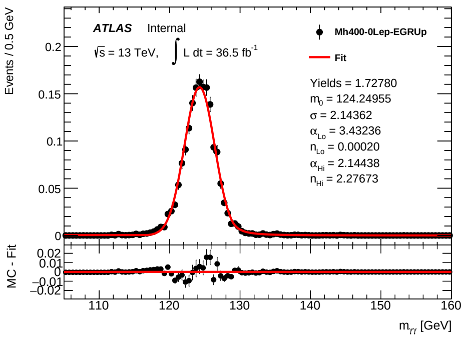

(c)

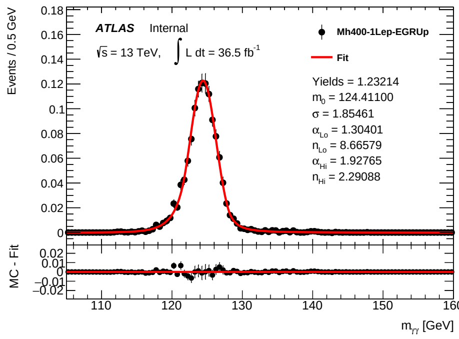

(d)

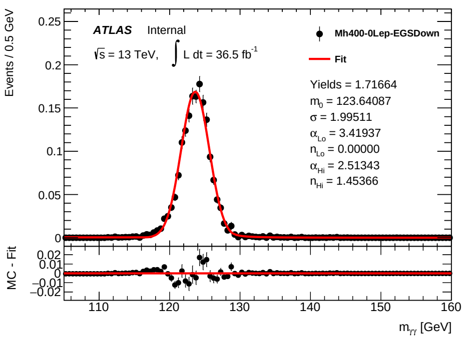

(e)

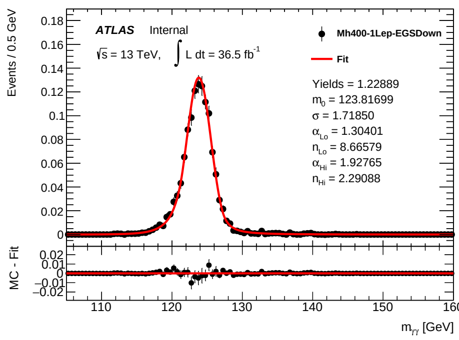

(f)

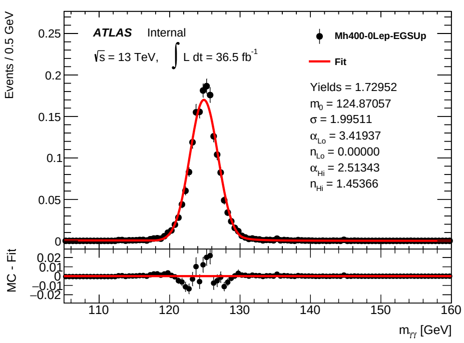

(g)

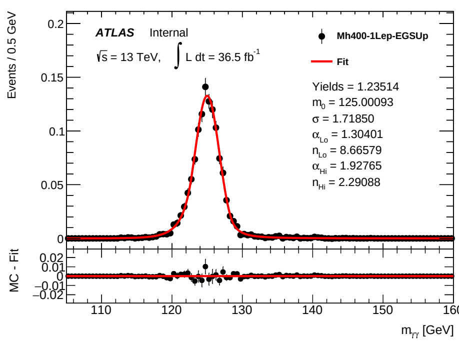

(h)

Figure 71: The fits for m_H = 400 GeV to obtain (a) σ_*Down* in zero lepton region, (b) σ_*Down* in one lepton region, (c) σ_*Up* in zero lepton region, (d) σ_*Up* in one lepton region, (e) m_0_*Down* in zero lepton region, (f) m_0_*Down* in one lepton region, (g) m_0_*Up* in zero lepton region, (h) m_0_*Up* in one lepton region.

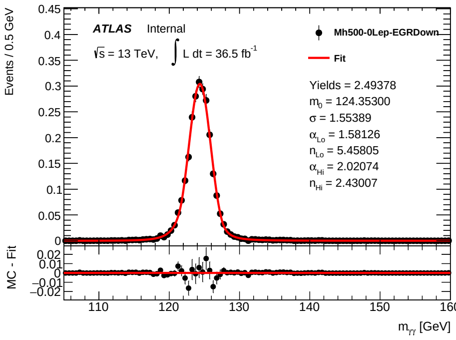

(a)

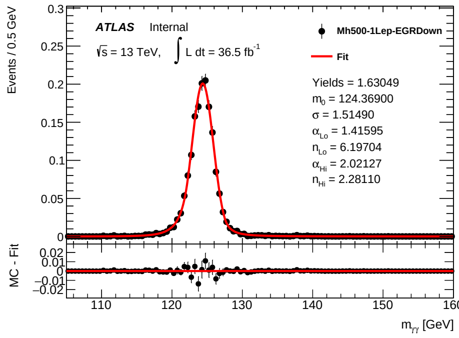

(b)

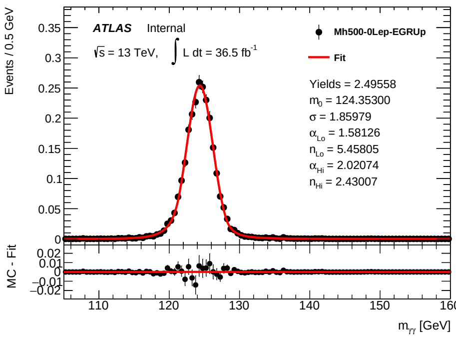

(c)

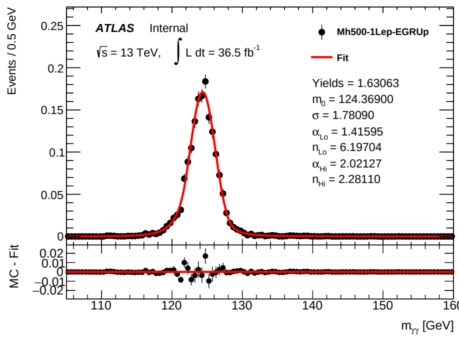

(d)

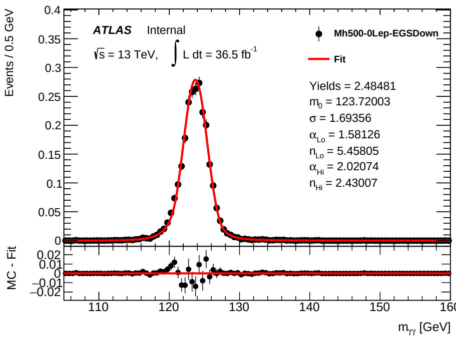

(e)

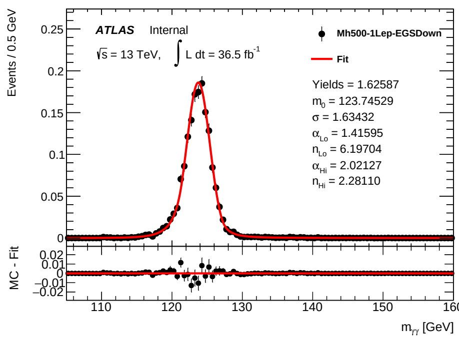

(f)

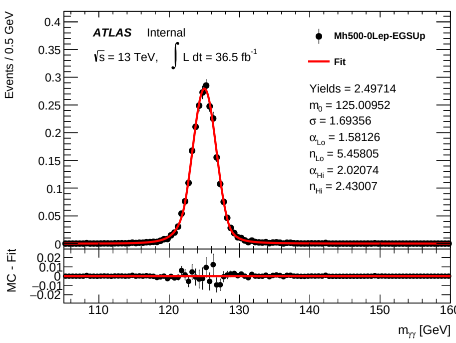

(g)

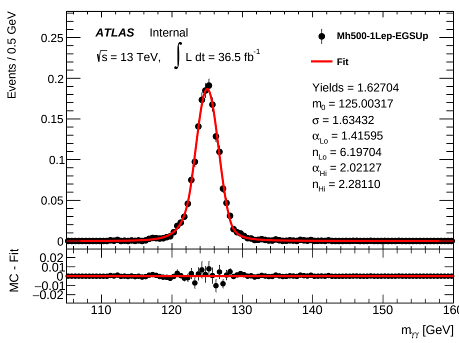

(h)

Figure 72: The fits for $m_H = 500$ GeV to obtain (a) σ_Down in zero lepton region, (b) σ_Down in one lepton region, (c) σ_Up in zero lepton region, (d) σ_Up in one lepton region, (e) m_0_Down in zero lepton region, (f) m_0_Down in one lepton region, (g) m_0_Up in zero lepton region, (h) m_0_Up in one lepton region.

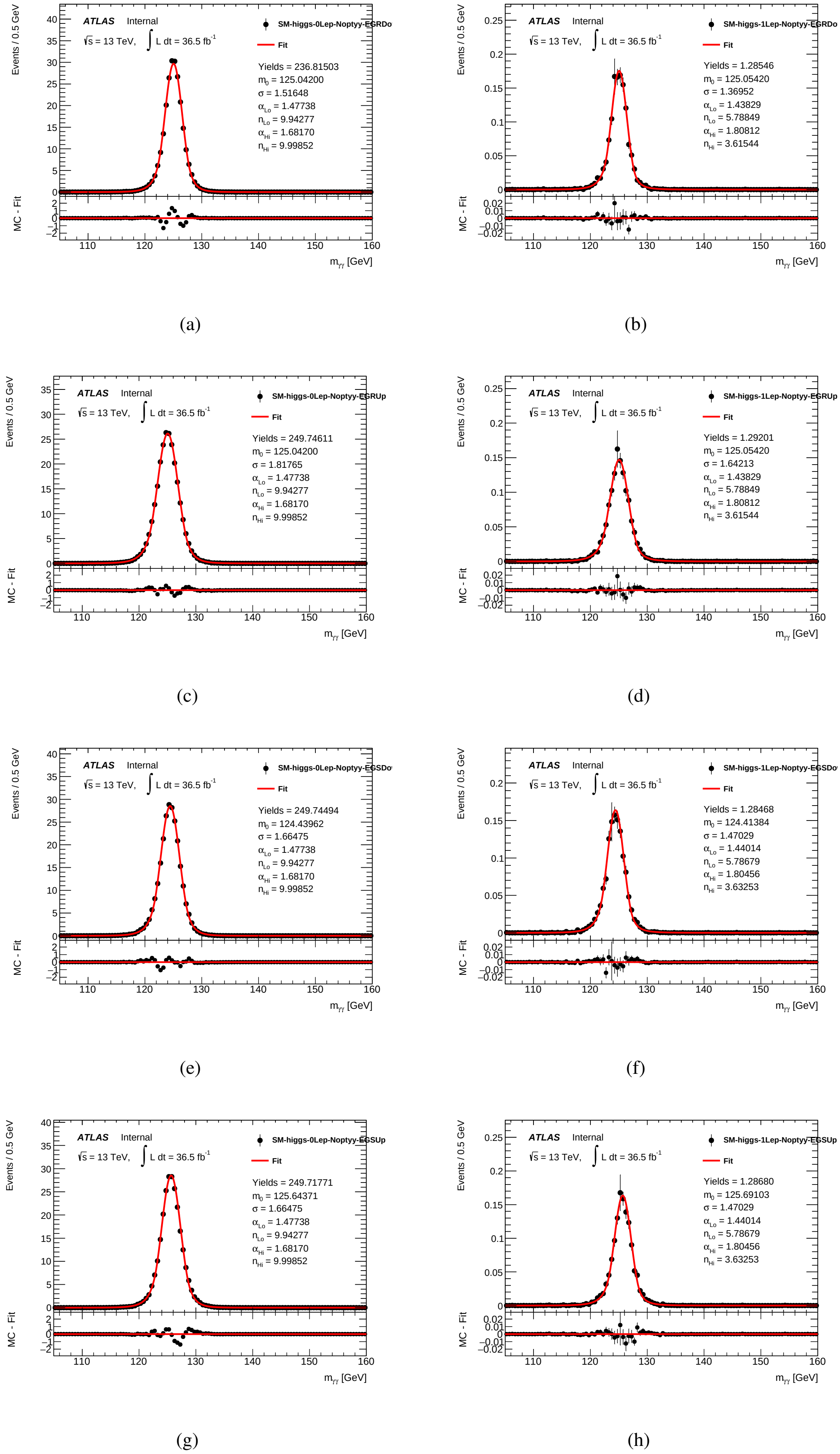

Figure 73: The fits for SM single higgs background to obtain (a) σ_Down in zero lepton region, (b) σ_Down in one lepton region, (c) σ_Up in zero lepton region, (d) σ_Up in one lepton region, (e) m_0_Down in zero lepton region, (f) m_0_Down in one lepton region, (g) m_0_Up in zero lepton region, (h) m_0_Up in one lepton region, without $p_T(\gamma\gamma)$ cut applied.

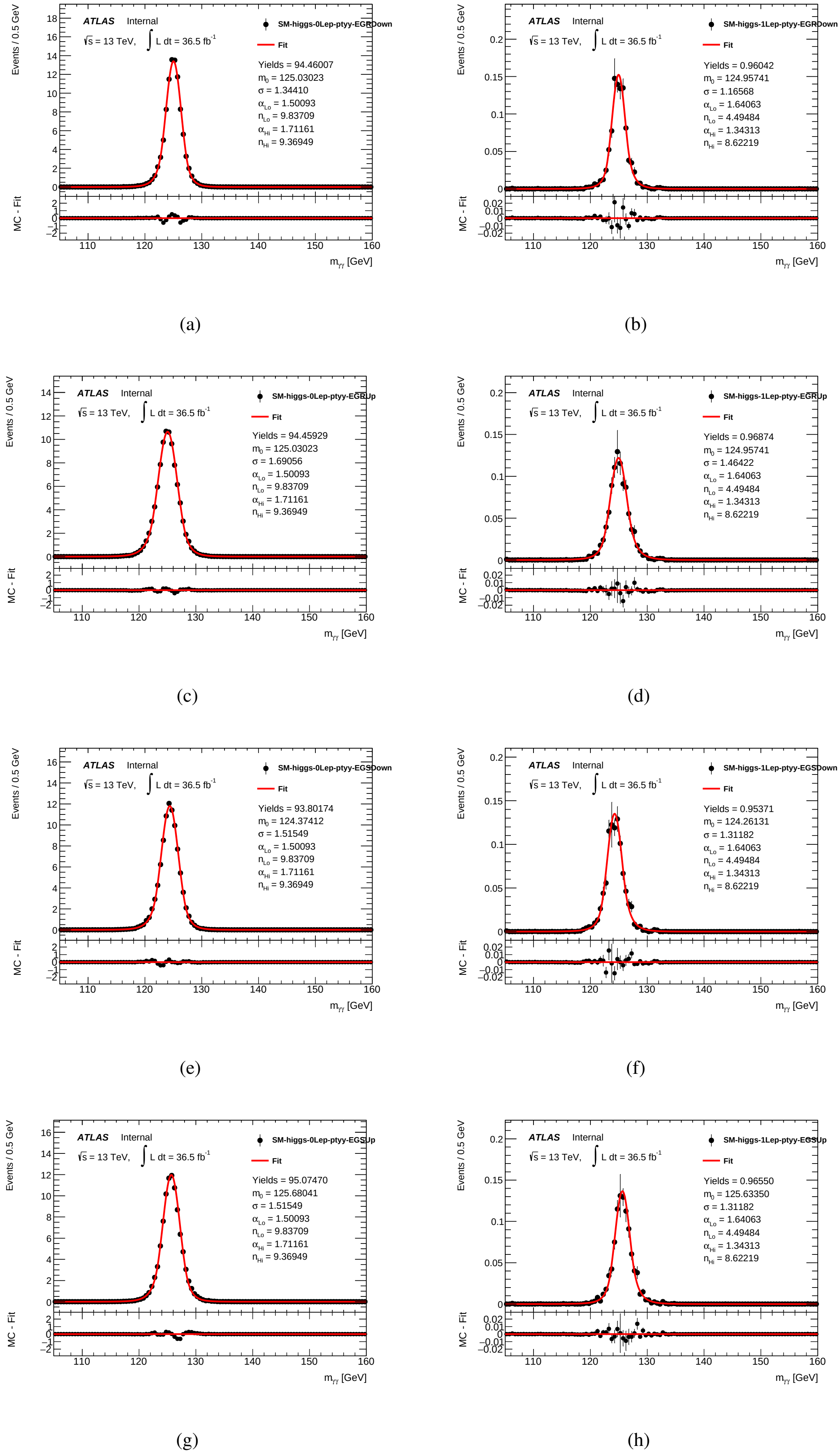

Figure 74: The fits for SM single higgs background to obtain (a) σ_Down in zero lepton region, (b) σ_Down in one lepton region, (c) σ_Up in zero lepton region, (d) σ_Up in one lepton region, (e) m_0_Down in zero lepton region, (f) m_0_Down in one lepton region, (g) m_0_Up in zero lepton region, (h) m_0_Up in one lepton region, with $p_T(\gamma\gamma)$ cut applied.

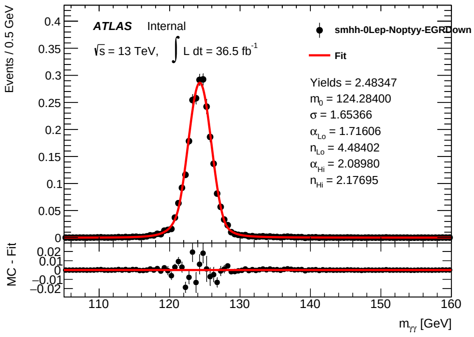

(a)

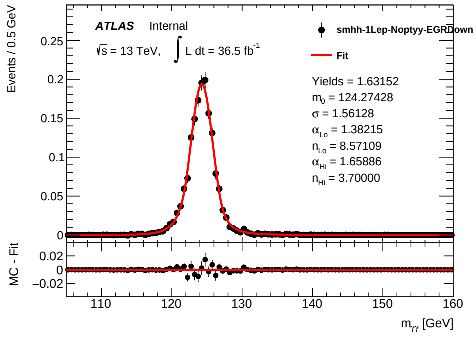

(b)

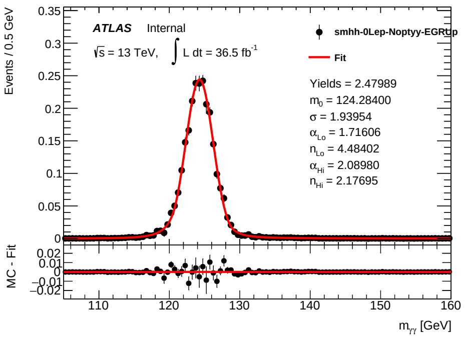

(c)

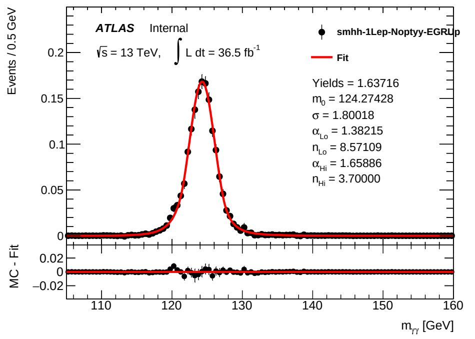

(d)

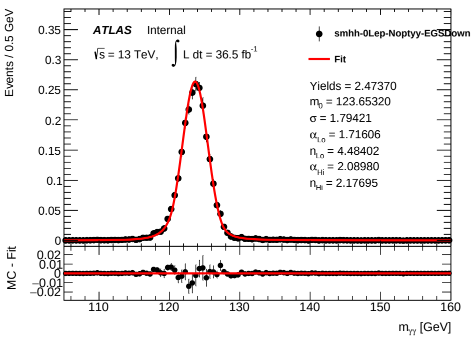

(e)

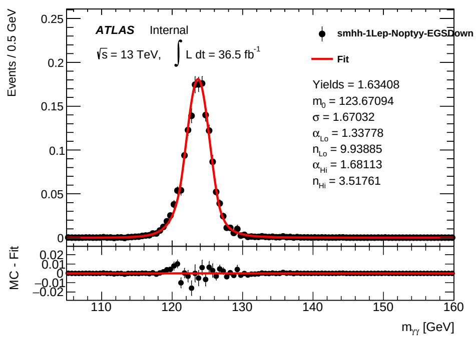

(f)

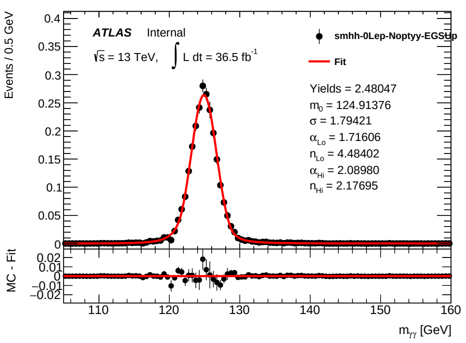

(g)

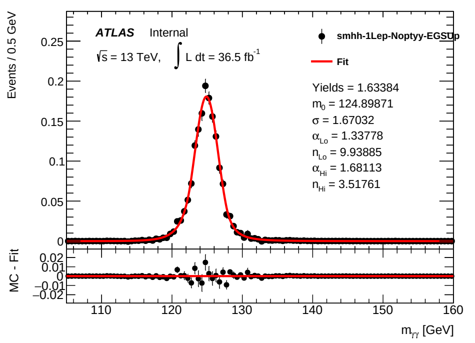

(h)

Figure 75: The fits for SM Higgs boson pair background to obtain (a) σ_Down in zero lepton region, (b) σ_Down in one lepton region, (c) σ_Up in zero lepton region, (d) σ_Up in one lepton region, (e) m_0_Down in zero lepton region, (f) m_0_Down in one lepton region, (g) m_0_Up in zero lepton region, (h) m_0_Up in one lepton region, with $p_T(\gamma\gamma)$ cut applied.